

CHEMICAL ENGINEERING DIVISION**FUEL CYCLE PROGRAMS
PROGRESS REPORT****October—December 1977****by**

**M. J. Steindler, Milton Ader, R. E. Barletta, J. K. Bates,
C. H. Bean, G. J. Bernstein, T. R. Cannon, K. F. Flynn,
T. J. Gerding, L. J. Jardine, B. J. Kullen, R. A. Leonard,
W. J. Mecham, K. M. Myles, R. H. Pelto, B. B. Saunders,
W. B. Seefeldt, M. G. Seitz, A. A. Siczek, L. E. Trevorrow,
A. A. Ziegler, D. S. Webster, and Leslie Burris**



U of C-AUA-USDOE

PROPERTY OF
ANL-W Technical Library

ARGONNE NATIONAL LABORATORY, ARGONNE, ILLINOIS

**Prepared for the U. S. DEPARTMENT OF ENERGY
under Contract W-31-109-Eng-38**

The facilities of Argonne National Laboratory are owned by the United States Government. Under the terms of a contract (W-31-109-Eng-38) between the U. S. Department of Energy, Argonne Universities Association and The University of Chicago, the University employs the staff and operates the Laboratory in accordance with policies and programs formulated, approved and reviewed by the Association.

MEMBERS OF ARGONNE UNIVERSITIES ASSOCIATION

The University of Arizona	Kansas State University	The Ohio State University
Carnegie-Mellon University	The University of Kansas	Ohio University
Case Western Reserve University	Loyola University	The Pennsylvania State University
The University of Chicago	Marquette University	Purdue University
University of Cincinnati	Michigan State University	Saint Louis University
Illinois Institute of Technology	The University of Michigan	Southern Illinois University
University of Illinois	University of Minnesota	The University of Texas at Austin
Indiana University	University of Missouri	Washington University
Iowa State University	Northwestern University	Wayne State University
The University of Iowa	University of Notre Dame	The University of Wisconsin

NOTICE

This report was prepared as an account of work sponsored by the United States Government. Neither the United States nor the United States Department of Energy, nor any of their employees, nor any of their contractors, subcontractors, or their employees, makes any warranty, express or implied, or assumes any legal liability or responsibility for the accuracy, completeness or usefulness of any information, apparatus, product or process disclosed, or represents that its use would not infringe privately-owned rights. Mention of commercial products, their manufacturers, or their suppliers in this publication does not imply or connote approval or disapproval of the product by Argonne National Laboratory or the U. S. Department of Energy.

Printed in the United States of America
Available from
National Technical Information Service
U. S. Department of Commerce
5285 Port Royal Road
Springfield, Virginia 22161
Price: Printed Copy \$6.50; Microfiche \$3.00

ANL-78-37

ARGONNE NATIONAL LABORATORY
9700 South Cass Avenue
Argonne, Illinois 60439

CHEMICAL ENGINEERING DIVISION
FUEL CYCLE PROGRAMS
QUARTERLY PROGRESS REPORT
October—December 1977

by

M. J. Steindler, Milton Ader, R. E. Barletta, J. K. Bates,
C. H. Bean, G. J. Bernstein, T. F. Cannon, K. F. Flynn,
T. J. Gerding, L. J. Jardine, B. J. Kullen, R. A. Leonard,
W. J. Mecham, K. M. Myles, R. A. Pelto, B. B. Saunders,
W. B. Seefeldt, M. G. Seitz, A. A. Siczek, L. E. Trevorow,
A. A. Ziegler, D. S. Webster, and Leslie Burris

Previous reports in this series

ANL-77-36
ANL-78-11

TABLE OF CONTENTS

	<u>Page</u>
ABSTRACT	1
SUMMARY	2
I. DEVELOPMENT OF ADVANCED SOLVENT EXTRACTION TECHNIQUES	7
A. Developments for the Processing of LWR Fuel	7
1. Introduction	7
2. Development of a 10 Mg/Day Contactor	7
3. Development of a Single-Stage Mini-Centrifugal Contactor	7
4. Development of an Eight-Stage Mini-Contactor	9
5. Extraction of Ruthenium and Zirconium in Centrifugal Contactors in the Purex Process	13
B. Developments for Reprocessing of FBR Fuel	19
1. Introduction	19
2. Development of 0.5 Mg/d Centrifugal Contactor	19
3. Solvent Cleanup	19
C. Aqueous Reprocessing Alternatives to the Thorex Process	22
1. Introduction	22
2. TCMA·NO ₃	23
3. DAAP and DHHP	23
4. HD(DIBM)P	23
II. ENVIRONMENTAL EFFECTS	24
A. Introduction	24
B. Explosive Dispersal of Metallic Uranium	24
C. Explosive Dispersal of Chemical Agents	27
1. Results	28
D. Study of the Effects of Diluents on the Dispersal of Chemical Agents	33
E. Models of Vaporization in Explosions	37
1. An Example: A Steel Ball	38
2. The Effect on Volatile Material: Water or Other Volatile Material	38
3. Limitations on Aerosol Formation from Vaporized Material	38
F. Propagation of Shock Waves in Ventilation Ducts	39
III. SEPARATION OF SELECTED ACTINIDES AND FISSION PRODUCTS FROM HLLW	40
A. Use of Various Organic Extractants in 2-cm-dia Centrifugal Contactor	40

TABLE OF CONTENTS (contd)

	<u>Page</u>
IV. PYROCHEMICAL AND DRY PROCESSING METHODS PROGRAM	41
A. Introduction	41
B. Program Management	41
C. Engineering Analysis	42
1. Materials Development	42
2. Carbide Fuel Processing	43
3. Thorium-Uranium Salt Transport Processing	48
D. Separations Processes	49
V. METAL MATRIX ENCAPSULATION OF HIGH-LEVEL WASTES	50
A. Introduction	50
B. Corrosion Rates of Candidate Matrix Metals	50
1. Preparation of Laboratory-Scale Metal Matrix Castings	50
2. High-Temperature/High-Pressure Corrosion of Metal Matrix Materials and Calcine in Saturated Brines	51
C. Chemical Interactions of Metal-Encapsulated Waste Forms	53
1. Experimental Procedures	54
2. Results and Discussion	54
3. Conclusions	56
D. Leach Rates of Simulated High-Level Waste Forms	57
1. Experimental Results	58
2. Conclusions	61
VI. ESTABLISHMENT OF TENTATIVE CRITERIA FOR HULL TREATMENT	64
A. Introduction	64
B. Progress in the Period	64
C. Reevaluation of the Criteria Base	65
D. A Tree-Structure Criteria Development Model	69
E. Zirconium Fines Behavior During Shearing Operations	73
VII. TRANSPORT PROPERTIES OF NUCLEAR WASTES IN GEOLOGIC MEDIA	78
A. Introduction	78
B. Rock and Solution Characterization	78
C. Column Infiltration Experiments	80

TABLE OF CONTENTS (contd)

	<u>Page</u>
D. Static-Absorption Experiments	83
E. Conclusions	84
VIII. TRACE-ELEMENT TRANSPORT IN LITHIC MATERIAL BY FLUID FLOW AT HIGH TEMPERATURE	85
A. Introduction	85
B. Experimental Method and Theoretical Consideration	85
C. Other Applications of Infiltration Experiments	86
D. Experimental Apparatus	87
E. Planned Experimental Program	89
REFERENCES	90

LIST OF FIGURES

<u>No.</u>	<u>Title</u>	<u>Page</u>
1.	Cross Section of a Single-Stage Centrifugal Contactor that has a Disk Base	8
2.	Effect of O/A Ratio and Rotor Speed on the Maximum Throughput	11
3.	Effect of O/A Ratio and Rotor Speed on the Maximum Throughput of the First Eight-Stage Centrifugal Contactor	12
4.	Effect of Total Flow Rate on Liquid Holdup Volume	13
5.	Histogram of Particle Size Distribution for Shot 6	25
6.	Particle Size Distribution Frequencies for Shot 6	25
7.	Effect of Pellet Compaction on Dispersal Effectiveness	29
8.	Effect of Casing on Dispersal Effectiveness	31
9.	Effect of Pellet Size on Dispersal Effectiveness	32
10.	Diagram of Miniature Bomb	34
11.	Bomb Dispersal Efficiency vs. Explosive Ratio	36
12.	Thermodynamic Stabilities of Some Actinide Carbides and Intermetallic Compounds	47
13.	Negative Natural Logarithm of the Penetration Depth, K, vs. the Reciprocal of Absolute Temperature	56
14.	Quantity of Dislodged Material as a Function of Chopped-Fuel Length	75
15.	Size Distribution of Zircaloy-2 and Uranium Particles Dislodged from Shearing Zircaloy-2-Clad UO ₂ Prototype Fuel Rods Into 2.5-cm Lengths	76
16.	Elution Curve for Tritium in a Shale Column of 17 cm ³ Volume	83
17.	Apparatus for Study of the Transport of Fluids Through Rock at High Temperatures and Pressures	88

LIST OF TABLES

<u>No.</u>	<u>Title</u>	<u>Page</u>
1.	Mass Transfer Efficiencies in Single-Stage Contactor	9
2.	Performance of Individual Stages in the First Eight-Stage Contactor	10
3.	Distribution Coefficients of Zirconium Nitrate Back-Extracted from 30% TBP/n-dodecane into 3M Nitric Acid at Ambient Temperature	16
4.	Distribution Coefficients of Ru(IV) Extracted by 30% TBP-nDD from ~0.01M Ru(IV) Nitrate Solution in ~3M HNO ₃ at Ambient Temperature	16
5.	Distribution Coefficients of Ru(IV) Back-Extracted from 30% TBP-nDD into 3M HNO ₃ at Ambient Temperature	17
6.	Distribution Coefficients of Ruthenium Nitrosyl Nitrate/Nitro Compounds Extracted by 30% TBP/nDD from ~0.01M Ruthenium Nitrosyl Solution in 3M HNO ₃ at Ambient Temperature	17
7.	Distribution Coefficients of Ruthenium Nitrosyl Nitrate/Nitro Compounds Back-Extracted from 30% TBP-nDD into 3M HNO ₃ at Ambient Temperature	18
8.	Characteristics of Particles from Explosive Tests that Dispersed Depleted Uranium Metal	26
9.	Effect of Pellet Compaction on Particle Size Mean	30
10.	Effect of Casing on Particle Size Mean	32
11.	Effect of Pellet Size on Mean Particle Size	33
12.	Particle Size Distributions Resulting from Explosive Dissemination of Resorcinol	35
13.	Probable Chemical and Physical States of Fission Products in Hyperstoichiometric Carbide Fuel, (U,Pu)C _{1+x}	44
14.	Results of 10-Day Autoclave Corrosion Test at 250°C and 5 MPa	52
15.	Experimental Conditions for Reactions of INEL Calcine, INEL Calcine-10 wt % SiO ₂ , and INEL Calcine-50 wt % SiO ₂ with Al-12 wt % Si Alloy	54

LIST OF TABLES (contd)

<u>No.</u>	<u>Title</u>	<u>Page</u>
16.	Rate of Penetration for Reaction Between INEL Calcine Plus 50 wt % SiO ₂ or 10 wt % SiO ₂ and Aluminum-12 wt % Si Alloy for the Uniform Reaction Zone	55
17.	First-Week Leach Rates for SWF Pellets Containing Fluid-Bed Calcine in 25°C Stagnant Distilled Water	59
18.	Leach Rates for SWF Pellets Containing Fluid-Bed Calcine and Aluminosilicate Flux in 25°C Stagnant Distilled Water	60
19.	Leach Rates in 25°C Distilled Stagnant Water for Lead Ingots Containing PW-7a Beads	62
20.	Seven-day Leach Rates in 25°C Distilled Stagnant Water for PW-7a Beads in Various Configurations	63
21.	Cladding Hull Accumulations Based on Plant Designs	67
22.	Development of Detail in Criteria	70
23.	Factors Conducive to Zircaloy Pyrophoricity in a Conceptual Fuel-Shear Design	74
24.	Estimated Amounts and Ratios of Particles from Shearing of LWR Fuel	77
25.	X-Ray Diffraction Analyses of Rocks Used in Nuclide Migration Experiments	79
26.	Total Dissolved Solids, Hydrogen Ion Concentrations, and Oxidation Potentials of Pre-Equilibrated Deaerated Solutions	80
27.	Activities of Tritium in Eluates from Four Column-Infiltration Experiments	82

CHEMICAL ENGINEERING DIVISION

FUEL CYCLE PROGRAMS
QUARTERLY PROGRESS REPORT

October—December 1977

by

M. J. Steindler, Milton Ader, R. E. Barletta, J. K. Bates,
C. H. Bean, G. J. Bernstein, T. F. Cannon, K. F. Flynn,
T. J. Gerding, L. J. Jardine, B. J. Kullen, R. A. Leonard,
W. J. Mecham, K. M. Myles, R. A. Pelto, B. G. Saunders,
W. B. Seefeldt, M. G. Seitz, A. A. Siczek, L. E. Trevorow,
A. A. Ziegler, D. S. Webster, and L. Burris

ABSTRACT

Fuel cycle studies reported for this period include studies of advanced solvent extraction techniques focussed on the development of centrifugal contactors for use in Purex processes. Miniature single-stage and eight-stage centrifugal contactors are being employed in performance studies applicable to larger units. In other work, literature on the dispersion of reagents as a result explosions is being reviewed to develop systematic data applicable to fuel reprocessing and useful in identifying source terms. In yet other work, scouting studies were performed to obtain criteria for identifying organic solutions suitable for the separation of actinides from fission products.

A program has been initiated on pyrochemical and dry processing of nuclear fuel. Literature reviews have been initiated on material development, carbide fuel reprocessing, and thorium-uranium reprocessing in fused salts. A review and evaluation of the encapsulation of high-level waste in a metal matrix is under way. Corrosion and leach rates of simulated waste forms are being measured and a model has been proposed to describe the reaction between solidified high-level waste and metals. In other work, criteria for the handling of fuel assembly hulls are being developed on the basis of past work on the pyrophoricity of zirconium alloys and related criteria from several sources.

Experimental work is under way to determine whether nuclear wastes can be safely confined in geologic formations. Information is being obtained on the migration of radionuclides in aqueous solution-rock systems.

SUMMARY

Development of Advanced Solvent Extraction Techniques

A single-stage 2-cm-dia centrifugal contactor was operated to measure uranium extraction efficiency in Purex-type extractions. At 6000 rpm, extraction efficiency was found to be in the range 90 to 92% when either a disk or radial vanes were installed on the housing bottom.

Also an eight-stage 2-cm-dia annular centrifugal contactor bank was tested for flow performance, for individual stages, and for all eight stages combined. At organic-to-aqueous ratios between 1.0 and 2.5, the contactor can operate reliably at total throughputs of 100 mL/min. Total liquid holdup in the eight-stage unit was found to increase from 125 mL at a total throughput of 40 mL/min to 180 mL at 120 mL/min.

An annular centrifugal contactor suitable for reprocessing reactor fuel at 0.5 Mg/d has been fabricated and installed in a test facility for mechanical and hydraulic testing.

Studies of extraction kinetics of the fission products, ruthenium, and zirconium, in a single-stage centrifugal contactor have been completed. They indicate that the extent of extraction of ruthenium and zirconium is reduced by about 30% in a short-residence-time (3-7 s) contactor as compared with a pulse column (5 min). The scrubbing efficiency is affected to about the same degree.

The importance of the chemistry of metal complexes of di-n-butylphosphoric acid (HDBP), the major impurity resulting from solvent degradation of tri-n-butyl phosphate (TBP) is discussed, and several areas to be investigated are highlighted. The four most important areas are:

- (1) The formation of HDBP by radiolysis and hydrolysis in the presence of heavy metals (Zr, U, Th, Pa, Pu);
- (2) The kinetics of complex formation, *i.e.*, the rates of extraction of the various metals by HDBP/TBP/nDD;
- (3) The kinetics of polymerization and metal retention, *i.e.*, the behavior of the initially formed complex as the solution is aged; and
- (4) The relative stabilities of the different metal complexes (a) as a function of time or "age of the solvent" and (b) with respect to the stabilities of aqueous complexes produced during solvent washing.

A new program has been initiated to investigate aqueous reprocessing alternatives to the Thorex process for the recovery of thorium-based reactor fuels and to test them in centrifugal contactors.

Environmental Effects

The purpose of this program is to develop a systematic and coherent body of knowledge as a basis for realistic source terms for accidents in fuel reprocessing plants.

The generation of source terms consists of three phases: the formation of aerosols, dusts, and mists by accident events; the modification of the characteristics of airborne material during its transport within a facility to an air-cleaning system; and the modification of the material by the air-cleaning system. Principal attention to date has been given to explosive events.

Experiments were conducted at another site in which hollow cylinders of metallic uranium were explosively dispersed. A bimodal particle size distribution was fairly characteristic; the small-particle-size mode approximated a lognormal distribution, and the large-particle-size mode did not. The large-particle-size mode became smaller as the amount of explosive was increased. The mass median diameters for the small-particle-size mode were 120 to 219 μm , and geometric standard deviations were close to 2.

In experiments in which hollow cylinders of solid materials were dispersed, the explosive ratio (weight of explosive/weight of inert material) was also found to be significant. High explosive ratios yielded distributions having low mass mean particle diameters. Dispersion (as measured by mass mean particle diameters) was found to decrease (1) when a casing was placed around the test device and (2) when the scale of the test was increased (with the explosive ratio held constant). Mass median diameters ranged from 7 to 30 μm .

Information is presented on a model of vaporization of materials due to explosive heating effects, and on the attenuation of blast effects by the physical configurations of ducts and other structures.

Separation of Selected Actinides and Fission Products from HLLW

Organic extractants are being evaluated for use in flow sheets for the separation of actinides from fission products. Results of scouting studies showed that they work well in commercial extraction equipment when the solvent (such as diethylbenzene) gives a low-viscosity solution. When the viscosity is high (*e.g.*, 4 times that for 30 vol % TBP in nDD), fairly satisfactory phase separations can still be achieved, but only by making significant reductions in throughput. Tentative criteria are given for identifying organic solutions that are suitable for use in commercial extraction equipment.

Pyrochemical and Dry Processing Methods Program

A Pyrochemical and Dry Processing Methods Program (PDPM) was established at the beginning of FY78 within the Fuel-Cycle Section, Chemical Engineering Division, at Argonne National Laboratory (ANL). This program is part of the national fuel-cycle program for reprocessing fuel by processes that will reduce the risk of proliferation of nuclear weapons. Argonne has been designed by DOE as the lead laboratory for PDPM, with various reprocessing tasks being performed at other DOE laboratories and by industrial contractors.

To carry out these activities, work packages have been established that include statements of work supplied by ANL and appropriate contractors. These statements of work each include objectives, a cost plan, a milestone plan, and a management plan. This material is then factored into the overall management plan.

Literature reviews have been initiated for three projects in this program--namely, material development, carbide fuel reprocessing, and thorium-uranium reprocessing in fused salts. This includes all pertinent thermodynamic information on the behavior of actinides, fission products, and cladding materials in metal and salt solvents. Conceptual flow sheets based on this information are being drawn up.

Preliminary literature searches have indicated a lack of data on thorium and protactinium partition and solubility in nonaqueous systems and laboratory experiments are being considered.

Metal Matrix Encapsulation of High-Level Wastes

Composites ($\sim 3\frac{1}{2}$ -cm ID by 10-to 23-cm long) of simulated waste forms (Al_2O_3 beads, glass beads, agglomerated-sintered INEL fluid-bed calcine) dispersed in metallic lead, an aluminum alloy, and Admiralty brass have been prepared in a vacuum and in an argon atmosphere.

Corrosion of metallic lead, an aluminum-12.5 wt % silicon alloy, and Admiralty brass in saturated-brine solutions at 250°C and ~ 5 MPa (750 psi) is being examined. A 10-day test of the aluminum alloy revealed severe attack (4-12 % weight losses) with the release of hydrogen. Lead suffered no significant effects under the same test conditions. Lead and Admiralty brass specimens from 30-day tests have been examined visually and appear to have encountered little corrosion. More detailed physical analyses are being done. Sixty-day tests of the latter two alloys are well under way.

A model has been proposed to describe the reaction between solidified HLW and metals in order to evaluate the importance of chemical reactions in the metal encapsulation concept for waste management. A simulated waste form consisting of 50 wt % fluid-bed calcine and 50 wt % SiO_2 has been selected for study. The Arrhenius activation parameters for this system have been determined ($E_a = 22.8$ kcal/mol), the extent of reaction with aluminum, based on these parameters, has been calculated for various temperature and time conditions. The extent of reaction is estimated to be ~ 10 wt % of the solidified HLW in 100 y of storage, it being assumed that the temperature reaches a maximum of 1000°C for a period of 1 h during the 100 y.

Further experiments have been performed using waste forms containing 10% SiO_2 rather than 50% SiO_2 . The reaction rates of these waste forms with aluminum were roughly one order of magnitude lower than those for waste forms containing 50% SiO_2 .

Leach rate studies of simulated solid waste forms associated with the metal matrix encapsulation technique have continued. Sintered waste forms (SWF), as well as lead matrix composites, have been evaluated during this report period, using a procedure based on neutron activation analysis. Satisfactory leach rates have been obtained for SWF when aluminosilicate fluxes were added to the calcined waste prior to sintering. Results of the leach rate tests of lead-matrix composites showed that there was a significant amount of leaching from the interior of the ingot. If a final waste form should exhibit this behavior, its leaching characteristics would be considered unsatisfactory. Additional investigation of the problem is in progress.

Establishment of Tentative Criteria for Hull Treatment

Criteria (or guidelines) are being developed for DOE for safe handling and disposal of fuel-assembly hulls and hardware that will be discarded after chopping and leaching of spent fuel at fuel reprocessing plants. In this program, a set of tentative criteria is to be assembled; the criteria are to be transmitted to appropriate industries, DOE, and the NRC for review and suggestions; and revised versions based on comments by reviewers are to be issued. To date, a draft criteria document has been written and is described herein. Also presented are (1) alternative bases for criteria, (2) a methodology for hull-handling criteria development, and (3) a prediction of the nature of zirconium fines in the shear cell.

Transport Properties of Nuclear Wastes in Geologic Media

An experimental program is under way to evaluate whether nuclear wastes can be safely confined in geologic formations. In laboratory experiments, quantitative data are being obtained describing the radionuclide-geologic material interactions that control the transport of radionuclides in geologic media.

Characteristics of the rocks and solutions used in the program were measured to describe materials used in the experiments. Mineral constituents of chalk, shale, and limestone were determined by X-ray diffraction analyses. Total dissolved solids, pH, and oxidation potential were determined on rock-equilibrated solutions used in the experiments. Total dissolved solids in solutions reacted with chalk, shale, and limestone were 110, 170, and 42 mg/L of solution, respectively; pH ranged from 8.0 to 7.6; and the oxidation potential from 0.269 to 0.277 V using a standard calomel electrode.

The properties of lithic columns can affect nuclide migration and are important to interpreting the results of experiments. In column infiltration experiments during this quarter, tritiated water was used to mark the advancing water front through columns of shale and chalk aggregate.

The tritiated water was seen to move through the columns with little dispersion, indicating that earlier observed migration of cesium was due to chemical properties of the cesium rather than hydrodynamic properties of the column.

Results of static absorption experiments performed to investigate the cause of apparent synergistic behavior between plutonium and americium (observed previously) were analyzed. From the experimental results, it is concluded that auxiliary chemicals accompanying the plutonium are responsible for the synergistic behavior, rather than the plutonium itself.

Trace Element Transport in the Material by Fluid Flow at High Temperature

This report introduces a new program for studying the migration of trace elements at high temperatures in geologic materials with which the trace elements interact.

Chemical reactions during fluid flow can cause chemical and mineralogical zoning in geologic formations, and attempts to calculate mass transport of major elements or trace elements by fluid flow are complex and are not always possible using data derived from static experiments.

In this program, a direct empirical approach is preferred: trace element transport by pumping aqueous fluids through packed chromatographic columns of powdered rock or mineral. A trace amount of a substance is introduced into the stream, and the effluent or the solid remaining in the column is analyzed to determine the migration rate.

Equipment for this work is described which is capable of pumping solutions through columns at uniform rates as low as 0.01 mL/min at temperatures up to 290°C and pressures up to 5×10^7 Pa (7300 psi). Different seals will permit use of this equipment up to 600°C. In initial experiments, transport of cesium and strontium in clay minerals is being studied.

I. DEVELOPMENT OF ADVANCED SOLVENT EXTRACTION TECHNIQUES

(G. J. Bernstein, Herbert Diamond,* E. P. Horwitz,*
R. A. Leonard, G. W. Mason,* B. B. Saunders, A. A. Siczek,
G. F. Vandergrift,* and A. A. Ziegler)

A. Developments for the Processing of LWR Fuel

1. Introduction

Work is continuing on various aspects of the program for development of advanced solvent extraction techniques for Purex reprocessing of light water reactor (LWR) fuel. This program is being carried out in cooperation with Savannah River Laboratory (SRL). The specific components of the ANL program are: (1) design, construction, and testing of single-stage miniature centrifugal contactors based on the annular mixing concept; (2) design, construction, and testing of multistage miniature contactors based on the annular mixing concept; (3) design, construction, and testing of a large annular centrifugal contactor with a capacity of 10 Mg/d of LWR fuel; (4) study of the chemistry and kinetics of solvent extraction of ruthenium and zirconium for the purpose of developing flow sheets capable of enhanced decontamination based upon differential extraction kinetics in short-residence-time contactors; (5) investigation of uranium-plutonium partition in short-residence or other types of contactors; and (6) investigation of alternative aqueous thorium processing systems, including causes and effects of solvent damage.

The contactors being used in work on these problems include a 2-cm-ID centrifugal contactor and an eight-stage mini-contactor, the individual stages of which are very similar to the single-stage unit (ANL-78-11).

2. Development of a 10 Mg/d Contactor (G. J. Bernstein)

An earlier report in this series (ANL-77-36) described the operating principles and showed the general configuration and dimensions of a large annular centrifugal contactor capable of processing LWR fuel at the rate of 10 Mg/d. This unit has a rotor of 25-cm-ID and 42-cm length (36-cm separating section and 6-cm weir section). The rotor will be driven at about 1750 rpm by a 3.7-kW (5-hp) commercial precision motorized spindle which has been purchased. Detailed design of the contactor is being deferred until a 0.5 Mg/d unit of similar design can be tested (see Section B.2 below). It is anticipated that successful operation of the smaller unit will provide a valid basis for the design and construction of the large unit.

3. Development of a Single-Stage Mini-Centrifugal Contactor (R. A. Leonard, A. A. Ziegler, and G. J. Bernstein)

In the preceding report in this series, ANL-78-11, it was stated that substantially higher throughputs were obtained when a circular disk (Fig. 1) covered the radial vanes on the bottom of the housing of the 2-cm-ID contactor. In the most recent report period, tests were made to compare extraction

* Chemistry Division, Argonne National Laboratory.

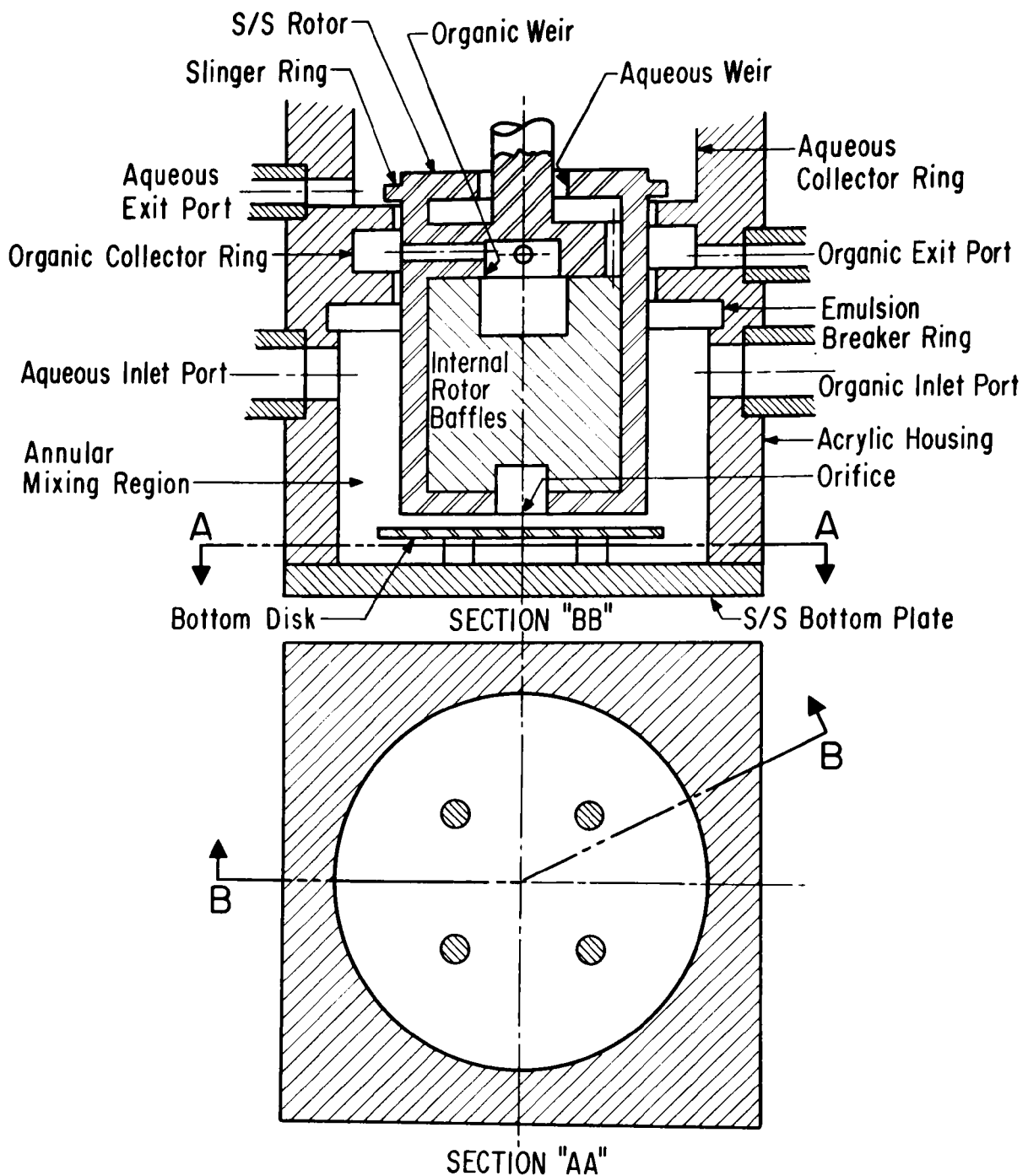


Fig. 1. Cross Section of a Single-Stage Centrifugal Contactor that has a Disk Base

efficiencies of the two types of housings. As shown in Table 1, extraction efficiency for uranium was higher with vanes uncovered at rotor speeds of 4000 rpm (94% *vs.* 81%), but both the vanes and the disc showed essentially the same efficiency (90-92%) at 6000 rpm.

Table 1. Mass Transfer Efficiencies in Single-Stage Contactor

Aqueous Feed: 0.011M Uranyl Nitrate in 3.0M HNO ₃ Organic Feed: 30 vol % TBP in nDD Rotor II					
Rotor Speed, rpm	Type of Base	Total Flow Rate, mL/min	O/A Ratio	Matl. Balance Recovery of U, %	Uranium Extraction Efficiency, ^a %
6000	I(Vanes)	40.8	1.00	94	90 ± 3
6000	XV(Disk)	41.6	1.00	101	92 ± 1
6000	XV(Disk)	160.1	0.962	99	90 ± 1
4000	I(Vanes)	80.0	0.975	96	94 ± 3
4000	XV(Disk)	80.0	0.975	101	81 ± 1
4000	XV(Disk)	81.6	0.980	105	82 ± 3

^aExtraction efficiency is defined as:

$$E_A = \frac{X_F - X_P}{X_F - X_{P,E}} \text{ and}$$

$$E_O = \frac{Y_P - Y_F}{Y_{P,E} - Y_F}$$

where X_F and Y_F = aqueous and organic feed concentrations

X_P and Y_P = aqueous and organic product concentrations

$X_{P,E}$ and $Y_{P,E}$ = concentrations of product streams if they are completely equilibrated.

4. Development of an Eight-Stage Mini-Contactor (R. A. Leonard, A. A. Ziegler, and G. J. Bernstein)

Hydraulic performance tests are continuing on the eight-stage miniature centrifugal contactor. This unit was described in the preceding report, ANL-78-11. It consists of eight stages (each similar to the single-stage contactor), arranged to operate in series and driven by a common variable-speed belt drive. In the eight-stage unit, the rotors were made about 1 cm longer than that in the single-stage contactor to reduce the likelihood that mixed phases in the annular mixing zone will rise into the organic-phase collector ring and contaminate the organic-phase effluent streams.

Preliminary tests were made to measure the hydraulic performance of each individual stage in the contactor. These tests were conducted at rotor speeds ranging from 3000 to 4800 rpm and at total throughputs up to 120 mL/min. The results, shown in Table 2, indicate some variation in performance for individual stages. Contamination is found almost exclusively in the organic effluent stream, and is greater when the O/A flow ratio is low. This suggests that the diameter of the aqueous weir may not be sufficiently larger than the diameter of the organic weir. As a result, the interface between the two phases in the rotor may be too close to the organic weir and allow some unseparated aqueous phase to escape with the organic phase. This condition will be investigated by modifying a rotor of a single-stage contactor.

Table 2. Performance of Individual Stages in the First Eight-Stage Contactor

Aqueous Phase (A): 3.0M HNO ₃ Organic Phase (O): 30 vol % TBP in nDD				
Total Flow, mL/min	40	40	80	120
Rotor Speed, rpm	3000	4800	3600	4800
O/A Ratio	1.0	0.2	1.0	1.0
Contamination: A in O (O in A), %				
Stage 1	0.4 (tr) ^a	5.0 (O)	2.8 (O)	1.7 (O)
Stage 2	0.4 (tr)	1.4 (O)	3.1 (O)	1.9 (tr)
Stage 3	0.2 (O)	2.9 (O)	3.6 (O)	0.3 (O)
Stage 4	0.9 (O)	8.4 (O)	4.0 (O)	0.7 (O)
Stage 5	0.3 (tr)	<.1 (tr)	0.9 (O)	0.3 (O)
Stage 6	0.3 (tr)	0.7 (O)	2.8 (O)	0.5 (O)
Stage 7	2.8 (O)	1.3 (tr)	4.5 (O)	5.9 (O)
Stage 8	.9 (O)	6.7 (O)	3.4 (O)	0.3 (tr)

^atr is trace amount.

A series of tests was also made on stage eight of this contactor to measure maximum acceptable throughput at a wide range of rotor speeds and O/A flow ratios. The performance of stage eight in these tests was generally better than it was in the tests shown in Table 2. The difference may be due to a difference in the manner in which the limiting operating condition was approached. Figure 2 shows that maximum throughput increases with rotor speed (between 3000 and 6900 rpm) and with O/A flow ratio (between 0.2 and 10). Throughputs above 200 mL/min were not attempted at the higher rotor speeds.

Hydraulic performance of the combined stages of the eight-stage contactor was measured at rotor speeds of 3600, 4800, and 6000 rpm. The effect of rotor speed on throughput at various O/A flow ratios is shown in Fig. 3. A significant increase in flow occurred when rotor speeds increased from 4800 to 6000 rpm. This suggests that a further increase in rotor speed would be

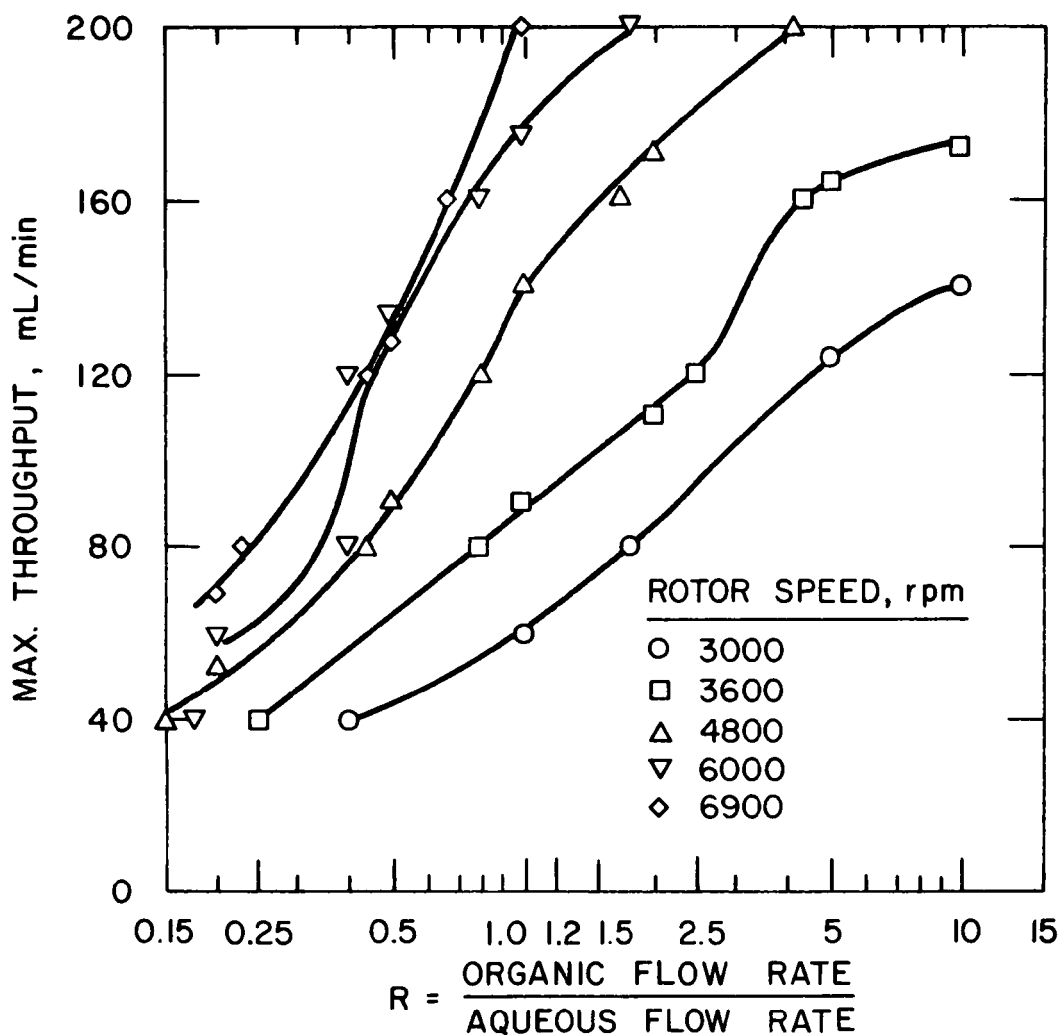


Fig. 2. Effect of O/A Ratio and Rotor Speed on the Maximum Throughput. Aqueous phase: 3M HNO₃. Organic phase: 30% TBP in nDD. Stage eight of eight-stage centrifugal contactor.

useful. A larger pulley on the drive motor will be obtained to achieve higher speeds.

A relatively sharp drop in throughput is evident (Fig. 3) when the O/A ratio falls below 1.0. This is similar to the performance of the stages when operated singly.

Liquid holdup volume when all eight stages were in operation was measured by stopping the rotor drive motor and feed pumps at the same time, then draining the contents of the contactor. Figure 4 shows that the total volume of each phase in the contactor increases as total flow rate increases.

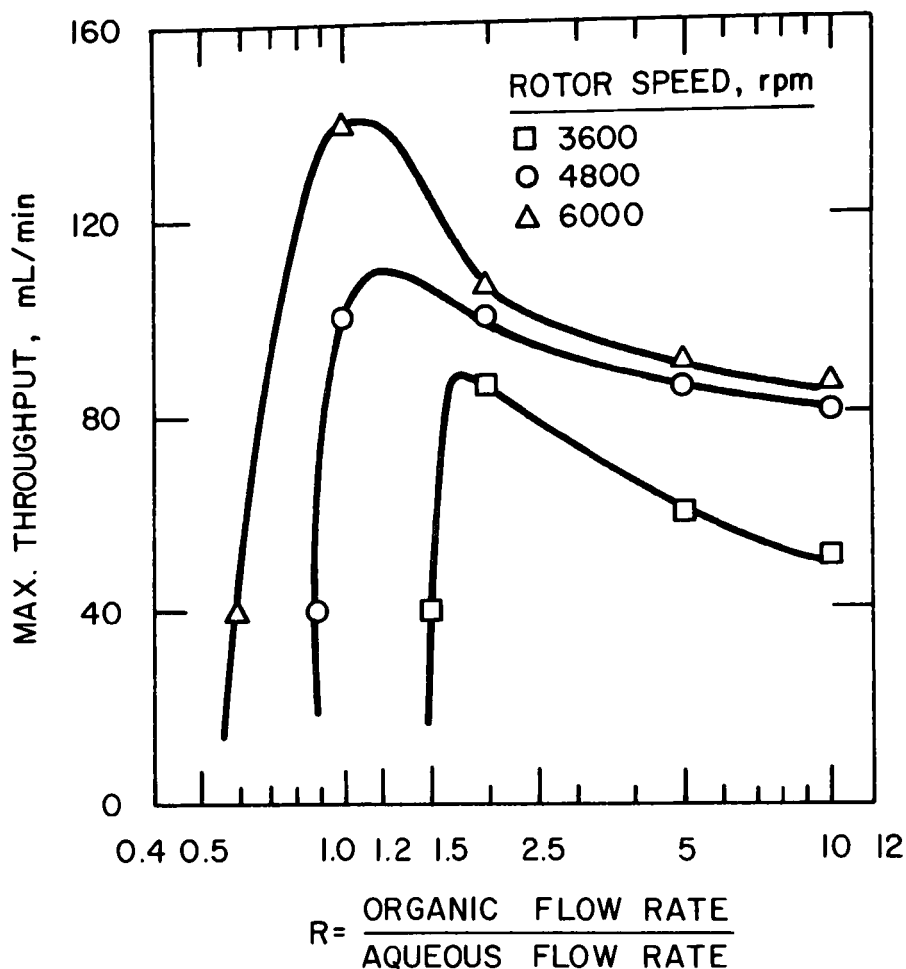


Fig. 3. Effect of O/A Ratio and Rotor Speed on the Maximum Throughput of the First Eight-Stage Centrifugal Contactor. Aqueous feed: 3M HNO_3 . Organic feed: 30 vol % TBP in nDD

In early tests, some difficulty was encountered with short operating lives of drive belts made of Buna-N or Viton* O-rings. Belt performance problems were solved by using a drive belt made of polyurethane. The polyurethane belt has the further advantage that it can be made to size by simple heat welding.

A second eight-stage contactor is now under construction. In view of the potential increase in throughput with disks, disks will be incorporated in this contactor. Hydraulic tests of the single-stage contactor showed that contamination of the organic discharge stream was often due to the surging of the mixture from the annulus up into the organic-phase collector ring. In the eight-stage contactors, the rotor was made slightly longer to reduce the effect of surging, and throughput seems to be limited by phase separation in the rotor. Thus, it is not clear that the increase in throughput found in the single-stage contactor based on the use of a disk will be realized in the second eight-stage contactor.

* Trademark, E. I. duPont de Nemours & Co., Inc., Wilmington, Delaware.

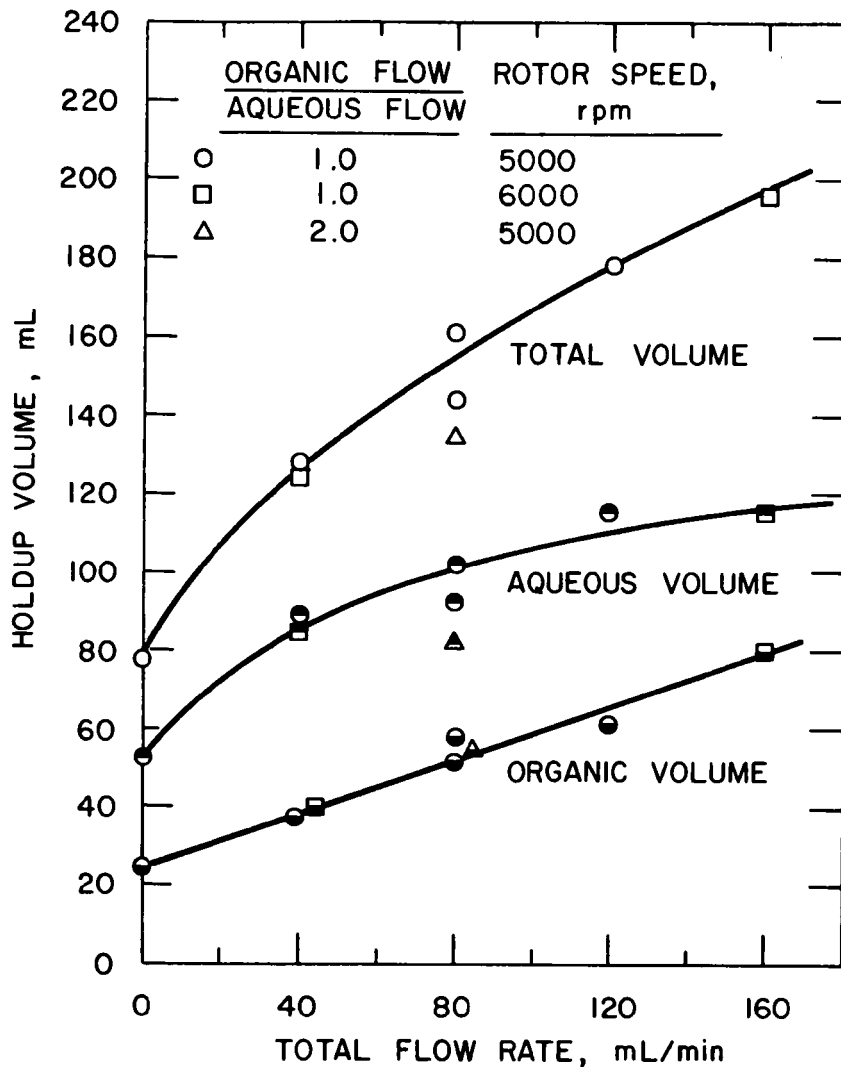


Fig. 4. Effect of Total Flow Rate on Liquid Holdup Volume. Equipment: eight-stage 2-cm centrifugal contactor no. 1. Aqueous phase: 3M HNO₃. Organic phase: 30 vol % TBP in nDD. Open points, total vol.; top half solid, aqueous vol.; bottom half solid, organic vol.

5. Extraction of Ruthenium and Zirconium in Centrifugal Contactors in the Purex Process
(A. A. Siczek)

The objective of this work is to develop improved Purex flow sheets for reprocessing spent reactor fuel in short-residence-time centrifugal contactors. The difference in effective extraction rates of (1) uranium and plutonium and (2) fission products can provide a basis for their improved separation, since the rates of extraction of the latter are lower than those of the former.

In centrifugal contactors, the phase contact time is only ~3-10 s per stage, a fiftyfold reduction in comparison with ~5 min in a pulse column. An extraction time of 3 to 10 s is adequate for the mass transfer of uranium, plutonium, and nitric acid since their extraction rates are diffusion-controlled [PUSHLENKOV]. The rate-controlling process in the extraction of zirconium and ruthenium involves the formation of solvates, as well as conversion among different chemical species and the formation of complexes.

Ruthenium exists in nitric acid solutions in the form of various nitrate, nitro, or mixed nitrate-nitro complexes of trivalent ruthenium nitrosyl (RuNO^{3+}) which have widely differing extractabilities. The equilibrium among them is established slowly ($t_{1/2} = 10$ to 60 min for nitrate ligands and $t_{1/2} = 1$ to 30 days for nitro groups at 20°C) [BROWN-1960]. Zirconium complexes in the nitric acid medium undergo hydrolysis and/or polymerization to produce polymers of very different extractabilities. The formation and interconversion among them is also slow [YAGODIN]. These processes are much slower than diffusion across a phase boundary, and the equilibrium state may not be reached for several minutes or more [BROWN-1960, YAGODIN].

The short contact time may also affect scrubbing efficiency because transfer of ruthenium and zirconium into the aqueous phase in the scrub section of the first extraction bank may not be complete. Nevertheless, short total extraction and scrubbing times may be beneficial because they do not allow the formation in the organic phase of those zirconium and ruthenium species that are very difficult to scrub. On the overall basis, short-residence-time contactors were reported to give better decontamination from zirconium and ruthenium than did mixer-settlers that have longer residence times [KISBAUGH, SCHLEA, ORTH].

To obtain data for the design of flow sheets, studies of the kinetics of the forward-extraction and back-extraction of ruthenium and zirconium in a single-stage annular centrifugal contactor were conducted during the past quarter. In addition to studies with ruthenium and zirconium only, a series of runs was made in the single-stage contactor to measure extraction and scrubbing coefficients of zirconium and ruthenium as a function of residence time and nitric acid concentration with both fission products present in the same solution. Additionally, extraction of ruthenium was investigated under conditions in which a low-acidity feed was spiked with more concentrated nitric acid just before flowing into the contactor. The purpose of these experiments is to establish conditions giving better decontamination for uranium and plutonium in short-residence-time contactors.

a. Experimental

The same experimental procedure was employed in all studies. The following reagents were used: ruthenium(IV) nitrates were purchased from Research Organic/Inorganic (Sun Valley, Calif.) and ruthenium nitrosyl nitrate crystals were obtained from Pfaltz and Bauer (Stanford, Conn.). The visible and infrared spectra of these reagents were determined* and were found to agree with the literature [FLETCHER-1958, FLETCHER-1959, BROWN-1960]. Zirconium nitrate crystals were obtained from A. D. Mackay (Darien, Conn.). Tri-n-butyl phosphate and n-dodecane were supplied by Kodak (Rochester, N.Y.). All reagents were of analytical grade.

* Acetone solutions were evaporated to dryness, and KBr pellets were made with the residue.

Aqueous solutions of ruthenium and zirconium nitrates (separately or both in the same solution) were prepared by dissolving the reagents in water and nitric acid to give final concentrations of $\sim 0.01M$ ruthenium and/or zirconium in $1-3M$ nitric acid. The organic solutions of ruthenium and/or zirconium were prepared by contacting with agitation aqueous solutions of these elements in $2M$ nitric acid with 30% tri-n-butyl phosphate (TBP) in n-dodecane (nDD) for 6-8 h. The concentrations of these elements in the organic phase are given in the tables. The aqueous solutions were contacted for a few seconds with 30% TBP-n-dodecane (forward-extraction) and the organics with nitric acid solution (back-extraction) in the single-stage 5-cm-ID (2-in.-ID) annular centrifugal contactor. The contactor used in the experiments was described previously in ANL-77-36 and ANL-78-11. Rotor speeds were monitored with a stroboscope and were held at 8500-9000 rpm. The flow rate ratio of organic phase-to-aqueous phase was set at approximately 1:1.

Aqueous and organic streams were pumped into the contactor by calibrated metering pumps. For the runs in which concentrated nitric acid was added to the aqueous feed stream, a third pump was used that was connected to the aqueous feed line through a tee. Flow rates were measured each time pumping rate was changed by diverting the inlet streams into graduated cylinders and were controlled to within 1 to 2% of desired rates. Residence times in the mixing annulus were varied by varying the total throughput. Effluent samples were taken by diverting the effluent streams into graduated centrifuge tubes. The samples were centrifuged in a standard laboratory centrifuge and were checked for entrainment of one phase in the other. To obtain data on contact times longer than ~ 10 s, the collected phases were equilibrated for five minutes by vigorous shaking. All experiments were performed at ambient temperature.

b. Results

Zirconium. The results for the zirconium forward-extraction were reported in ANL-78-11. It was found that the distribution coefficients for forward extraction were essentially constant within the initial 7 s of contact time and the transfer represented about 60% of the zirconium equilibrium distribution coefficient value. The zirconium distribution coefficients (D_{Zr}) for freshly prepared solution of zirconium nitrate and for solution aged 10 days were not found to differ significantly.

Results of scrubbing (back-extraction) tests with zirconium show that approximately 70% of the zirconium was scrubbed from 30% TBP/nDD into $3M$ HNO_3 solution in 3-7 s, in comparison to that scrubbed out in $1/2$ h contact time (Table 3).

Ruthenium. The analytical results for similar tests with tetravalent ruthenium nitrates (this form is also present in a fuel dissolver solution) and ruthenium nitrosyl nitrate/nitro compounds are presented as distribution coefficients in Tables 4-7. The values of the distribution coefficients for both $Ru(IV)$ and $RuNO^{3+}$ nitrates are in very good agreement with literature data [BROWN-1957]. The efficiency of extraction of the ruthenium complexes is about 70% in 3-7 s contact time. The efficiency of scrubbing ruthenium nitrosyl species (Table 7) is about 60% and is lower than that for $Ru(IV)$ (Table 5).

Table 3. Distribution Coefficients of Zirconium Nitrate Back-Extracted from 30% TBP/n-dodecane into 3M Nitric Acid at Ambient Temperature. Rotor speed: 9000 rpm. O/A = 1

Series	Approx. Contact Time	Concentration, mg/mL		D_{Zr}
		Organic	Aqueous	
a	1.5 s	0.026 7	0.056 0	0.48
a	4.0 s	0.026 6	0.067 3	0.40
a	7.0 s	0.026 8	0.067 2	0.40
a	3 min	0.022 5	0.063 0	0.36
b	10 min	0.044 0	0.123	0.36
b	30 min	0.041 5	0.125	0.33

^aInitial concentration of zirconium in the organic solvent was 0.09 mg/mL.

^bInitial concentration of zirconium in the organic solvent was 0.16 mg/mL.

Table 4. Distribution Coefficients of Ru(IV) Extracted by 30% TBP-nDD from ~0.01M Ru(IV) Nitrate Solution in ~3M HNO₃ at Ambient Temperature. Rotor speed: 9000 rpm. O/A = 1

Approx. Contact Time	Concentration, mg/mL		$D_{Ru(IV)}^a$
	Organic	Aqueous	
1.5 s	0.009 6	1.307	0.007
4.0 s	0.008 9	1.331	0.006
5 min	0.015 5	1.010	0.015
1 h	0.016 9	1.000	0.017

^aThe initial concentration of Ru(IV) was ~1.39 mg/mL. Final concentrations of nitric acid were: 0.5M in the organic phase and 2.5M in the aqueous.

Table 5. Distribution Coefficients of Ru(IV) Back-Extracted from 30% TBP-nDD into 3M HNO₃ at Ambient Temperature.^a
Rotor speed: 9000 rpm. O/A = 1

Test	Approx. Contact Time	Concentration, mg/mL		D _{Ru(IV)}
		Organic	Aqueous	
1	1.5 s	0.031 5	0.056 8	0.55
	4.0 s	0.036 7	0.062 1	0.59
2	5 min	0.052 9	0.117 8	0.45

^aThe initial concentrations of Ru(IV) were 0.085 mg/mL in Test 1 and 0.105 mg/mL in Test 2.

Table 6. Distribution Coefficients of Ruthenium Nitrosyl Nitrate/Nitro Compounds Extracted by 30% TBP/nDD from ~0.01M Ruthenium Nitrosyl Solution in 3M HNO₃ at Ambient Temperature. Rotor speed: 9000 rpm. O/A = 1

Test	Approx. Contact Time	Concentration, mg/mL		D _{RuNO³⁺} ^a
		Organic	Aqueous	
1	1.5 s	0.124	1.406	0.09
	4.0 s	0.116	1.421	0.08
	7.0 s	0.153	1.389	0.11
	1 min	0.175	1.315	0.13
2	5 min	0.140	1.220	0.12

^aFinal concentrations of nitric acid were 0.5M in the organic phase and 2.5M in the aqueous phase.

The tests on ruthenium extraction from a 1M nitric solution which was spiked with concentrated (7M) nitric acid (final concentration of 3M HNO₃) just prior to being contacted with the organic solvent are encouraging. The runs of 2 and 4 s gave a distribution coefficient, D_{Ru}, of ~0.011, which is smaller by about a factor of 10 than a D_{Ru} obtained with a 3M HNO₃ aqueous phase. This effect will be tested further.

c. Discussion

The studies of ruthenium and zirconium extraction in the single-stage centrifugal contactor indicate a comparatively small kinetic effect; the amounts of these two elements extracted into the organic phase are reduced only by about 30% compared with pulse columns. Nevertheless, if this reduction

Table 7. Distribution Coefficients of Ruthenium Nitrosyl Nitrate/Nitro Compounds Back-Extracted from 30% TBP-nDD into 3M HNO₃ at Ambient Temperature.^a Rotor speed: 9000 rpm. O/A = 1 for first four periods.

Approx. Contact Time	Concentration, mg/mL		$D_{\text{RuNO}^{3+}}$
	Organic	Aqueous	
1.5 s	0.193	0.283	0.68
4.0 s	0.229	0.295	0.77
7.0 s	0.225	0.319	0.80
1 min	0.151	0.360	0.42
5 min ^b	0.214	0.609	0.35

^aThe initial RuNO³⁺ concentration was 0.511 mg/mL.

^bVolume ratio, org/aq = 2:1.

is repeated in every extraction stage, it would lead to a significant improvement in decontamination. Single-stage extraction experiments allow observation of only the effects due to the major ruthenium species, and these probably do not determine final decontamination from ruthenium. For study of the minor species, multistage studies are required and will be conducted.

The behavior of ruthenium and zirconium in the scrubbing section also should be established. The kinetic effect causes the scrubbing efficiency to be lower in short contact times. However, it is not known what the overall efficiency in the scrub section of a multistage system will be. The latter will be measured in tests conducted in the eight-stage miniature contactor. Even if the overall scrubbing efficiency is lower than it is in pulse columns, a decrease in the amount of fission products extracted into the organic phase may offset this effect.

d. Future Work

Studies of the extraction kinetics of uranium, ruthenium, and zirconium in the eight-stage miniature centrifugal contactor are planned in order to determine the number of stages required for the extraction of uranium and the extent of transfer of ruthenium and zirconium into the organic solvent in these stages. The number of stages in the scrub section necessary for removal of the fission products from the organic solvent will also be established. Initially, four extraction and four scrubbing stages will be tested. These will provide base-line data in developing flow sheets for performing the Purex process in centrifugal contactors.

B. Developments for Reprocessing of FBR Fuel

1. Introduction

Work is continuing on the program to develop improved solvent extraction techniques for Purex reprocessing of fast breeder reactor (FBR) fuels. This work is being carried out in cooperation with Oak Ridge National Laboratory (ORNL). The main objectives of the ANL program are: (1) design, construction, and testing of an annular centrifugal contactor of 0.5 Mg/d capacity, (2) adaptation of a Purex flow sheet for use in short-residence centrifugal contactors, and (3) a study of solvent cleanup techniques in fast contactors aimed at improving the cleanup process and reducing the impact of solvent cleanup upon waste handling.

2. Development of 0.5 Mg/d Centrifugal Contactor (R. A. Leonard, A. A. Ziegler, and G. J. Bernstein)

An annular centrifugal contactor sized to process about 0.5 Mg/d of FBR fuel has been designed and built. This unit has a rotor 9 cm in diameter and about 27-cm long, which makes it critically safe for all possible concentrations of plutonium solutions in the Purex process. The rotor is coupled directly to a 0.75-kW (1-hp) commercial precision motorized spindle which rotates at about 1750 rpm. The rotor design incorporates an air-controlled weir, with the air being supplied through a rotary air seal mounted on top of the hollow shaft of the motorized spindle. A description of the contactor appeared in ANL-78-11.

Fabrication of the contactor was completed during this report period, and the contactor has been installed in the test facility. Mechanical and hydraulic tests will begin in January 1978.

3. Solvent Cleanup (B. B. Saunders)

a. Introduction

There is widespread disagreement in the literature over the extent of solvent damage that occurs in the Purex or Thorex processes and over the specific compounds in the tri-n-butyl phosphate (TBP)-diluent systems that are responsible for the extraction of zirconium and the retention of zirconium, plutonium, and thorium. However, there is general agreement that the major product of the degradation of the TBP by both radiolysis and hydrolysis is di-n-butyl phosphoric acid (HDBP).

In relation to extraction processes, the kinetics of complex formation of HDBP with heavy metals is one of the most important areas to study. As equipment design permits shorter contact times and faster extractions, the kinetics of extraction, not the stabilities of the complexes at equilibrium, become the dominant principles governing extraction.

The behavior of complexes after the extraction step is also important to an understanding of solvent degradation and purification. If the complexes initially formed slowly transform into more stable compounds or polymers, it will be more effective to use purification techniques designed

to treat the solvent within a very short time of the initial extraction so that milder chemicals and conditions can be used. On the other hand, the "aging" of the solvent may occur quickly, *i.e.*, the complexes initially formed may react quickly to form polymers and more stable compounds; in this case, more reactive chemicals and more elaborate techniques will be required to remove these compounds from the solvent. Even though the emphasis of this study is on the behavior of HDBP, other degradation products (present in much smaller concentrations) which form complexes with uranium, zirconium, plutonium, protactinium, and thorium may exhibit similar behavior.

b. Formation of HDBP

The formation of HDBP by hydrolysis and radiolysis has been studied by many workers [HEALY]. Radiolysis studies and G values for various systems have been reported--neat TBP, water-saturated TBP, water- and nitric acid-saturated TBP, TBP in diluents, TBP dissolved in water, etc. The G values in all of these systems are generally close to 1. Instead of attempting to resolve the individual contributions of radiolysis and hydrolysis [BRODDA], it is recommended that it would be more practical and realistic to determine experimentally the amount of HDBP formed when TBP/diluent/nitric acid systems are intimately mixed for known periods of mixing while being subjected to specific radiation dose rates and temperatures.

Degradation of TBP is also influenced by the presence of heavy metals, although this effect has not been adequately studied. Burger [BURGER] reported that the presence of UO_2^{2+} decreased the amount of solvent damage. Other workers [BRESCHET, MOFFAT] found that the presence of zirconium complexes of HDBP increased the TBP degradation. Experiments are needed that would be designed to measure and compare the effects of the different heavy metals, uranium, thorium, plutonium, and zirconium, upon the rate of formation of HDBP, the extent of degradation of TBP, and the amount of heavy metals retained.

c. Extraction of Heavy Metals by HDBP

A major complication in this study related to removal of the dibutyl phosphate complexes of uranium, plutonium, thorium, and zirconium is the variation of complexes and mixtures of complexes and the formation of different polymers, depending upon the conditions of extraction. Dibutyl phosphate complexes are known to be stable but very little quantitative information on their stability is available. If stability constants were known, it would be easier to estimate the relative efficiencies of various complexing agents in removing uranium, plutonium, thorium, protactinium, and zirconium butyl phosphate complexes from TBP/n-dodecane(nDD) solvent.

There are conflicting reports concerning even the relative stabilities of uranium, plutonium, and zirconium complexes. Tsujino [TSUJINO] has attributed the following sequence of stabilities of HDBP complexes to Hahn [HAHN]: $\text{Zr(IV)} > \text{Pu(IV)} > \text{UO}_2^{2+} > \text{RuNO}^{3+} > \text{Nb(V)}$. However, there is no mention of this sequence in Hahn's paper. On the other hand, in 1958, Brown gave the following order for formation constants of HDBP complexes: $\text{Pu(IV)} > \text{Zr(IV)} > \text{Nb(V)} > \text{UO}_2^{2+}$ [BROWN-1958]. Maya [MAYA] reports that the stability of the uranyl complex must be less than that of the zirconium complex because zirconium is extracted, even under conditions where the zirconium concentration is 10^{-5} that of UO_2^{2+} in nitric acid. However, the presence of

UO_2^{2+} in nitric acid decreases the amount of Zr(IV) extracted. This may reflect a difference in the kinetics of extraction of UO_2^{2+} and Zr(IV) rather than the uranyl complex being stronger.

Solovkin and coworkers have identified and studied the polymers and complexes of HDBP with zirconium, uranium, thorium, and plutonium nitrates and have done some work on the rate of extraction by HDBP. They report that Pu(IV) is extracted from nitric acid by HDBP in Syntin* in less than 10 s to form $\text{Pu}(\text{NO}_3)_2(\text{DBP})_2$ [SOKHINA]. However, when TBP is also present, the reaction times are much longer (~ 2 h). The reactions of Th(IV) nitrate with HDBP in nDD produce $\text{Th}(\text{DBP})_4$ which forms "slowly" [SOLOVKIN-1971], but the time was not specified. The rate of extraction of Zr(IV) into HDBP/TBP solutions has not been thoroughly investigated, although experiments performed at ANL and reported in ANL-78-11 demonstrated that Zr(IV) extraction into 30% TBP/nDD/ $10^{-3}M$ HDBP takes at least several minutes. Twice as much Zr(IV) had been extracted into the organic layer after 5 min of stirring than after 1 min of stirring.

d. The Retention of Heavy Metals by HDBP

The uranium, plutonium, and zirconium complexes of HDBP are more soluble in the TBP/nDD organic solution than in aqueous solutions and are thus responsible for the retention of those heavy metals in the organic phase. Solovkin *et al.* have isolated some of the dibutyl phosphate complexes of uranium, zirconium, thorium, and plutonium [TETERIN-1971A, TETERIN-1971B, SOLOVKIN-1969, SOLOVKIN-1971, and SOKHINA]. In general, these complexes are precipitated from HDBP solutions and are polymeric. The HDBP or DBP often acts as a bridging anion between two metal ions, and as many as 10 or 14 structural units have been reported.

The complexes isolated may not be the same as those formed during the initial extraction of uranium, thorium, plutonium, and zirconium. Several workers have noted that zirconium retention in TBP solutions increases with the age of the solution, *i.e.*, as the solution ages, it becomes more difficult to "wash out" or strip zirconium from solutions of HDBP in TBP. If an organic solvent containing butyl lauryl phosphoric acid (HBLPA) is loaded with Zr(IV) and is immediately stripped with aqueous solutions of HNO_3 or distilled water, the zirconium can be removed [MAYA]. If an organic Zr-containing solution is allowed to age, zirconium retention increases. It seems likely (especially for zirconium and probably for plutonium) that once the metal is extracted into the organic solution, the HDBP (and perhaps even TBP) more slowly form polymers with the metals which are more difficult to remove from the organic solvents. If an aqueous solution of a complexing agent (that forms a water-soluble complex with the metal) is used in the washing step, reaction times longer than those obtained in short-residence-time contactors may be needed for "aged" organic solutions. This would be especially important to consider in the case of a process shutdown.

* Syntin is an alkane mixture used as a diluent.

e. Conclusions and Proposed Experiments

Even in a simple system consisting of HDBP and one type of metal ion, the nature and behavior of the complexes formed are not well known. Polymeric complexes are formed, but the rates of formation and the identities of the different complexes present under process conditions are not known. The changes in radiolysis and hydrolysis yields of HDBP caused by the presence of individual ions in $\text{HNO}_3/\text{TBP}/\text{nDD}$ systems are not known; consequently, the change caused by the presence of several ions during processing cannot be predicted in HDBP/nDD and TBP/nDD solutions. The behavior of individual ions and of mixtures of ions typical of those from dissolved fuel will be investigated.

The behavior of HDBP is important in solvent degradation and solvent cleanup because this is the degradation product in largest concentration. Our experimental efforts are designed to investigate the following:

1. The kinetics of the extraction of uranium, thorium, plutonium, zirconium, and protactinium by HDBP/TBP/nDD systems, especially where there are mixtures of the ions;
2. The kinetics of polymerization of HDBP complexes of uranium, thorium, plutonium, zirconium, and protactinium, *i.e.*, the kinetics of aging of used solvent;
3. The use of complexing agents or other methods to remove the compounds responsible for heavy metal retention in TBP/nDD.

One major consideration in the design of our experiments will be to make certain that conditions are such that direct comparisons (1) between the experiments and (2) between laboratory experiments and process conditions will be possible.

C. Aqueous Reprocessing Alternatives to the Thorex Process (Herbert Diamond,* E. P. Horwitz,* G. W. Mason,* C. S. Sabau,* and G. F. Vandergrift*)

1. Introduction

Investigation of aqueous reprocessing alternatives to the Thorex process is in progress. The objective of the process is to recover the thorium, uranium, and plutonium present after irradiation of mixed Th-U oxide fuel. Uranium-238 is present in the original mixed fuel in order to "denature" the ^{233}U . Protactinium will decay 1000-fold during cooling and will not be an important source of ^{233}U . The plutonium, which is produced from the ^{238}U in the fuel, must be recovered along with sufficient fission-product contamination to require processing within a heavily shielded facility.

The extractants for plutonium, uranium, and thorium to be investigated initially are: tricaprylmethylammonium nitrate (TCMA-NO_3) [KOCH], bis (2,6-dimethyl-4-heptyl) phosphoric acid [HD(DIBM)P] [PEPPARD], di-n-amyl n-amylphosphonate (DAAP), and di-n-hexyl n-hexylphosphonate (DHHP) [SIDDAL]. Each extractant has advantages and disadvantages. A summary is given below.

* Chemistry Division, Argonne National Laboratory.

2. TCMA·NO₃

The extractant, TCMA·NO₃, will be tested in diethyl benzene diluent in the range, 0.4 to 0.6M (~30 vol %). The extraction of Th(IV) is high from 1 to 10M HNO₃ whereas the K_d of U(VI) is just adequate in the range of 4 to 8M HNO₃. The separation of Th(IV) and U(VI) from fission products is excellent and the Th(IV)/U(VI) alpha is very large. Third phase formations on loading Th(IV), as well as extraction cleanup from radiolytic degradation products, are possible problems.

3. DAAP and DHHP

The extractants, DAAP and DHHP, will be tested in n-dodecane diluent in the 1M concentration range (~30 vol %). Extraction of Th(IV) and U(VI) is high in the 0.8 to 10M HNO₃ range. However, the U(VI)/Th(IV) separation factor is relatively small (~3). Attempts will be made to improve this alpha by selective back-extraction of Th(IV) with carboxylic acids. Decontamination from fission products should be good, and the extraction of Zr(IV) could be regulated by the HNO₃ concentration. The solubility properties of these extractants are favorable.

4. HD(DIBM)P

This extractant will be tested in both aliphatic and aromatic diluents. The K_d for U(VI) is high in 2M HNO₃; however, Th(IV) extraction is somewhat low at this HNO₃ concentration. Lower acidities will probably be required to extract Th(IV). The separation factor for U(VI)/Th(IV) is excellent, and separation of these two elements can probably be achieved with HNO₃. Separation of thorium and uranium from fission products is not completely known. Fission product zirconium will extract with the uranium and plutonium, but this could be an advantage. Decontamination from most fission products should be good. The solubility of macroconcentrations of thorium in HD(DIBM)P is unknown.

II. ENVIRONMENTAL EFFECTS

(W. B. Seefeldt and W. J. Mechem)

A. Introduction

An objective of this work is to provide a compilation of information to aid in the prediction of accident consequences in LWR fuel reprocessing facilities. The scope encompasses (1) definition of source terms from hypothetical accidents in reprocessing plants in terms of physical and chemical properties of materials released to the first stage of air cleaning, (2) determination of modifications of the properties of airborne materials undergoing transport to the first stage of an air cleaning system, (3) quantitative estimation of the penetration of radionuclides through various stages of air cleaning, and (4) definition of corresponding properties of the products of accidents as they are released to the environment at the stack or a similar boundary of the plant.

Work continued during the period on obtaining information considered germane to the determination of the characteristics of material becoming airborne as a result of an explosive event. Desired information includes airborne mass concentration, particle size distribution, and chemical form. Since no experimental work directed toward such objectives for fuel reprocessing plants has been performed, work in other fields was examined to develop information that may be useful. Because operations in a processing plant are concerned mostly with liquids, the dispersion of liquids is of principal concern in this study, although solids are not ignored. Most information in the literature pertains to solids, however.

In the preceding report, a review of literature concerning nuclear-related testing, blasting and quarrying operations, and coal mining was reported. During this report period, literature concerning the explosive dispersal of metallic uranium and chemical agents* has been studied.

B. Explosive Dispersal of Metallic Uranium

Information from the Sandia Laboratories concerning explosive tests made with metallic uranium [LUNA] has been examined. The purpose of the tests was to provide basic data for evaluating health and safety effects of an accidental detonation of the high-explosive portion of a nuclear weapon.

A test device consisted of a 41-kg hollow cylinder of depleted uranium metal surrounded by shaped explosives (identified as PBS 9404). The method of uranium fabrication was not given. Explosive charge-to-metal mass ratio was the principal parameter of the test series. Actual values of this ratio were not given in the reference; the values are characterized as low, intermediate, and high. Some initial tests were conducted with aluminum, iron, and cerium rather than uranium, but their results were not described. Detonation produced (a) a compact puff of smoke from a combination of explosive combustion products and uranium metal vapors, and (b) brilliantly incandescent streamers radiating in all directions for distances up to 300 m. The streamers were particles of

* In the U.S. Army investigation (reviewed here) to study the dispersion of a chemical agent by explosion of a bomb [ALLAN], resorcinol was used as the stand-in for chemical agents.

uranium heated by self-oxidation. The characteristics of the metallic fragments (size and velocity) were determined from greased plates and electron microscope grids that intercepted the radiating particles at distances one or two meters from the event. The details of actual measurement methods are given in the reference [LUNA].

The debris analyses for tests were presented as (1) histograms (see Fig. 5., for example) for small-particle-size ($<250 \mu\text{m}$) ranges and (2) plots of $\ln (dN/dD)$ vs. $\ln D$ (see Fig. 6, for example) covering all particle size ranges. (D is particle diameter, and N is the number of particles per unit area of the collecting surface.) From this basic presentation, the information given in Table 8 was developed.

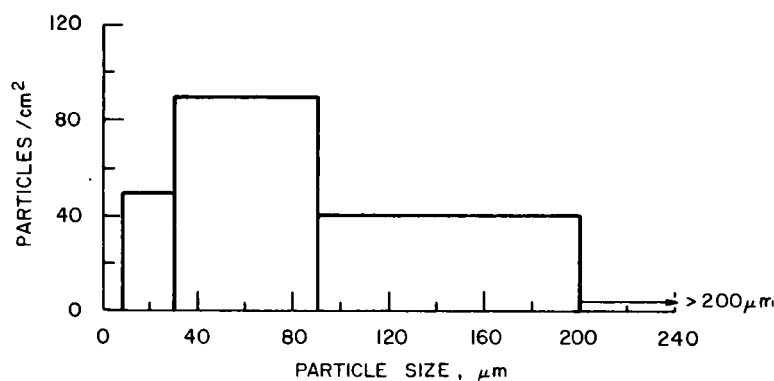


Fig. 5. Histogram of Particle Size Distribution for Shot 6 [LUNA]

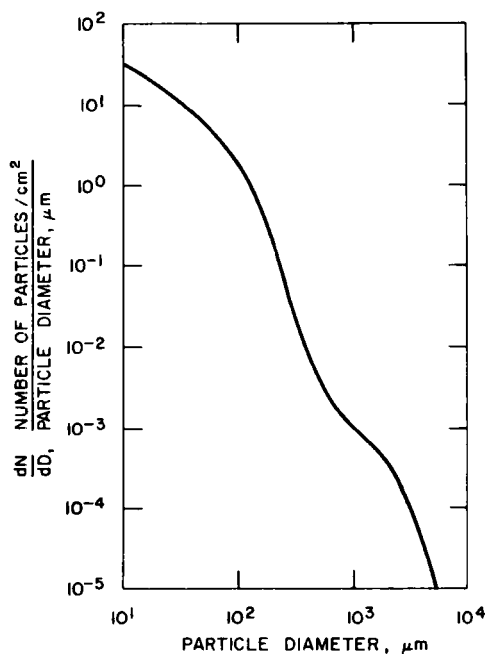


Fig. 6.
Particle Size Distribution
Frequencies for Shot 6 [LUNA]

Table 8. Characteristics of Particles from Explosive Tests that Dispersed Depleted Uranium Metal^a

	Test		
	Shot 6	Shot 7	Shot 8
Explosive to metal ratio ^b	Low	Intermediate	High
Largest particle observed	6250 μm	2500 μm	250 μm
Wt % of particles in small-particle size mode	$\sim 4.1\%$	$\sim 50\%$	$\sim 100\%$
The diameter dividing the small- from the large-particle-size modes	$\sim 600 \mu\text{m}$	480 μm	250 μm
<u>Data calculated from histograms^c</u>			
Mean diameter based on:			
Number of particles	50 μm	N/A	41 μm
Mass	213 μm	N/A	254 μm
Geometric standard deviation	2.0	N/A	2.2
<u>Data calculated from plot of (dN/dD) vs. D of Reference^c</u>			
Mean particle diameter based on:			
Number of particles	41 μm	48 μm	35 μm
Mass	219 μm	159 μm	120 μm
Geometric standard deviation	2.1	1.9	1.9

^aReference: [LUNA].

^bActual values were not reported--probably because of security classification.

^cSee the text; these data are for the small-particle-size mode only.

Some observations are as follows:

1. The particle size distributions can be divided into two modes: a lower mode (small-particle size) that approximates a log normal distribution, and an upper mode (large-particle size) that does not.
2. As the ratio of explosive to uranium increases, the fraction of debris appearing in the lower mode increases. Note, for example, 4.1% for shot 6 (low ratio) as compared with $\sim 100\%$ for shot 8 (high ratio).
3. The particle diameter that divides the two modes appears to decrease with increasing ratio (600 μm for shot 6 and 250 μm for shot 8).

4. The mean particle diameter (based on the number of particles) of the smaller-particle-size mode ranges from 35 to 50 μm , with geometric standard deviations centering around 2. The corresponding mass mean particle diameters range from 120 to 220 μm .

5. The particle size distributions obtained by the two different methods of plotting the data correlated very well for shot 6 (low explosive to metal ratio), but poorly for shot 8 (high ratio).

6. From the data obtained (Table 8) from plots of $\ln (dN/dD)$ vs. $\ln D$, it can be concluded that increasing the explosive ratio results in smaller airborne particles being formed.

7. In the small-particle-size mode, the number of particles smaller than 10 μm is less than 4% for all shots.

8. In the small-particle-size mode, the mass of particles smaller than 10 μm is less than 0.01% for all shots.

Airborne mass concentrations either were not measured or were not reported. If it is assumed that the initial dispersion cloud had a radius of 300 m (this number was mentioned as a maximum dispersal distance), an average mass concentration of $\sim 10^{-2}$ mg/m^3 is calculated. This value would constitute a lower limit.

Data of this kind is expected to be useful in making estimates for our purposes, but difficulties of extrapolating to events in reprocessing plants are posed. This includes the relative magnitudes of the events, differing materials, and differences in confinement (these events were unconfined; events in a plant would have some degree of confinement).

C. Explosive Dispersal of Chemical Agents

The explosive dissemination of chemical agents is an effective technique. For a typical chemical bomblet, only a few percent of the total energy of the explosive is theoretically required for the aerosolization of an agent. However, bomblets would not have a high dissemination efficiency, particularly in the production of fine aerosols of 10 μm or less, unless the weight of explosive used is on the order of one-half of the total bomblet weight.

A rather extensive experimental program has been conducted to study the dispersion of solids [ALLAN]. Though the ultimate application of the study is very different from ours, it is hoped that some information can be extracted from the results that will be useful to us.

The solid material selected for the work was resorcinol ($\text{C}_6\text{H}_6\text{O}_2$), an organic material with moderate thermal stability for which reliable analytical techniques are available. Two initial forms of the material were used, a powder consisting of crystalline filaments ranging in size from 50 to 600 μm , and chips as large as several millimeters. These materials were used either as received, or as modified by ball milling, pelletizing, casting, or additives. The reference test configuration was that of a cylinder 3.8 by 3.8 cm (1.5 in. by 1.5 in.) having a central cavity filled with the explosive. The cavity size allowed the amount of explosive used to be varied, which in turn influenced a

principal parameter, the mass ratio. The latter is defined as the ratio of the weight of inert material (*i.e.*, nonexplosive) to the weight of explosive. We have chosen to use the term, explosive ratio, which is the inverse of the mass ratio.

$$\text{Explosive Ratio (ER)} = \frac{1}{\text{Mass Ratio (MR)}} = \frac{\text{Weight of Explosive}}{\text{Weight of Inert}}$$

The forms of resorcinol for which we are reporting results are loose powder, cast material, and material compacted to pressures of 39,045 kPa (5663 psi). (Additional compacting pressures were included in the original work but are not covered in our analysis.) The explosive was identified as Composition C-4 plastic, fired with an E-83 electrical detonator.

The detonations were carried out in a 170-m³ (6000 f³) chamber 610 cm by 914 cm by 305 cm (20 ft by 30 ft by 10 ft) in which the test device was centrally suspended. The resulting airborne material was sampled for a period of thirty minutes; during this time, two stirring fans were operated for maintaining homogeneity.

The primary data obtained consisted of the percentage of the bomblet's initial resorcinol charge remaining airborne *vs.* time. This information was subsequently converted via a "Dimmick" curve fitting technique to the percentage of initial resorcinol (also called fill) appearing as particles smaller than 10 μm .

We have further manipulated the data based on two assumptions that are not verifiable from the report. The first is that the particle size distributions are distributed lognormally. It is inherent in this assumption that distributions are unimodal, which is consistent with other data we are aware of for systems generated at high explosive ratios. We believe that this assumption is not unreasonable. The second assumption--a more tenuous one--is that the geometric standard deviation of the distribution is two. This assumption is quite reasonable for airborne materials that have aged. We are less sure about its applicability to the initial dispersion at time zero. These two assumptions permit us to estimate the mass mean diameter of the distributions.

1. Results

For inclusion in this report, we have concentrated on three principal effects as they relate to particle size distributions: (1) the degree of compaction of the resorcinol (fill), (2) the presence of confining casing material, and (3) test scale. The explosive ratio is a parameter for all effects. For each effect, a figure is included showing the primary data extracted from the reference, followed by a table showing our translation to mean particle size based on the assumptions given above.

a. Effect of Compaction (Fig. 7 and Table 9)

Uncompacted resorcinol yielded the smallest mean particle diameters for all explosive ratios (ER), ranging from 18.5 μm for an ER of 0.2 to 7.2 μm for the more energetic ER of 1. Of the various compaction pressures used, 39,045 kPa (5700 psi) yielded the largest mean particle diameters, but

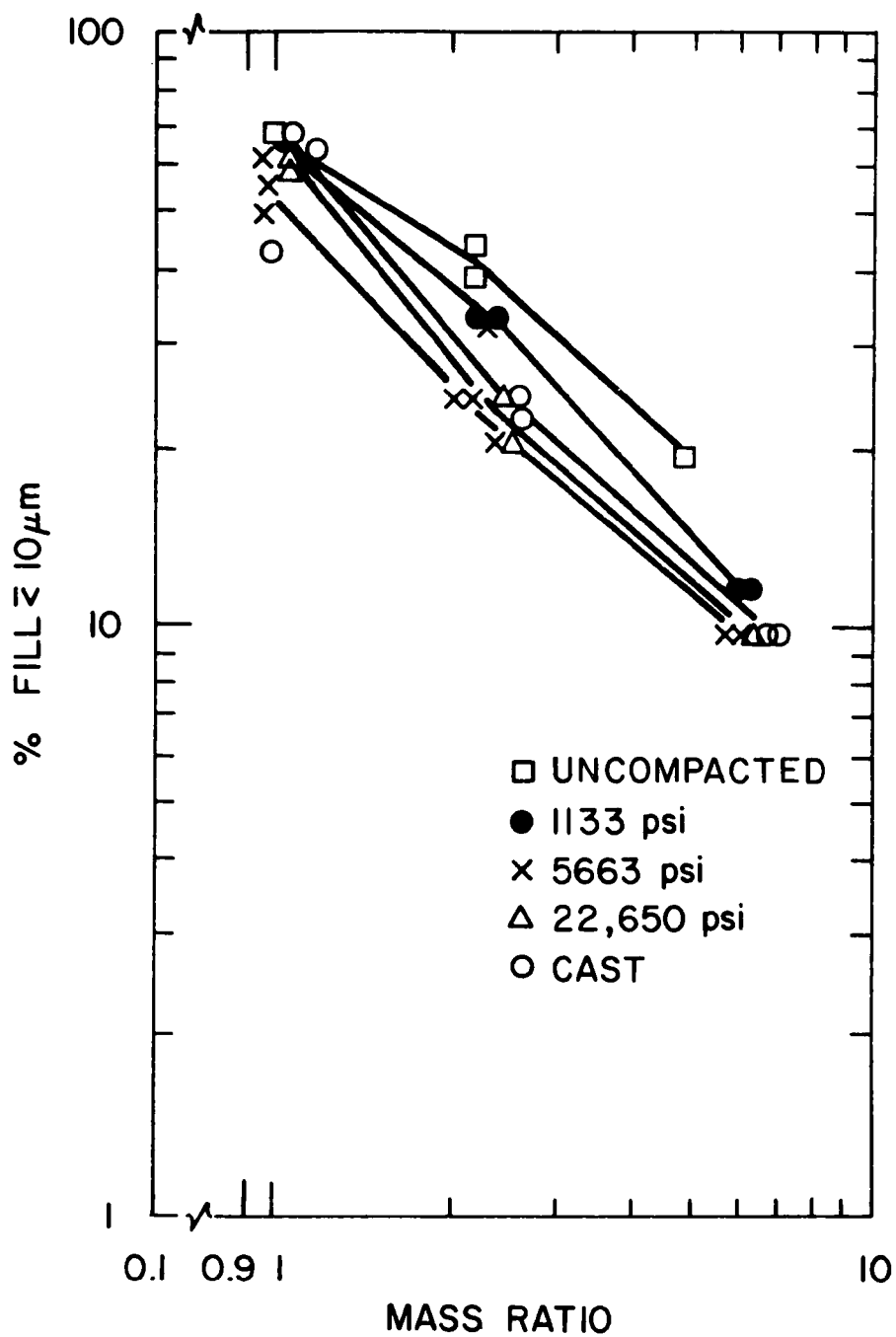


Fig. 7. Effect of Pellet Compaction on Dispersal Effectiveness [ALLAN]

Table 9. Effect of Pellet Compaction on Particle Size Mean.^a
 Pellet size: 3.8 cm by 3.8 cm (1.5 in. by 1.5 in.)
 Casing: thin or none

Density Parameter	Explosive Ratio	Mean Particle Diameter, μm^b
Uncompacted	0.2	18.5
Uncompacted	0.5	11.5
Uncompacted	1.0	7.2
Compacted to 39,045 kPa	0.2	23.5
Compacted to 39,045 kPa	0.5	16.1
Compacted to 39,045 kPa	1.0	10.0
Cast	0.2	22.7
Cast	0.5	14.5
Cast	1.0	8.6

^aComputed from data presented in Fig. 7, based on the following assumptions:

1. Particle size distributions are lognormal.
2. Geometric standard deviation is 2.

^bBased on mass of particles.

the increases cannot be considered to be substantial. Resorcinol in the cast form (the most compact form) might have been expected to yield quite a different result, but the mean particle diameters were comparable to those of resorcinol compacted at 5663 psi.

The differences attributable to explosive ratios are significant, as expected, being greater than differences attributable to compaction.

b. Effect of a Casing (Fig. 8 and Table 10)

The effect of confinement during an explosive event has been recognized to be an important parameter affecting particle size distributions. These tests [ALLAN] give us some clue as to what the effect may be.

The data shown for no casing (Fig. 8 and Table 10) is comparable to that reported in Table 9 and Fig. 7. Note that the addition of casing decreases the effectiveness of dispersion, resulting in larger mean particle sizes.

These data indicate that an accidental explosion in a fuel reprocessing plant will have the greatest consequences in the absence of confinement. The reason for this is our knowledge that as particles become larger, as is the case when material is unconfined, (1) more of them settle out and do not reach the air-cleaning system of a fuel reprocessing plant and (2) the probability of particles being intercepted by the air-cleaning system increases.

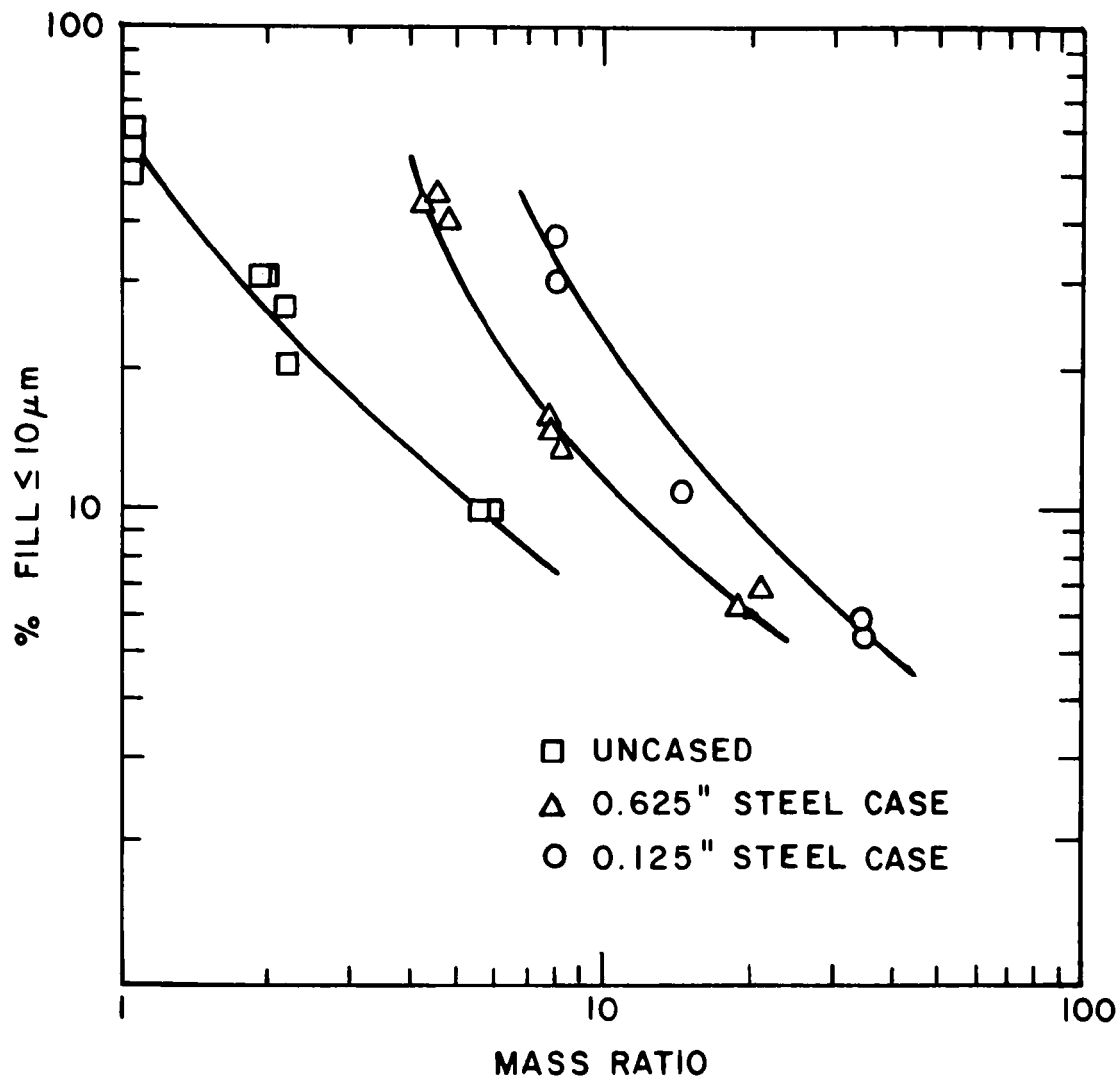


Fig. 8. Effect of Casing on Dispersal Effectiveness
[based on data points from ALLAN]

c. Effect of Scale (Fig. 9 and Table 11)

Tests were conducted with three different pellet sizes: half that of the reference size (1.9 cm by 1.9 cm), the reference size (3.81 cm by 3.81 cm), and double the reference size (7.62 cm by 7.62 cm). In each test series the explosive ratio (ER) was held constant.

Differences of mean particle sizes are significant for low ERs (an ER of 0.2), but essentially disappear for more energetic events (ER = 1.0). As the pellet size increases (for a constant ER), dispersion appears to become less efficient, as evidenced by larger mean particle sizes.

Table 10. Effect of Casing on Particle Size Mean.^a Pellet size: 3.8 cm by 3.8 cm (1.5 in. by 1.5 in.)
Compaction pressure: 39,045 kPa (5663 psi)

Casing	Explosive Ratio	Mean Particle Diameter, μm^b
None	0.2	24.8
None	0.5	15.8
None	1.0	8.7
1.65 mm Steel	0.2	28.8
1.65 mm Steel	0.5	21.0
1.65 mm Steel	1.0	11.1
3.18 mm Steel	0.2	30.2
3.18 mm Steel	0.5	23.5
3.18 mm Steel	1.0	13.5

^aComputed from data presented in Fig. 8 based on the following assumptions:

1. Particle size distributions are lognormal.
2. Geometric standard deviation is 2.

^bBased on mass of particles.

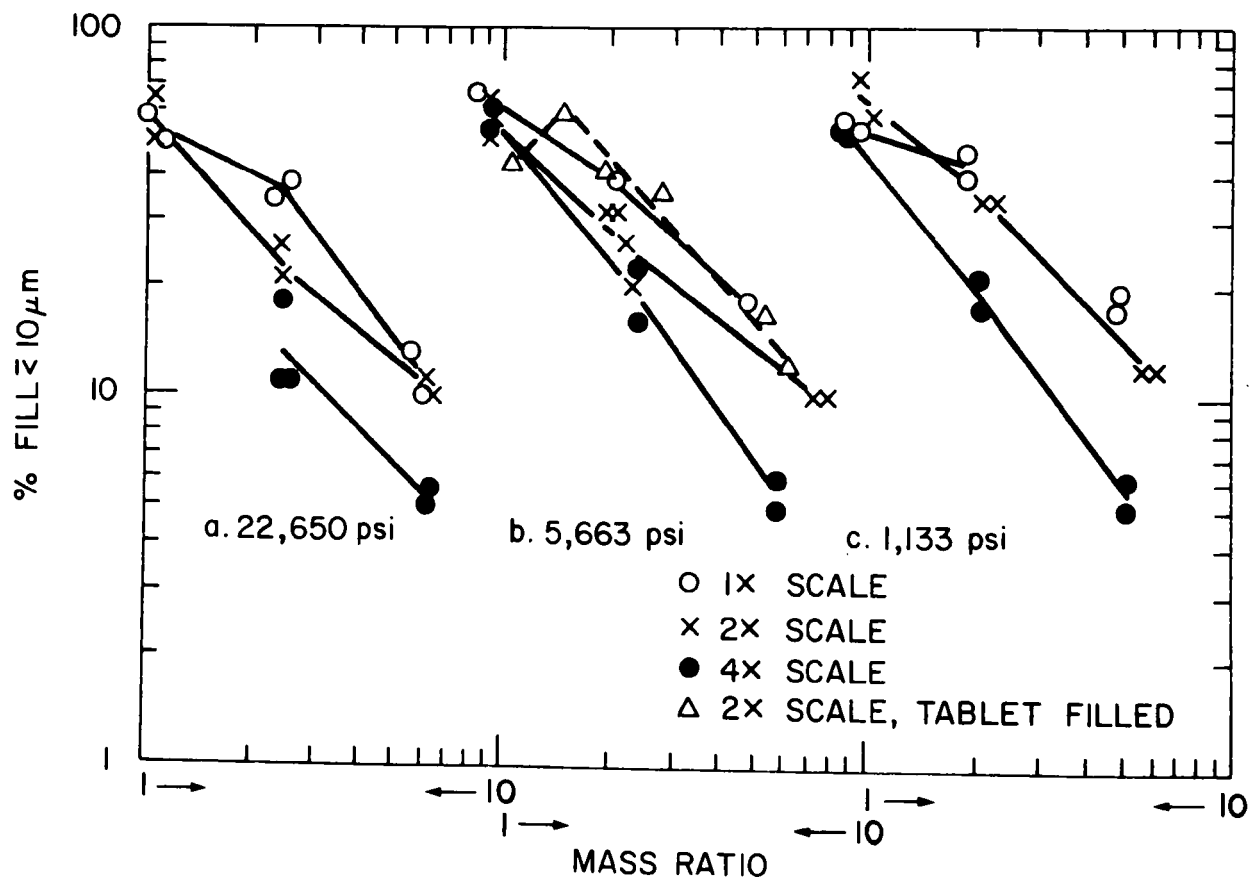


Fig. 9. Effect of Pellet Size on Dispersal Effectiveness [ALLAN]

Table 11. Effect of Pellet Size on Mean Particle Size.^a
 2X: Reference pellet size: 3.8 cm by 3.8 cm
 1X: One-half size: 1.9 cm by 1.9 cm
 4X: Double size: 7.6 cm by 7.6 cm

Scale	Explosive Ratio	Mean Particle Diameter, μm^b
1X	0.2	19.4
2X	0.2	21.6
4X	0.2	28.7
1X	0.5	12.1
2X	0.5	15.1
4X	0.5	16.8
1X	1.0	9
2X	1.0	9
4X	1.0	9

^aComputed from data presented in Fig. 9 based on the following assumptions:

1. Particle size distributions are lognormal.
2. Geometric standard deviation is 2.

^bBased on mass of particles.

d. Additional Comments

The series of tests described in this reference [ALLAN] are quite energetic, as is seen from the explosive ratios used. For comparing these results with the results of other tests in which solids were dispersed, we are in need of a normalizing standard (such as energy) to compensate for the fact that the explosive ratio *per se* is insufficient to describe a system. We are further hampered since for some systems reported, *e.g.*, explosive dissemination of metallic uranium, described above, these ratios are identified as simply low, high, or intermediate.

D. Study of the Effects of Diluents on the Dispersal of Chemical Agents

The U.S. Army performed work directed towards improving the dispersion of resorcinol (as a simulant for chemical agents) by the use of various diluent materials, as described by Goldenson [GOLDENSON]. The work is old, dating back to 1951. Miniature bombs using tetryl pellets as the explosive (high explosive, HE) were detonated in chambers having volumes of 5.966 and 159 m³. Figure 10 shows the two sizes of miniature bombs used. The outer volume was filled with measured quantities of the material (filler material) to be dispersed; the central cavity was filled with the burster (the explosive) and the detonator. The device was suspended centrally in a chamber. The cloud of airborne material generated upon explosion was sampled at intervals of up to four hours by drawing measured volumes of the dust through filter paper. The samples on filter paper were then analyzed for resorcinol. From this raw data, the percentage of fill material airborne as a function of time was determined.

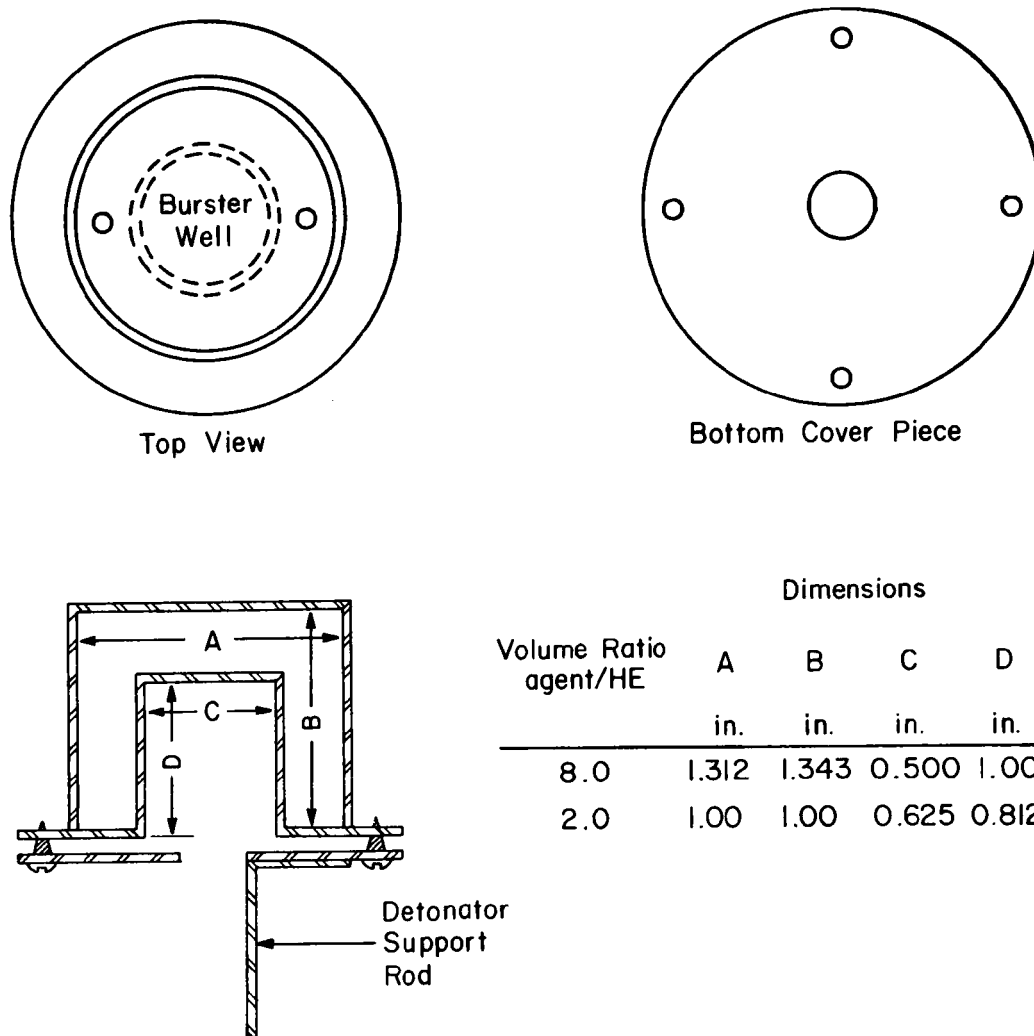


Fig. 10. Diagram of Miniature Bomb (two sizes) [GOLDENSON]

The particle size distribution of the airborne cloud was calculated by the investigators by application of a combination of Oden's method of tangential intercepts and Stokes law. From the manner in which the data is reported, it appears that the authors concluded that the distributions were lognormal, but insufficient data is shown in the reference [GOLDENSON] to allow this conclusion to be independently verified. The text describes a variety of procedures for preparing the filler material; included is ball milling followed by compaction at pressures ranging from 0-3450 kPa (0 to 500 psi). In several tests, a paste was prepared by adding either CCl_4 or $\text{CHCl}_2\text{-CHCl}_2$ to the filler.

Table 12 shows the results that are significant for our area of interest. The data were assembled from several tables of the original report [GOLDENSON]. Particle size distributions in the original report were each recomputed to show the mean diameter (expressed as μm) and the geometric standard deviation. From the descriptions appearing in the text, we have concluded that the material appearing in dust form had been ball milled and compacted at a pressure of about 350 kPa (50 psi).

Table 12. Particle Size Distributions Resulting from Explosive Dissemination of Resorcinol

Test No.	Volume Chamber, L	Carrier Diluent	ER ^c	Form of Filler	Lognormal Distribution Parameters ^a	
					Mean Particle Diameter, μm	σ_g^b
1	5 966	Silica	1.54	Dust	32	5.8
2	5 966	Aerogel	2.70	Dust	44	9.5
3	5 966	Aerogel	1.28	Dust	15	46
4	5 966	Aerogel	1.69	Dust	11	11
5	5 966	Aerogel	0.30	Dust	660	~ 90
6	5 966	Aerogel	0.43	Dust	2 600	~ 300
7	5 966	Aerogel	0.40	Dust	680	~ 200
8	5 966	Aerogel	0.38	Dust	680	~ 200
9	5 966	Aerogel	0.26	Dust	2 000	~ 45
10	5 966	Silica gel	0.22	Dust	52	~ 9
11	5 966	Fuller's earth	0.28	Dust	1 350	~ 80
12	5 966	Fuller's earth	1.19	Dust	18	~ 11
13	159 000	Aerogel	0.41	Dust	36	10
14	159 000	Santocel, CX	0.30	Dust	43	4.3
15	159 000	Santocel, CR	0.29	Dust	29	2.4
16	159 000	Santocel, CF	0.37	Dust	80	11
1	5 966	Aerogel	0.13	Paste ^d	18	2.8
2	5 966	Aerogel	0.43	Paste ^d	18	3.4
3	5 966	Aerogel	0.12	Paste ^e	36	3.3
4	5 966	Aerogel	0.42	Paste ^e	18	2.9
5	5 966	Aerogel	0.45	Paste ^e	16	2.8

^aBased on number of particles (not mass).^bGeometric standard deviation.^cExplosive ratio: wt of explosive/wt of filler plus diluent.^dMade by adding CCl_4 .^eMade by adding CHCl_2 - CHCl_2 .

Notable about the results in Table 12 are the extremely high geometric standard deviations (σ_g) obtained in the dust tests in the small chamber at low explosive ratios. In reviews of other work, we found that values of σ_g ranged from about 1.5 to 10. The authors' data indicate that values of σ_g ranged into the hundreds, with values of mean particle diameter as high as 2 600 μm . Similar tests with comparable explosive ratios conducted in the large chamber did not show high geometric standard deviations.

Consistent with information from other reviews, increasing the explosive ratio increased the degree of dispersion as measured by small mean particle diameters (Tests 1 through 4 in the first grouping). An exception was test 2 with the largest explosive ratio, which did not yield the smallest mean.

The five tests in which the filler was originally in the form of paste (last group of tests numbered 1 through 5) yielded much finer dispersions than the other tests even though explosive ratios were very low.

Figure 11 shows graphically the effect of explosive ratio on dispersion efficiency where the latter is defined as the weight of airborne material associated with particles having diameters smaller than 6 μm .

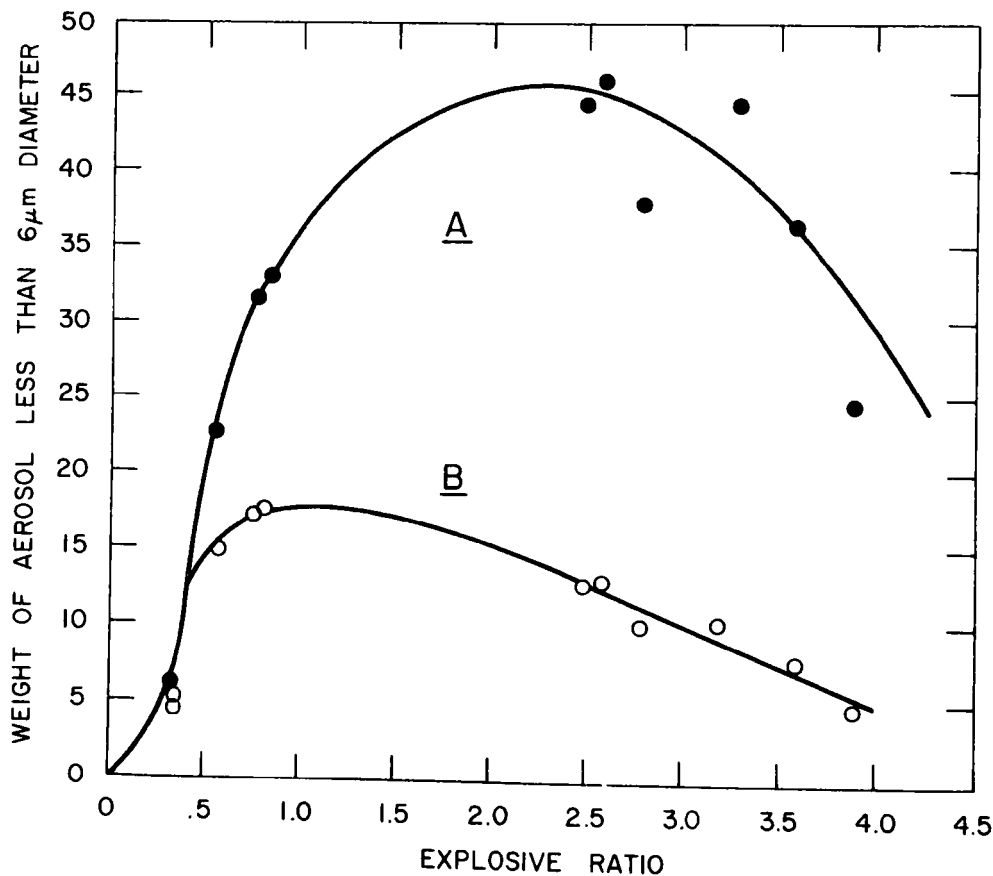


Fig. 11. Bomb Dispersal Efficiency vs. Explosive Ratio [GOLDENSON]. Curve A: Weight of aerosol produced by a bomb having a constant weight of explosive at the indicated explosive ratios. Curve B: Weight of aerosol produced by a constant unit weight bomb at the indicated explosive ratios.

Some of the authors' conclusions [GOLDENSON] regarding these tests are:

- (1) Grinding and sieving of the filler materials is not critical because evaluation of samples with and without diluent shows they have approximately the same properties.
- (2) On the basis of dispersibility, the aerogel type carriers are superior to others tested (Table 12). The optimum mixture contains about 15% carrier.
- (3) For each type of munition, there is an optimum mixture of explosive to filler which produces the maximum amount of aerosol.
- (4) The use of carrier dusts shows promise for the dispersal of agents, but much more work is required to improve dispersal efficiencies.

E. Models of Vaporization in Explosions

The information presented above concerns the degree of fracturing and subsequent dissemination of solids due to explosive forces. The particles are generally rather coarse, and it is expected that further analysis will show that many of the particles, if present in a fuel reprocessing plant, would settle while enroute to an air cleaning system. However, if the heat of an explosion results in considerable vaporization of surrounding materials followed by gas phase condensation, the airborne materials will approach much more closely the particle sizes of aerosols. Such aerosols will have considerable stability and will be carried almost quantitatively to the air cleaning system. Our model of vaporization presented below is intended to give some insight into this subject.

The detonation energy of TNT, as measured in a calorimeter, is about 1.00 kcal/g TNT. Since C_v , specific heat at constant volume, for the gaseous products of TNT is about 0.215 cal/(g)(°C), the initial temperature of the (unexpanded) detonation gas "fireball" is about 4 300°C or 4 500 K. The ideal gas pressure is about 2×10^6 kPa (20 000 atm).

The dynamics of an explosion in open air can be calculated simply on the basis that the radius of the sphere of expanding gas accelerates to the velocity of sound in ambient air (330 m/s). This value would be in error for large explosions in which the velocity of sound increases in the compressed gas of the shockwave, but it is not greatly in error for small explosions of a few kg of TNT. For 1 kg of TNT, the average temperature of the detonation gases drops below 1 000 K in about 5 ms. By general principles and from empirical scaling laws for open-air explosions, the above time interval increases proportionately to the one-third power of the amount of TNT. That is, for 10 kg of TNT, the gas temperature would fall below 1 000 K in $5 \times 10^{1/3} = 10$ ms.

The amount of vaporization that occurs in this short time would depend on several factors:

1. the rate of energy transfer from the hot gases to the solid or liquid material that is a candidate for vaporization,
2. the heat conduction and temperature change within this material, and
3. the vapor pressure of this material as a function of temperature.

1. An Example: A Steel Ball

In order to clarify how these factors operate, consider a steel ball near the center of the expanding fireball. The initial density is about 7.9 g/cm^3 —higher than that of the detonation gas. The melting point of the steel is $1\,530^\circ\text{C}$ and the boiling point is $3\,000^\circ\text{C}$. With its higher density, ρ_{steel} , and volumetric heat capacity, C_{steel} , the steel acts as a local heat sink. For the temperature to rise to $3\,000^\circ\text{C}$ for a given mass of steel, the surrounding high-pressure gas would have to lose an equal amount of thermal energy. Thus, we consider distances from the center of the steel ball, where r_0 is the radius of the steel ball, r is the general radial distance outward into the hot gas, and C is specific heat:

$$\left(\frac{4\pi}{3} r_0^3\right)(\rho_{\text{steel}})(C_{\text{steel}})(3\,000) = \frac{4\pi}{3} (r^3 - r_0^3)(\rho_{\text{gas}})(C_{\text{gas}})(4\,300 - 3\,000) \quad (1)$$

If it is assumed that $C_{\text{steel}} = C_{\text{gas}}$, that $\rho_{\text{steel}}/\rho_{\text{gas}} = \frac{7.9}{1.65} = 4.8$, and that $r_0^3 < r^3$, Eq. 1 simplifies to $r \geq 2.23 r_0$. Actually, the gas sphere would not be evenly reduced in temperature to $3\,000^\circ\text{C}$, and the sphere of reduced temperature would be somewhat larger, say, $r \geq 3 r_0$. Thus, it appears possible to heat a 1-cm steel ball to $3\,000^\circ\text{C}$.

How much time would be required for such heat transfer? The maximum rate of heat transfer in steel is rapid, *i.e.*, at the speed of sound. Also, heat transfer in gas is rapid, since above $3\,000^\circ\text{C}$, radiation transfer is dominant. Thus, a steel ball apparently could be heated to about $3\,000^\circ\text{C}$ in 5 ms. The effect depends on the amount of TNT exploded and the amount of steel.

However, even if the steel were heated to the atmospheric boiling point, it would not enter the vapor state, since it would be under a pressure of several hundred thousand kilopascals. Apparently, the steel would not vaporize but would be a sphere of superheated liquid which would vaporize upon collapse of the detonation pressure. As stated above, this would occur in about 6 ms for 1 kg of TNT, and the time interval would increase proportionately to the $1/3$ power of the amount of TNT for larger "bombs." The amount of vaporization would thus depend on the degree of superheating of the steel as well as the heat of vaporization relative to the heat capacity. It is likely that the gas turbulence would also act to break up the ball of molten steel after collapse of the fireball.

2. The Effect on Volatile Material: Water or Other Volatile Material

Water is heated somewhat like steel is, except that the critical constants of water are 374°C , 21350 kPa (218 atm), and 0.325 g/cm^3 . Thus, water would enter the vapor state directly and would mix with the detonation gases and air.

Hydrocarbons, which are generally thermally decomposed into gaseous products, are readily gasified by a fireball.

3. Limitations on Aerosol Formation from Vaporized Material

Not all vaporized material becomes aerosol. Aerosols are formed by condensation of vapor only under certain conditions in which condensible vapor is mixed with noncondensable vapor and then the whole mass of gas is cooled

so that condensation occurs on airborne nuclei rather than on cold surfaces. Where mixing and bulk cooling are absent, aerosols are not formed; ordinary surface condensation occurs instead. Thus, although vaporization is the only efficient way of making aerosols, vaporization alone is not enough, but the proper fluid flow, mixing, and heat transfer must occur also. Aerosol production is affected by these conditions during the explosion proper, as well as in the post-explosion period in a reference reprocessing plant.

F. Propagation of Shock Waves in Ventilation Ducts

The amount of radioactive material released in an accidental explosion depends on the performance of the air cleaning system and its ability to withstand stresses from the explosion.

Detonations of explosive materials can form supersonic shock waves which propagate in air with potentially damaging effects on the air-confinement system and ventilation components. Protection of structures by blast shields [PORZEL] and attenuation of shock waves in pipes by orifices [DRESNER] has been shown to be practical; the analysis of blast propagation in tunnels indicates little effectiveness of a simple right-angle bend in attenuating a shock wave [VIECELLI].

Further detailed analysis [KOT] also supported this judgment, but experimental confirmation was suggested by Kriebel to validate these conclusions [KRIEBEL]. This experimental verification was obtained for hydrogen explosions propagated in air in 13-cm (5 in.)-dia pipes [PORTER] and for shock tube generation of pressure waves in water and propagated in 4-cm (1.5-in.)-dia pipes [HISHIDA]. In recent modeling of explosion-generated shock waves in air ducts, the lack of measurable attenuation at bends was again confirmed [BUSBY]. The effect of bends is expected to be manifest, not in shock dynamics, but in Bernoullian flow resistance, as modeled, for example, in another recent study [GREGORY]. Apparently, integration of results in this field has not yet been achieved.

III. SEPARATION OF SELECTED ACTINIDES AND FISSION PRODUCTS FROM HLLW (E. P. Horwitz,* G. W. Mason,* R. A. Leonard, W. B. Seefeldt, and M. J. Steindler)

A. Use of Various Organic Extractants in 2-cm-dia Centrifugal Contactor

Scouting studies were made to determine whether organic extractants being proposed for flow sheets for the separation of actinides from fission products can be used in commercial liquid-liquid extraction equipment. The extractants of interest include 0.25M tricaprylmethylammonium nitrate (TCMA·NO₃) in diethylbenzene (DEB), 0.5M dihexoxyethylphosphoric acid (HDHoEP) in DEB, and 0.25M HDHoEP in 2-ethylhexanoic acid (2-EHA). A criterion for selecting appropriate extractants for process equipment is also desirable.

An organic solution was evaluated by testing it for flow performance in a single-stage 2-cm-dia. centrifugal contactor described elsewhere in this report and in an earlier ANL report (ANL-78-11). Flow performance is based on the degree of phase separation in the two existing streams and on the absence of flooding in the annular mixing region. To rate the organic phase, its performance was compared with the behavior of 30 vol % tri-n-butyl phosphate (TBP) in n-dodecane (nDD) with the concentration of HNO₃ in the aqueous phase, the organic and aqueous flow rates, the rotor design, the rotor speed, and the base geometry the same.

For the extractants in DEB solutions, the flow performance was satisfactory, being essentially similar to that of the TBP in nDD. These DEB solutions have low viscosities (similar to those of the nDD solutions). For the extractant in 2-EHA, the flow performance is poorer than that of TBP in nDD. The 2-EHA solution has a viscosity of 7.4 mPa·s (7.4 cP) as compared with 1.73 mPa·s (1.73 cP) for 30 vol % TBP in nDD. Also, the density is higher being 914 kg/m³ (0.914 g/mL) as compared with 814 kg/m³ (0.814 g/mL). Nevertheless, it was still possible to get 98% phase separation in the exiting streams for the extractant in 2-EHA if (1) the disk base was used in place of the radial vane base, (2) lower flow rates (10 to 50% of rated throughput) were used, (3) high rotor speeds were used at low organic-to-aqueous (O/A) flow ratios, and (4) low rotor speeds were used at high O/A ratios.

Based on these results, two design criteria are suggested for evaluating organic solutions and process flow sheets in the 2-cm centrifugal contactors. First, the O/A density ratio should not exceed 0.90 since the 2-cm-dia. unit is designed with this upper limit. The 2-EHA solution with 1.0M HNO₃ had an O/A ratio of 0.89 and so was pushing this limit. Second, the viscosity of the organic solution should not exceed 7.4 mPa·s (7.4 cP) and, preferably, should be 2 mPa·s (2 cP) or less. However, these restrictions on O/A density ratio and organic viscosity would not apply to plant-scale contactors where the use of an air-controlled weir allows for extending the operable range of density ratio and viscosity. If it becomes necessary to test in the mini-contactors a flow sheet involving O/A ratios greater than 0.90, new rotors designed for such service can be built.

* Chemistry Division, Argonne National Laboratory.

IV. PYROCHEMICAL AND DRY PROCESSING METHODS PROGRAM

(C. H. Bean, K. M. Myles, L. J. Jardine, B. B. Saunders, Milton Ader, J. K. Bates, T. F. Cannon, T. J. Gerding, and M. J. Steindler)

A. Introduction

A Pyrochemical and Dry Processing Methods Program (PDPM) was established at the beginning of FY78 within the Fuel-Cycle Section, Chemical Engineering Division, at Argonne National Laboratory (ANL). This program is part of the national fuel cycle program for reprocessing fuel by processes that will reduce the risk of proliferation of nuclear weapons. Argonne has been designated by DOE as the lead laboratory for PDPM, with various reprocessing development investigations being performed at other DOE laboratories and by industrial contractors.

B. Program Management

The management objective for PDPM is to control the development of non-aqueous reprocessing systems in order to achieve established program objectives within scheduled cost and time frames. These objectives are achieved by applying the DOE Uniform Contractor Reporting Guidelines within the framework of administrative procedures and controls established by ANL. A management plan, a milestone plan, and a cost plan provide a baseline for authorizing, measuring, regulating, documenting, and reporting the status of individual tasks, subtasks, and work packages identified in a work breakdown structure (WBS). Probable future tasks are in-plant waste treatment, general support, and major facilities.

Proposals solicited by ANL from DOE laboratories, industry, and others for R&D in support of PDPM were evaluated. Those judged capable of making a contribution to PDPM were re-scoped by ANL. The changes included (1) requirements for a background survey or engineering analysis before process separation work is started and (2) the deferment of large-scale demonstrations for approximately two years. The revised proposals were the baseline effort recommended by ANL for support of PDPM. This, in turn, established the baseline program that was approved by DOE.

The research and development effort of the program is divided into work packages. Individual work packages are (01) Materials Development for PDPM, (02) Carbide Fuel Processing, and (03) Th-U Salt-Transport Processing, Argonne National Laboratory; (04) U-Pu Salt-Transport Processing, and (05) Fabrication of Process-Size Refractory-Metal Vessels, Rockwell International - Rocky Flats; (06) Aluminum-Alloy Processing of Th- and U-Based Fuels, IRT Corp.; (07) Chloride-Volatility Processing of Th-Based Fuels, Babcock and Wilcox, (08) AIROX, CARBOX, and RAHYD Processing Systems, Rockwell International - Atomics International; (09) Molten Nitrate-Salt Oxidation Processes for Ceramic Fuels, Pacific Northwest Laboratory; (10) Molten Salt Processes Applied to Ceramic Fuels, Oak Ridge National Laboratory; (11) Reprocessing of Thoria-Urania Fuel in Molten Salts Containing ThCl_4 , AMES; (12) Molten-Tin Processes for Reactor Fuels, Lawrence Livermore Laboratory. A specified scope of work, objectives, milestones, and budget limitations apply to each work package.

In the first quarter of FY78, most of the program management effort has been spent in obtaining the proper documentation, authorization, and approval for contracted effort on work package Nos. 04 through 11. A preliminary statement of work (SOW) was prepared by ANL for each work package and was transmitted to key contractor personnel. The technical, administrative, and financial conditions were negotiated, and a final SOW was then approved by both ANL and the contractor.

A detailed financial plan was prepared with a cost breakdown by WBS subtask for each work package. The financial plan was the basis for review and approval by ANL accounting and budget personnel. Procurement requisitions were submitted to the ANL Budget Office for approval, but no procurements had been authorized by the Laboratory as of December 31, 1977.

A preliminary program plan that identified program objectives and described the individual work packages under investigation for the PDPM was submitted to DOE on December 15. This will be expanded into a PDPM Management Plan after individual contractors are authorized to start work and submit individual management plans for each work package. The final management plan will describe all program objectives, the management structure, the technical approach, work breakdown structure, management controls, and test plans as appropriate for all work packages. This plan will be updated as needed to reflect changes in technical approach or program guidance. A new management plan will be prepared at the start of each fiscal year.

C. Engineering Analysis

Literature reviews have been initiated to examine techniques for nonaqueous processing of irradiated nuclear reactor fuels. The first studies have focussed on carbide fuel processing and salt transport processing, as well as materials problems related to such processing. Other processes will be examined by other contractors as soon as contracts are signed. From the literature studies, preliminary flow sheets will be developed.

1. Materials Development

(David Stahl,* J. Y. N. Wang,* and J. W. Hafstrom*)

This work package involves the determination of materials problems related to PDPM, including vessels, pumps, and lines, and the solution of those problems by analytical and experimental means. The fuel state will also be examined to identify and resolve hazards.

Much of the available U.S. literature (up to 1969) on nonaqueous reprocessing has been reviewed. A topical report will be prepared summarizing the information found. The number of acceptable materials for transfer tubing and components other than crucibles for the uranium and plutonium separation steps is fairly extensive. No detailed analyses are available of the nature of the corrosive attack on metals and ceramics by the various molten metal-salt systems used in these processes. Containment materials such as tungsten alloys and beryllia (which is not wet by U/Pu), have been satisfactorily used in EBR-II fuel-cycle studies. Although graphite containment material is not attacked by the liquid metal solvents or fused-salt carriers employed, uranium and plutonium are retained in the form of carbides. Iron-based alloys in transfer lines are susceptible to severe attack by molten salts. Areas of

* Materials Science Division, Argonne National Laboratory.

interest that require further materials work are: (a) the development of a coating or lining for inexpensive or readily fabricable crucible materials to replace or reduce the amount of tungsten or beryllia, (b) thorough analyses of the corrosion behavior of containment and tubing materials in molten metal-salt systems, and (c) fabrication and/or joining processes for these materials.

For various PDPM processes, there may be substantially different requirements for containment materials. No one set of materials is expected to meet the needs of all potential processes. The selection of materials requires consideration of possible interactions between the container or transfer tubing and precipitated species, liquid metal solvents, and molten salts, each containing different amounts and types of fuel constituents that may alter the local chemistry. The compatibility of the containment materials with constituents of the vapor phase (often halides) also must be considered. A critical assessment of the materials problems requires input from the various subcontractors within PDPM who are responsible for defining the processes.

2. Carbide Fuel Processing (M. J. Steindler and K. M. Myles)

The objective of this work package is to develop and test flow sheets for the reprocessing of spent carbide fuels in nonaqueous media. Of prime interest are monocarbide fuels for light-water and breeder reactors using U-Pu, Th-U, and Th-U-Pu fuels. Any reprocessing scheme proposed must meet antiproliferation criteria (*i.e.*, production of a concentrated, decontaminated fissile-material stream is to be avoided). The initial conceptual flow sheets will employ separation procedures based on information already in the literature, particularly procedures that exploit chemical properties unique to the carbides. Accordingly, expedient steps such as the combustion of the carbides to oxides will not be considered since oxide fuel reprocessing is being developed and evaluated in other parts of the program.

A major part of the initial investigation is review of the literature dealing with reactions and reprocessing of carbide fuels. This includes the collection and evaluation of all pertinent thermodynamic information--especially that concerning the behavior of actinides, fission products, and cladding materials in metal and salt solvents. In effect, "reprocessing . . . in non-aqueous media" is restricted to pyrochemical processing in liquid metals and salts; other nonaqueous media such as organic solvents are apparently unsuitable because they tend not to react with (dissolve) carbide fuels or they suffer radiolytic decomposition. The use of gaseous reagents to partition actinides from each other or from fission products is being considered in other work packages.

The initial separation concepts will deal with UC, PuC, ThC, and fission product carbides as distinct entities. However, it is recognized that spent fuel contains mainly a solid-solution monocarbide phase and possibly some sesqui-, and dicarbide phases, ternary carbides, intermetallic compounds, metallic halides, etc. Predictions of the chemical state of irradiated (U,Pu)C_{1+x} have been made, using simulated burnup studies [SMAILOS], cladding compatibility studies [HOFMANN-1974], and free-energy and phase-relationship data for fission product elements and fuel [FEE-1975A]. The predictions and conclusions from these studies, summarized by Jardine [JARDINE] are presented in Table 13. There are many possible species, and chemical separations could

Table 13. Probable Chemical and Physical States of Fission Products in Hyperstoichiometric Carbide Fuel, $(U,Pu)C_{1+x}$ [JARDINE]

Chemical Groups	Physical States
3H	?
Xe, Kr	Elemental gas.
I, Br	Elemental vapor; I combined with Cs or Rb.
Cs, Rb	Elemental (cool regions); combined with I (or Br).
La, Ce, Pr, Nd, Pm, Sm, Eu, Gd, Tb, Dy, Ho, Er	Form monocarbides dissolved in fuel matrix; di- and sesquicarbides (immiscible with UC) are more stable than monocarbides, and so they may be present as a separate phase.
Ba, Sr	Form stable dicarbides which may precipitate as a separate phase; it is unknown if monocarbides are soluble and stabilized in fuel matrix.
Y, Zr, Nb	Dissolved as monocarbides (solid solution) in fuel matrix.
Mo, Tc, Ru, Rh	Form separate ternary carbides [$UMoC_2$, $UTcC_2$, U_2RuC_2 , U_2RhC_2 or $U_2(Rh_xRu_{1-x})C_2$]; small amounts may dissolve in $(U,Zr)C_{1+x}$ phase; Mo_2C and Mo_3C_2 possible too; also found are some intermetallic phases $(U,Pu)(Ru,Rh,Pd)_3$; weak evidence that some MoC may dissolve.
Pd	Forms intermetallic UPd_3 (does not form $UPdC$); may dissolve in $U_2(Rh_xRu_{1-x})C_2$; reacts with $(U,Zr)C_{1+x}$ to give $(U,Zr)Pd_3$, $(U,Zr)Pd_4$.
Se, Te	Forms U_2TeC_2 and binary intermetallic USe (no Se ternary); USe_2 $<1000^\circ C$, $1600^\circ C > U_3Se_5 > 1000^\circ C$; $UTe_3 < 700^\circ C$, $UTe_{2-x} < 1000^\circ C$, $U_7Te_{12} < 1200^\circ C$, $U_2TeC_2 > 1200^\circ C$; may also form complex carbides with UC_{1+x} ; Se may form cesium selenide; Se may prevent U_2TeC_2 formation.
Ag, Cd, In, Sn, Sb	?

be adversely affected. For example, if some of the ternary carbide or intermetallic compounds containing uranium or plutonium prove to be extremely stable, their dissolution in metallic solvents might be incomplete. Such questions can be answered only by laboratory investigation.

a. Decladding
(Milton Ader)

The first step in any reprocessing flowsheet is the separation of fuel from cladding (and possibly other fuel-assembly hardware). Currently, preferred cladding materials for carbide pellets are 316 SS, 330 SS, several other Fe-Ni-Cr alloys [FEE-1975B], and Zircaloy.* Three general decladding procedures can be considered: mechanical or physical separation, chemical removal of cladding, and chemical removal of fuel.

Mechanical removal of the cladding by means of a cutting tool would be the method of choice if a successful tool could be developed. However, a small fraction of fuel would be expected to adhere to the cladding after long-term irradiation. The adhering carbide could be recovered by a different process than that used for the bulk of the fuel; *e.g.*, combustion in oxygen would convert the carbide to an oxide powder which could be readily separated from stainless steel cladding and subsequently reconverted to carbide. Adding steps to a flow sheet, however, is usually unattractive.

Decladding by melting stainless steel away from UO_2 pellets at $1450\text{--}1600^\circ\text{C}$ has been shown to be feasible [WINSCH-1974]; however, the high temperature required may lead to fuel-cladding interactions for carbide fuel.

Chemical removal of cladding from carbide fuels may prove to be more difficult than chemical removal from oxide fuels because of the generally lower thermodynamic stability, *i.e.*, the greater reactivity, of carbides. For example, stainless steel and Zircaloy-2 cladding is easily dissolved in liquid zinc at 800°C [WALSH] without affecting UO_2 fuel (and the same absence of reactivity is expected for ThO_2). However, ThC , PuC and some UC may dissolve in zinc along with stainless steel; this would be an undesirable complication. For Zircaloy-clad carbides, hydrochlorination at $350\text{--}400^\circ\text{C}$ volatilizes ZrCl_4 . This may be a satisfactory way of removing cladding while leaving the carbides unaffected. This will have to be tested.

Decladding of stainless steel with chlorine is possible; FeCl_3 would be volatilized and chromium and nickel chlorides would be left behind. However, the higher temperature required for this reaction ($\sim 600^\circ\text{C}$) is likely to cause constituents of the carbide fuel to react and to volatilize, in effect leading to a volatility process.

Dissolution of carbide fuel away from the cladding is a potential separation technique that is comparable to the chop-leach aqueous process for LWR urania fuel. Separation from stainless steel might be achieved by reacting carbides with an oxidant such as ZrCl_4 or ZnCl_2 dissolved in a molten salt medium. Calculations indicate favorable thermodynamics for these reactions. Furthermore, previous work [KATELEY] on the reaction of very inert ThO_2 with ZrCl_4 in LiCl-KCl or KCl-MgCl_2 at $560\text{--}650^\circ\text{C}$ offers promise that similar reactions with actinide carbides will proceed.

* Zircaloys are zirconium-based alloys (~ 98 wt % zirconium) containing small amounts of tin, iron, chromium, and, in some cases, nickel.

b. Carbide Dissolution and Preparation in Metal Solvents
(B. B. Saunders)

Uranium carbides, thorium carbides, and plutonium carbides have been reported to dissolve in certain metals (*e.g.*, ThC dissolves in bismuth, and PuC and UC dissolve in zinc [CHITTY, CRAIG, RICE, ROBINSON]) and have been synthesized from others (*e.g.*, UC has been prepared from Zn-Mg alloys [PETKUS]). A literature review was begun to determine the feasibility of reprocessing spent carbide fuel by selectively "dissolving" or reacting some of the actinides and fission products in a liquid metal while leaving behind the bulk of carbide fuel. The thermodynamics of various metal systems was reviewed; the free energies of formation of the actinide carbides and of several actinide inter-metallics are presented in Fig. 12.* From these data, the following inferences can be made:

- (a) UC will not dissolve in bismuth, cadmium or, for certain temperatures, in zinc.
- (b) ThC will dissolve in bismuth and zinc and should dissolve in cadmium.
- (c) PuC will dissolve in cadmium and zinc and probably in bismuth.
- (d) UC, PuC, and ThC will all dissolve in tin.
- (e) (U,Pu)C fuel can be treated with cadmium, bismuth, or zinc, and the plutonium (and some of the fission products) should dissolve, many of these metals leaving behind the UC.
- (f) A simple metal solvent system that would dissolve UC and possibly PuC but not affect ThC does not appear to be available.
- (g) UC can be prepared from bismuth, cadmium, and zinc. The data indicate that ThC can be prepared from zinc at high temperatures and that PuC cannot be prepared from any of the metal solvents.

With regard to the attempted synthesis of plutonium carbide from liquid metals, attempts to prepare PuC from Zn-Mg alloys yielded the sesquicarbide Pu_2C_3 [WINSCH-1962]. This is not a surprising result since estimates for $\Delta G_f^\circ(\text{PuC}_{1.5})$ are 4 to 10 kcal/g-atom Pu more negative than for PuC [HOLLEY]. Thus, with an excess of carbon, Pu_2C_3 is thermodynamically favored.

* Data in Fig. 12 for UC and $\text{PuC}_{0.9}$ are from [FEE-1975A], for $\text{ThC}_{0.97}$ and $\text{ThC}_{1.94}$ from [RAND], and the remainder from [JOHNSON]. The curve for $\text{Th}_2\text{Zn}_{17}$ is based on ΔG_f° (kcal/mol) = $-106.9 - 263.3 \times 10^{-3}T + 99.0 \times 10^{-3}T \log T$ [CHIOTTI]; the equation in [JOHNSON] contains a typographical error.

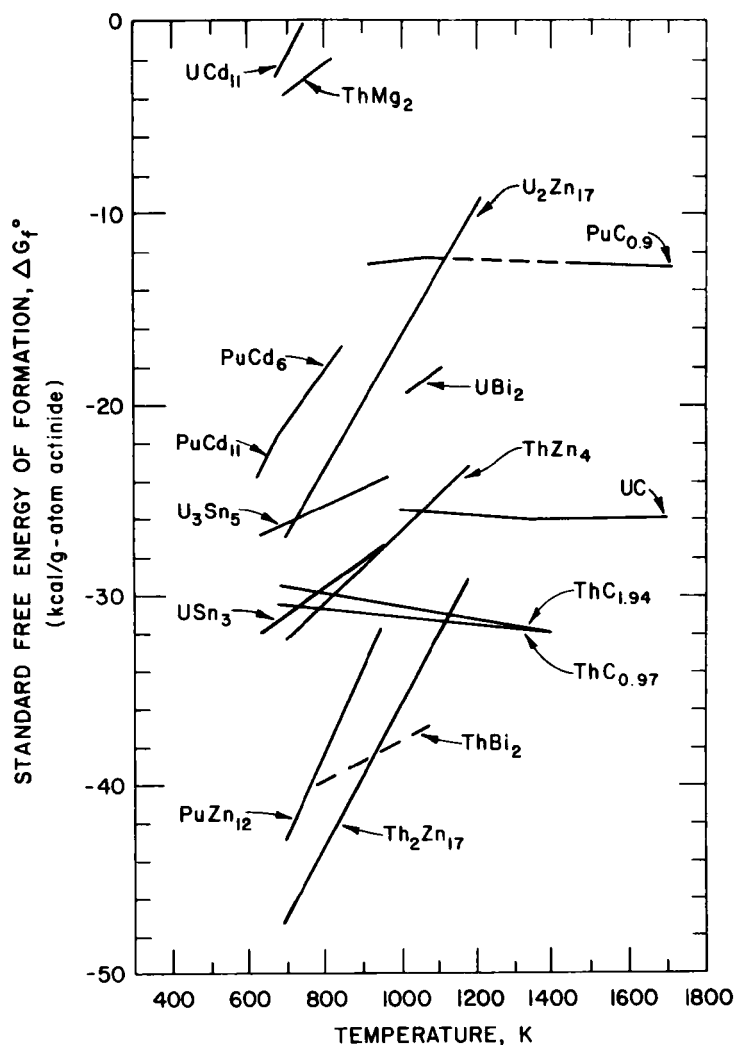


Fig. 12. Thermodynamic Stabilities of Some Actinide Carbides and Intermetallic Compounds [FEE-1975A, RAND, JOHNSON]

It is obvious from the previous discussion of the reactivity of carbides with metals that in pyrochemical processing, carbide fuels may have a distinct advantage over oxide fuels. Metal systems can even dissolve ThC without additional reagents such as are needed to dissolve ThO₂, which is very stable.

No experiments to investigate the rates of carbide dissolution in a metal solvent are reported, but occasionally the minimum times required to reach equilibrium in a particular system [CHITTY, RICE] are noted.

c. Carbide Dissolution and Preparation in Molten Salts
(B. B. Saunders)

Carbide fuels have been reprocessed in fused-salt systems by electrolysis and halogenation reactions that convert fuel to the halides [HANSEN, ROBINSON]. This type of reaction is not unique to the carbides and

can be used for oxide fuels as well. The halides can then be reduced to metals, oxidized to the oxides, or converted directly to the carbides [VOGLER, TOTH]. Selective halogenation of the carbides as a preliminary separation scheme may be possible. Ideally, the bulk of the fission products and a small amount of the actinides would be halogenated and dissolved in the molten salt, leaving the bulk of the carbide fuel unreacted. UC_2 is reported to be the stable species in fluoride salts [TOTH]. If this is the case for other molten salt systems, preparation of the carbides from metals to produce the monocarbide will be preferable. As with the metal systems, much work is needed to determine the conditions and rates for dissolving and preparing carbides in molten salts.

3. Thorium-Uranium Salt Transport Processing (M. J. Steindler, K. M. Myles)

The objective of this work is to examine nonaqueous reprocessing concepts for the selective transfer of spent-fuel constituents (thorium, uranium, protactinium, plutonium, and fission products) between molten alloys and molten salts in order to develop reprocessing flow sheets for spent fuel. Major emphasis will be given to salt-transport-type separations for thorium-based oxide and metal fuels requiring major Th-U separations, and less effort will be directed at uranium-based fuels requiring major U-Pu separations. Separations of U-Pu must also be addressed to some extent for thorium-based spent fuels, which would contain denatured uranium (*i.e.*, ^{238}U would be added to thorium-based fuels to dilute the fissile ^{233}U and satisfy any likely non-proliferation criteria). For shorter-cooled spent fuels, the chemical behavior of protactinium in any flow sheet would have to be determined because of the relatively long half-life (*i.e.*, ~ 27 days) of ^{233}Pa coupled with its decay to fissile ^{233}U . Such information should identify potential situations that could lead to the "milking" of protactinium to yield pure fissile ^{233}U . For oxide and metallic fuels, the chemical behavior of thorium, uranium, protactinium, plutonium, and selected fission products in molten alloys and salts will be studied in order to develop and establish the feasibility of process flow sheets.

a. Conventional Salt Transport (J. K. Bates)

The literature is being examined for flow sheets, concepts, and data that may be applicable to conventional salt transport. Flow sheets for the more promising concepts will be constructed from these reviews, and further analyses will be done utilizing published data and thermodynamic evaluations. Missing data will be identified. The absent data and the flow sheets will serve to guide laboratory-scale experiments aimed at establishing the feasibility of process flow sheets.

The literature reviews reveal a lack of appropriate data for thorium and protactinium in molten alloys and salts. Such data are required to identify potential donor and acceptor alloys for salt-transport-separations flow sheets similar to those previously examined for uranium and plutonium separations at ANL [STEUNENBERG, KNIGHTON]. If further literature searching does not yield the required data, laboratory-scale experiments directed at providing these critical data (primarily solubilities and distribution coefficients) will be initiated.

b. Molten Salt Processing Concepts
(L. J. Jardine and T. J. Gerding)

In addition to investigating salt-transport-type flow sheets, schemes are being examined which utilize variations in the oxygen potential of molten salts to achieve separations of the constituents of spent oxide fuels. For example, [WENZ] reported that in mixtures of UO_2 - PuO_2 in molten salts containing MgCl_2 , PuO_2 was "selectively" reacted to form a soluble oxychloride (PuOCl) while UO_2 remained unreacted. In a complementary series of reactions in molten salts containing MgCl_2 [AVOGADRO], sparging with HCl/O_2 resulted in the formation of a soluble oxychloride (UO_2Cl_2) while the PuO_2 remained essentially insoluble. Recovery of the soluble oxychloride by changing the oxygen potential has been reported [AVOGADRO, GORBUNOV]. Thus, it appears that either PuO_2 or UO_2 may be recovered by controlling the oxygen potential. Some information has been found on the behavior of thorium [LYON]. Possible flow sheets based upon this concept and their likely problem areas (*e.g.*, phase separations, etc.) will be examined further.

D. Separations Processes
(K. M. Myles and M. J. Steindler)

Any need for experimental data will be indicated by the results of the literature survey and the preliminary flow sheets.

V. METAL MATRIX ENCAPSULATION OF HIGH-LEVEL WASTES

(L. J. Jardine, R. E. Barletta, K. F. Flynn,
R. H. Pelto, and T. F. Cannon)

A. Introduction

The major objectives of this task are to identify the advantages and disadvantages of encapsulating solidified radioactive high-level waste (HLW) forms in a metal matrix. The net attributes of metal encapsulation are to be identified by comparisons with waste form properties and fabrication methods for the well-developed solidification alternatives of calcination and glass monoliths. A series of laboratory-scale investigations are in progress specifically aimed at generating data required to further assess probable or unresolved problem areas. Major experimental areas studied during this report period include (1) the corrosion rates of candidate matrix metals in saturated brine solutions at 250°C and ~5 MPa (700 psi) pressure, (2) the chemical interactions between simulated waste forms and proposed matrix metals, and (3) the leach rates at 25-100°C of simulated waste forms encapsulated (dispersed) in a metal matrix in aqueous solutions.

B. Corrosion Rates of Candidate Matrix Metals

1. Preparation of Laboratory-Scale Metal Matrix Castings

Laboratory-scale castings of lead, aluminum, and copper alloys (~3 1/2-cm ID by 10-to 23-cm long), cast in partial vacuum [95 kPa (28 in. Hg)] and inert (Ar) atmospheres, have been investigated. Materials used to simulate solidified waste forms included (1) Al₂O₃ (1-5 mm) beads, (2) borosilicate glass beads (~5 mm), (3) INEL* fluid-bed calcine-10 wt % metakaolin mixtures which had been disc-pelletized (~10 mm) and sintered [BELL], and (4) granular Molecular Sieve (~3-mm × 6-mm cylinders) pellets. Simulated waste forms were preloaded into baskets fabricated of stainless steel with 6-12 mesh openings. The baskets, in turn, were lowered into crucibles containing previously melted alloys. The temperature was controlled by conventional induction or resistance heating. Copper crucibles were used for the lead castings, and graphite crucibles for the aluminum and copper alloys. This fabrication approach was designed to produce composites which each had an outer protective layer of matrix metal (ANL-77-36).

The general procedure consisted of establishing either an argon atmosphere or a vacuum and then lowering the basket of simulated waste into the melt. In some experiments, the basket was agitated (*i.e.*, partially raised and lowered) in an attempt to enhance metal penetration around the simulated wastes. Lead castings were done at 400-480°C for periods up to 1 h; a temperature of ~730°C was used in casting aluminum.[†] The copper alloy selected was Admiralty brass (71 wt % Cu, 28 wt % Zn, 1 wt % Sn), with casting done at ~1040°C.

* Idaho Nuclear Engineering Laboratory. These simulated waste form pellets were provided by J. Berreth of Allied Chemical at INEL.

† ALCAN alloy No. 46020: Al plus 11-13 wt % Si, 0.6 wt % Fe, 0.3 wt % Mn, 0.05 wt % Cu, 0.05 wt % Zn, 0.01 wt % Ca, and all others <0.15 wt %.

Most of the lead and aluminum alloy composite castings had a region with a vertical void zone (or "pipe" formation) in the upper center regions of the composites. Such zones are believed to be more characteristic of the cooling properties and geometry of the system used than of other factors and should be correctable by proper design. In general, the metal adequately penetrated the basket of simulated waste and surrounded the individual waste forms. No conclusions can be made from these experiments as to whether it is preferable to cast in argon, air, or vacuum.

The castings with Admiralty brass in argon yielded a very poor composite, perhaps due to the poor flow characteristics of the melt. The higher temperature requirements ($>1000^{\circ}\text{C}$) for brass probably would introduce additional fabrication difficulties (*e.g.*, materials, volatility) in an actual process, and no further brass castings are likely to be prepared.

2. High-Temperature/High-Pressure Corrosion of Metal Matrix Materials and Calcine in Saturated Brines

Placement of solidified high-level waste (that has been immobilized in a metal matrix) deep in natural salt formations for terminal storage has been proposed. Data will probably be desired for the corrosion rates of metal matrix materials in the presence of salt under high hydrostatic pressures and at temperatures approaching 250°C . Reference metals of metallic lead, an aluminum-12.5 wt % silicon alloy, and Admiralty brass are being investigated in a high-pressure autoclave system. The procedure developed consisted of sealing the metal samples in glass (Pyrex) capsules along with water and excess salt* to saturate the solution at 250°C . One-half of the capsules were sealed in air, and the other half were sealed in either vacuum or inert (N_2) atmosphere. Sealed capsules were then loaded into an autoclave which contained ~ 60 vol % water. At a steady state temperature of $\sim 250^{\circ}\text{C}$, the autoclave pressure approximately matched the pressure inside the capsule and thus reduced the risk of rupturing the glass capsules by overpressurization. To simulate a possible environment expected at the surface of the waste container, the autoclave was operated at $\sim 250^{\circ}\text{C}$ [~ 5 MPa (750 psi) of saturated steam pressure].

After a continuous 10-day exposure, the lead samples showed little sign of attack and no significant weight change (see Table 14). The commercial aluminum-12.5 wt % Si alloy (ALCAN No. 46020) showed extreme attack, and all of the glass sample capsules had ruptured. The aluminum alloy metal surfaces were badly pitted and were coated with a white residue. The weight loss ranged between 4.4 and 12.1 wt % (see Table 14). X-ray diffraction analysis[†] of the aluminum alloy specimens revealed that the metal surface was pure silicon (*i.e.*, depleted in aluminum) and that the white residue was a compound having the approximate composition, $\text{Al}_4\text{Si}_5\text{O}_{14}(\text{OH})_4\text{Cl}$.

*The salt used is a salt core from 800 m below the surface at the proposed location of the high-level-waste terminal storage in New Mexico (*i.e.*, Waste Isolation Pilot Plant Project).

[†]Performed by B. S. Tani of the Chemical Engineering Division.

Table 14. Results of 10-Day Autoclave Corrosion Test
at 250°C and 5 MPa (750 psi)

Specimen	Capsule Atmosphere	Capsule Volume, cm ³	Initial wt, g	Final wt, g	Change in wt, g	Change in wt, %
<u>Lead</u>						
Pb 1	air	~0.56	0.928 14	0.928 51	+0.000 37	---
Pb 2	air	~0.56	0.667 89	0.667 89	---	---
Pb 3	vacuum	~0.56	0.701 55	0.701 31	-0.000 24	---
Pb 4	vacuum	~0.56	0.123 37	0.124 59	+0.001 22	---
<u>Aluminum alloy</u>						
Al 1	air	~0.24	0.083 16	0.079 21	-0.003 95	4.8
Al 2	air	~0.24	0.081 76	0.078 20	-0.003 56	4.4
Al 3	N ₂	~0.56	0.122 26	0.107 46	-0.014 80	12.1
Al 4	N ₂	~0.56	0.130 58	0.122 18	-0.008 48	6.4

Further, if it is assumed that all of the aluminum weight loss was due to reaction with water and that 3/2 moles of H₂ was liberated per mole of aluminum consumed inside the sealed capsule of known volume (pressure calculated assuming ideal gas law at 250°C, the estimated increase in capsule pressure would exceed 4 MPa (600 psi). The maximum pressure that the glass (4.75-mm ID by 1-mm wall) tubing used can withstand is estimated to be ~3 MPa (400 to 500 psi). All of these data indicate that a significant surface reaction of aluminum alloy with water occurred. This was probably initiated by the saturated brine solution attacking and removing any protective oxide coating on the aluminum alloy.

Conclusions from the 10-day corrosion tests are that the commercial Al-12.5 wt % Si alloy is not compatible with the conditions expected in salt deposits. Such an alloy would generate hydrogen and would undergo very accelerated corrosion, which might not be consistent with future waste management criteria. Other aluminum alloys may need to be examined similarly.

A 30-day corrosion experiment in which Admiralty brass (71% Cu, 28% Zn, 1% Sn) and lead samples were exposed to a saturated brine solution at 250°C was completed, and detailed results are not yet available. Visual inspection revealed that the brass surface had a distinct copper color. This is most likely due to some surface dezincification but appears to be very minor; there was no extensive pitting that would indicate more severe attack. The lead samples show very little visible signs of corrosive attack.

Further testing of lead and copper alloys in progress includes sixty-day experiments with both lead and Admiralty brass specimens. Also, thirty-day experiments are proceeding with stabilized calcine pellets [SAMSEL] and type 360 brass (61.5% Cu, 35.5% Zr, 3% Pb).

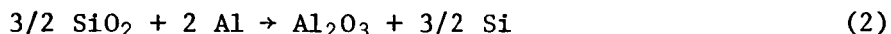
C. Chemical Interactions of Metal-Encapsulated Waste Forms

In order to evaluate the metal matrix concept of waste management, it is necessary to determine the nature and extent of chemical reactions which may occur between a high-level waste (HLW) form and an encapsulating metal. If such reactions occur, the HLW oxides (M) would be reduced and the encapsulating metal (A) oxidized.



It can be assumed that the metallic HLW reaction product would diffuse into the matrix metal and the oxide product would adhere to the solid HLW oxide.

Such a model appears to describe the aluminothermic reduction of silica



as well as the reaction of aluminum with a number of other oxides. In the case of the aluminum-silica reaction, the Arrhenius rate parameters have been determined for the conditions of both solid [GERSHINSKII] and liquid [STANDAGE] aluminum.

It remains to be seen if the model is applicable to a situation in which the oxide reactant is really a mixture of many oxides. Further, one would like to know how the reaction kinetics of the mixture compares with that of the component oxides since previous experiments (ANL-78-11) had shown no visible reaction between the simulated HLW calcine* used and furthermore, silica mixed with the calcine was still reactive. Mixtures of calcine* and silica were chosen for study. It was decided to study two extremes in reactive oxide mixtures:

1. HLW forms in which the reactive component was a relatively large proportion of the oxide mix. This was represented by a mixture of 50 wt % silica and 50 wt % calcine.
2. HLW forms in which the reactive component was a relatively small proportion of the oxide mix. For this case, a mixture of 10 wt % SiO_2 and 90 wt % calcine was chosen. This mixture represents the relative amount of SiO_2 which might actually be present in solidified sintered HLW forms.

A further check of the reactivity of the simulated high-level-waste calcine with aluminum was also performed during this period to provide a guide to interpreting these studies.

* Fluid-bed calcine, which was obtained from Idaho Nuclear Engineering Laboratory, Allied Chemical Corp.

1. Experimental Procedures

The simulated solidified HLW forms used in these experiments were 1.3 cm-diameter pellets, pressed and sintered from (1) INEL* fluid-bed calcine or (2) mixtures of INEL calcine plus SiO_2 in the relative proportions indicated above. All pellets were cold-pressed at 7×10^4 kPa (10^4 psi) and sintered at 900°C for ~ 2 h under an argon purge.

The pellets were immersed in molten aluminum-12 wt % silicon alloy (m.p. 577°C) at the temperature and time conditions shown in Table 15. After they were cooled to room temperature, the samples were sectioned and polished by standard techniques. The samples were then examined with an optical microscope, and the depth of penetration of the reaction zone was measured.

Table 15. Experimental Conditions for Reactions of INEL Calcine, INEL Calcine-10 wt % SiO_2 , and INEL Calcine-50 wt % SiO_2 with Al-12 wt % Si Alloy

	Temperature, $^\circ\text{C}$	Time, h
INEL Calcine	700	15
INEL Calcine	1004	19.7
INEL Calcine-10 wt % SiO_2	700	≥ 72
INEL Calcine-10 wt % SiO_2	908	42.5
INEL Calcine-10 wt % SiO_2	1008	21.7
INEL Calcine-50 wt % SiO_2	684	187
INEL Calcine-50 wt % SiO_2	849	20
INEL Calcine-50 wt % SiO_2	886	22
INEL Calcine-50 wt % SiO_2	1004	19.7

2. Results and Discussion

In the two experiments with pellets made from calcine alone, no reaction zone was observed by microscopic examination, using a magnification of 50X. Since one can easily see a reaction zone of 0.01-0.02 mm, the reaction rate of the calcine alone must be less than 10^{-4} cm/h. These experiments again emphasize the relative inertness to reduction by aluminum of the simulated HLW used for this study.

For those pellets which contained silica, it was possible to observe a reaction zone for all samples except the 10 wt % SiO_2 -90 wt % calcine pellet which was reacted at 700°C . The reaction zones observed were uniformly distributed around the circumference of the pellet, and the penetration rates of these uniform zones are given in Table 16. In addition to the uniform reaction layer, two areas of accelerated attack were observed in the calcine-50 wt % SiO_2 pellet reacted at 849°C . In these areas, the reaction zone

* Idaho Nuclear Engineering Laboratory, Allied Chemical Corp.

Table 16. Rate of Penetration for Reaction Between
(1) INEL Calcine Plus 50 wt % SiO₂ or
10 wt % SiO₂ and (2) Aluminum-12 wt % Si
Alloy for the Uniform Reaction Zone

	Temperature, °C	Penetration Rate, cm/h
INEL Calcine plus 50 wt % SiO ₂	684	1×10^{-4}
	849	5.0×10^{-4}
	886	9.2×10^{-4}
	1004	2.0×10^{-3}
INEL Calcine plus 10 wt % SiO ₂	700	no reaction observed
	908	1.5×10^{-4}
	1000	1.8×10^{-4}

penetrated to depths of 0.12 cm and 0.17 cm. This increased penetration was presumably caused by some as-yet-undetermined surface characteristics of the pellet, but the reaction product appeared to be the same as for the areas of uniform reaction.

The uniform reaction zone was characterized using the calcine-50% SiO₂ pellet which had been reacted with the aluminum alloy at 886°C. The zone was examined using energy-dispersive X-ray analysis and was found to be enriched in aluminum and depleted in silica. Presumably, then, the reaction products are the same as those of the aluminothermic reduction of pure SiO₂, *i.e.*, Si and Al₂O₃ (Eq. 2). These results appear to indicate that the product aluminum oxide adheres to the pellet while the silica is dispersed in the encapsulating metal as postulated in the model for these experiments.

The reaction rate for a diffusion-limited reaction such as the one occurring here between the aluminum and the silica-containing pellets may be expressed by:

$$K = Z \exp (-E_a/RT) \quad (3)$$

where K is the penetration rate (depth per unit time) of the reaction zone, R is the gas constant, and T is the absolute temperature. The pre-exponential factor, Z, and the activation energy, E_a, are the so-called Arrhenius rate parameters. One may obtain the Arrhenius parameters from a plot of log_e (ln) of the penetration rate *vs.* the reciprocal of the absolute temperature (Fig. 13). The activation energy (slope) and the log_e of the pre-exponential factor (cm/h) (intercept) were found to be 22.8 ± 1.4 kcal/mol and 2.8 ± 0.6 , respectively, by using a least squares analysis of the data for the calcine-50% SiO₂ reaction with the aluminum-12 wt % Si alloy. Thus, Eq. 3 becomes

$$K = 15.9 \exp (-22.8 \text{ kcal} \cdot \text{mol}^{-1}/RT), \text{ cm/h} \quad (4)$$

Although it is not yet possible to perform a least-squares analysis of the calcine-10% SiO₂/aluminum reaction data due to lack of sufficient data, it is possible to compare it to the results obtained using pellets containing

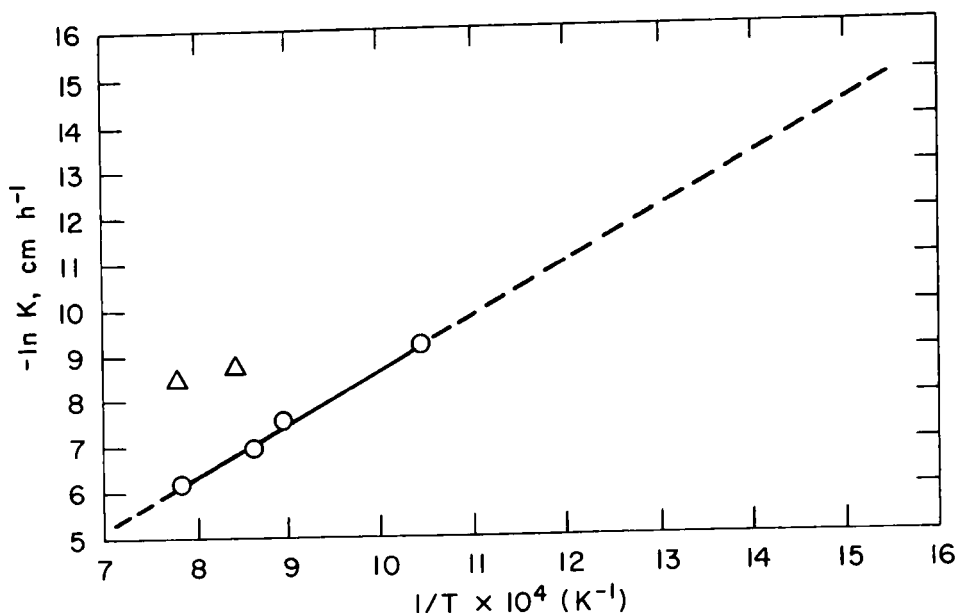


Fig. 13. Negative Natural Logarithm of the Penetration Depth, K , vs. the Reciprocal of Absolute Temperature. Circles represent 50 wt % INEL Fluid-bed calcine-50 wt % SiO_2 Pellets reacted with aluminum-12 wt % Si alloy. Triangles represent 90 wt % INEL fluid-bed calcine-10 wt % SiO_2 pellets reacted with aluminum-12 wt % Si alloy

50 wt % SiO_2 . In the two cases where the reaction could be observed, the measured rates were roughly one order of magnitude lower than the corresponding rate for 50 wt % SiO_2 pellets. For the reaction done at 700°C , it is possible to estimate that the rate is at least seven times lower for calcine-10% SiO_2 pellets than for 50% SiO_2 pellets since a reaction zone of 1×10^{-3} cm is discernible and since a 50 wt % SiO_2 pellet would have produced a zone of 7×10^{-3} cm if reacted at 700°C for that time period. Experiments with pellets containing 10 wt % SiO_2 to obtain an estimate of the Arrhenius parameters for the reaction are continuing.

3. Conclusions

Several conclusions may be made from these experiments. The rate parameters obtained for pellets containing a high concentration of reactive material (50 wt % SiO_2) are much different from those obtained for pure SiO_2 material. This would indicate that the presence of calcine has more of an effect than just dilution of the silica. This leads to the conclusion that it is necessary to measure reaction rates in the multicomponent system. In estimating the stability of the waste form/metal system, then, studies of the reactions of pure components with the encapsulating metal will give only a rough idea about the reactivity of that material.

Further dilution of the reactive material to lower concentrations in the pellet, however, does not appear to have as significant an effect. Based on the limited data obtained thus far, it would appear that the effect of dilution is only a linear correction. This would imply that the activation energy in the reaction of calcine-silica pellets with aluminum remains relatively constant. Nevertheless, confirmation of this must await the determination of activation parameters for reactions of the 10 wt % silica pellets.

Finally, it is possible to use Eq. 4 to make a worst-case estimate of the rate of reaction between the solidified HLW form and the encapsulating metal. This is reasonable since the system studied contains a reactive metal (aluminum) plus a multicomponent oxide, and the reaction rate of the calcine alone, though not measured, can be estimated to be at least one order of magnitude less than that of the calcine mixed with SiO_2 . Three temperature-time regions have been selected which might represent reasonable fabrication, interim storage, transportation accident, and terminal storage conditions:

- (1) 250°C for 100 y
- (2) 700°C for 10 h
- (3) 1000°C for 1 h

The extent of reaction in these three cases would be 41 μm , 12 μm , and 19 μm , respectively. The total of these reaction layer thicknesses would represent an extent of reaction of ~11% of the solidified HLW, assuming spherical solidified HLW particles ~4 mm in diameter. One might use these data to infer some of the long-term and accident properties of metal-encapsulated solidified HLW composites.

D. Leach Rates of Simulated High-Level Waste Forms

Immobilization of radioactive wastes presupposes the formation of a solid matrix that cannot be readily leached by waters which may come in contact with the waste during terminal storage. One of the solid waste forms being considered for terminal storage is the "metal matrix." This waste form consists of either a calcined or a sintered waste dispersed in a metal matrix.

In order to evaluate the suitability of this waste form, it is necessary to determine the resistance to dispersion of waste constituents by groundwater. The first step necessary for dispersion to occur is aqueous leaching of radioactivity from the solid matrix. The studies reviewed in this report deal with the rate at which leaching occurs for various radionuclides under various aqueous leachant conditions, using various simulated solid waste forms. A description of the neutron activation analysis (NAA) technique* used in these measurements, as well as initial results, have been reported in ANL-78-11.

*The gamma-emitting radioisotopes present in neutron-irradiated simulated waste following neutron activation are assayed by gamma ray analysis, using a lithium-drifted germanium (GeLi) detector.

1. Experimental Results

Sintered waste form (SWF) pellets containing Idaho Nuclear Engineering Laboratory (INEL) fluid-bed calcine (simulated high-level waste) mixed with aluminosilicate fluxes (50 wt %/50 wt %) [SAMSEL] were cold-pressed with an 11-Mg (12-ton) laboratory press at $7 \cdot 10^4$ kPa (10^4 psi) into 1.3-cm (1/2-in.) diameter pellets of various thicknesses (~ 0.5 to ~ 2 cm). Similar pellets of INEL calcine only were also made. Water (up to 5 wt %) was used as a binder. These pellets were sintered at $\sim 900^\circ\text{C}$ for several hours. The sintered pellets were irradiated in the isotope tray (flux of $\sim 6 \times 10^{12}$ n/cm²-s) of the Argonne National Laboratory (ANL) CP-5 Research Reactor for 24 h.

Sequential leach tests of approximately one-week duration have been performed on these pellets, using 25°C stagnant distilled water open to the atmosphere. The leach solutions were gamma ray analyzed, using a GeLi detector, and the fraction of specific isotopes leached from the solid matrix was determined. The principal leachable activation product from these pellets was ^{134}Cs . Leach rates from the first-week leach test based on ^{134}Cs as well as on total weight loss are given in Table 17. These leach rates have been calculated from the following relationship:

$$L = \frac{A_t}{A_0} \frac{W_0}{S t} \quad (5)$$

where A_t = amount of material A removed in time t

A_0 = initial amount of material A in solid

S = surface area of the solid material (cm²)

W_0 = initial weight of the solid material (g)

t = leaching period (d)

L = leach rate (g/cm²·d)

A_t/A_0 = fraction leached.

The surface area of each leach pellet was calculated, assuming it had the surface area of a right circular cylindrical shape (ANL-78-11).

The pellets composed only of calcine were leached at very high rates, as exemplified by the large weight losses as well as the fact that virtually all of the cesium was leached out during the one-week test (see Table 17). These results are in substantial agreement with the data of Samsel and Berreth [SAMSEL]. The pellets containing aluminosilicate fluxes had significantly less leaching (in some cases, as little as 10^{-5} g/cm²·d). The loss of cesium by leaching in these pellets during the initial leaching period seems to be lower than the loss of total mass as determined by weight loss. However, at low leach rates, the weight loss determinations are subject to large uncertainties because of the difficulties associated with evaluating small differences between large numbers.

Table 17. First-Week Leach Rates for SWF Pellets Containing Fluid-Bed Calcine in 25°C Stagnant Distilled Water

Sample No.	Pellet Composition	Analysis Method	Fraction ^a	Fraction ^a per d	Fraction ^a per d per cm ²	(g/cm ² ·d) ^b
1-3	Calcine fines	¹³⁴ Cs	0.92	1.3×10^{-1}	2.8×10^{-2}	4.0×10^{-2}
		wt loss	0.25	3.6×10^{-2}	7.6×10^{-3}	1.1×10^{-2}
1-4	Calcine fines	¹³⁴ Cs	0.93	1.3×10^{-1}	2.8×10^{-2}	3.6×10^{-2}
		wt loss	0.22	3.1×10^{-2}	6.5×10^{-3}	8.4×10^{-3}
2-1	Calcine fines	¹³⁴ Cs	0.89	1.1×10^{-1}	2.4×10^{-2}	2.5×10^{-2}
		wt loss	0.17	2.2×10^{-2}	4.8×10^{-3}	5.1×10^{-3}
2-2	Calcine fines	¹³⁴ Cs	0.99	1.3×10^{-1}	2.7×10^{-2}	2.9×10^{-2}
		wt loss	0.18	2.2×10^{-2}	4.8×10^{-3}	5.1×10^{-3}
2-5	Bed calcine	¹³⁴ Cs	0.94	1.2×10^{-1}	1.7×10^{-2}	7.5×10^{-2}
		wt loss	0.084	1.1×10^{-2}	1.5×10^{-3}	6.6×10^{-3}
2-6	Bed calcine	¹³⁴ Cs	0.99	1.3×10^{-1}	1.8×10^{-2}	8.2×10^{-2}
		wt loss	0.069	8.8×10^{-3}	1.3×10^{-3}	5.9×10^{-3}
1-1	19-7 flux ^c + bed calcine ^c	¹³⁴ Cs	0.012	1.8×10^{-3}	3.8×10^{-4}	4.5×10^{-4}
		wt loss	0.009	1.3×10^{-3}	2.9×10^{-4}	3.4×10^{-4}
1-6	19-7 flux ^c + bed calcine ^c	¹³⁴ Cs	0.033	4.7×10^{-3}	5.6×10^{-4}	2.6×10^{-3}
		wt loss	---	---	---	---
2-3	19-8 flux ^c + bed calcine ^c	¹³⁴ Cs	3.0×10^{-4}	3.8×10^{-5}	8.1×10^{-6}	8.8×10^{-6}
		wt loss	2.5×10^{-3}	3.2×10^{-4}	6.8×10^{-5}	7.4×10^{-5}
2-4	19-8 flux ^c + bed calcine ^c	¹³⁴ Cs	2.0×10^{-4}	2.6×10^{-5}	4.9×10^{-6}	1.1×10^{-5}
		wt loss	1.5×10^{-3}	1.9×10^{-4}	3.5×10^{-5}	7.7×10^{-5}

^aFraction of cesium leached or weight lost.

^bIdentified from equation five in the text.

^cAluminosilicate flux and calcine--composition defined in [SAMSEL].

The results of continued tests on the pellets composed of calcine mixed with flux are indicated in Table 18. In some cases, it was possible to resolve the neutron activation product ^{60}Co from the gamma ray spectrum. The ^{60}Co data, where available, tended to corroborate the ^{134}Cs results, indicating that cesium was not being preferentially leached from these pellets. Previous experimental results (ANL-78-11) have already indicated that ^{60}Co leaches at the same rate as the total mass in sintered waste forms.

Table 18. Leach Rates for SWF Pellets Containing Fluid-Bed Calcine and Aluminosilicate Flux^a (50 wt %/50 wt %) in 25°C Stagnant Distilled Water

Sample No.	Pellet Composition	Analysis Method	Leach Rate, g/cm ² ·d	
			1st Week Leach ^b	2nd Week Leach ^b
1-1	19-7 flux ^a + bed calcine	^{134}Cs	4.5×10^{-4}	3.5×10^{-5}
		^{60}Co	2.7×10^{-4}	3.0×10^{-5}
		wt loss	3.4×10^{-4}	3.1×10^{-5}
1-6	19-7 flux ^a + bed calcine	^{134}Cs	2.6×10^{-3}	9.8×10^{-5}
		^{60}Co	---	---
		wt loss	---	---
2-3	19-8 flux ^a + bed calcine	^{134}Cs	8.8×10^{-6}	2.2×10^{-5}
		^{60}Co	---	---
		wt loss	7.4×10^{-5}	---
2-4	19-8 flux ^a + bed calcine	^{134}Cs	1.1×10^{-5}	7.4×10^{-6}
		^{60}Co	---	8.8×10^{-6}
		wt loss	7.7×10^{-5}	---

^aAluminosilicate flux and calcine composition defined in [SAMSEL].

^bSequential one-week leach tests.

Although during the first week of leaching, those pellets containing the aluminosilicate flux [SAMSEL] identified as 19-7 had significantly higher leach rates than did the pellets containing the 19-8 flux, the leach rates for the 19-7 flux pellets decreased appreciably during the second week of leaching (see Table 18), bringing them into closer agreement with the pellets containing the 19-8 flux. This effect could be at least partly ascribed to problems in the preparation of the pellets. Additional studies using pellets containing the 19-8 flux are planned.

The leach rates for the SWF containing the aluminosilicate flux observed in these measurements were about two orders of magnitude higher than the leach rates observed by Samsel and Berreth [SAMSEL] for similar materials. However, their measurements were based on BET measurements* of the surface

*Brunauer-Emmett-Teller gas absorption technique.

area of crushed and powdered samples which were subjected to the leaching medium. Leach rates based on BET surface area measurements of crushed samples are probably lower than would be observed for large samples in natural environments since the surface area available to nitrogen adsorption (BET measurements) is likely to be larger than the surface area available to a solution. On the other hand, the assumption of a geometry of impervious cylinders used in determining the surface area leads to a higher rate than would be observed for large samples in natural environments since the pellets have some porosity. The drying rate of these pellets after leaching indicates that a significant amount of porosity exists.

Several metal-encapsulated composites consisting of SWF beads^{*} encapsulated in a metallic lead matrix were prepared. The composites were irradiated in the ANL CP-5 Research Reactor for 24 h and subsequently were gamma ray analyzed, using a GeLi detector, to determine the neutron-induced radioactivities present. Sequential one-week leach tests were performed on these composites, using 25°C stagnant distilled water open to the atmosphere. Three metal-encapsulated irradiated composites containing close-packed SWF beads were studied. Descriptions of these composites, together with a tabulation of the leach rates based on the first one-week test, are given in Table 19. Although the bead density was approximately the same in all three ingots, the fraction of exposed bead surface was much larger in the smaller ingots. Despite this, the leach rates for elements concentrated in the SWF beads (particularly cesium) were not dramatically different for the three ingots tested. This indicates that there was significant leaching from the interior of the ingot. The rate at which the ingots dried after leaching also indicated significant porosity, which tends to corroborate this observation. Again, as in the case of the sintered pellets, the weight loss measurements are subject to some ambiguity because of the difficulties associated with determining small differences between large numbers.

2. Conclusions

If significant leaching from the interior of a waste form (*i.e.*, an ingot) takes place, the assumed surface area (*i.e.*, the exterior surface area of the cylindrical ingot) is not the true surface area exposed to the leachant. Hence, leach rates reported as "per cm²" would be misleading. As has been pointed out before (ANL-78-11), caution is required in reporting leach rates, particularly if they are to be extrapolated to large ingots in geologic storage or compared with results of other workers.

Comparisons of the "g/cm²·d" leach rates in Table 19 with similar results for PW-7a beads (ANL-78-11) suggests that encapsulation in a lead matrix increases the leach rate. This results from the surface area used in these calculations. A more realistic comparison is made in Table 20, where the values for "fraction leached per day" of three isotopes are compared. In this comparison it can be seen that there is a significant shielding effect by the lead matrix (*i.e.*, the fractions of ⁶⁰Co and ⁶⁵Zn leached are lower from the large ingot than from the beads). However, the results from Table 19

^{*}These sintered waste form (SWF) beads were obtained from PNL. They were prepared on a disc pelletizer by agglomerating 85 wt % PW-7a [BONNER] spray calcine and 15 wt % glass frit, followed by sintering for 1 h at 1000°C.

Table 19. Leach Rates in 25°C Distilled Stagnant Water
for Lead Ingots Containing PW-7a Beads (Composites)

Ingot No.	Total Wt, g	Surface Area, cm ²	No. of Beads	Isotope Analyzed	Fraction Leached	Fraction Leached per d	Fraction Leached per d per cm ²	(g/cm ² ·d) ^a
23	23.364	10.6	54	⁶⁰ Co	1.0E-4	8.4E-6	7.9E-7	1.8E-5
				⁶⁵ Zn	1.1E-4	9.2E-6	8.6E-7	2.0E-5
				¹²⁴ Sb	7.2E-4	6.1E-5	5.7E-6	1.3E-4
				¹³⁴ Cs ^b	2.5E-1	2.1E-2	2.0E-3	4.7E-2
				¹⁴¹ Ce ^c	3.8E-4	3.2E-5	3.0E-6	7.0E-5
				wt loss	1.7E-2	1.4E-3	1.4E-4	3.3E-3
7	7.548	6.1	17	⁶⁰ Co	3.0E-4	2.5E-5	4.1E-6	3.1E-5
				⁶⁵ Zn	1.7E-4	1.4E-5	2.3E-6	1.7E-5
				¹⁷⁴ Sb	1.7E-3	1.4E-4	2.3E-5	1.7E-4
				¹³⁴ Cs ^b	1.3E-1	1.1E-2	1.7E-3	1.3E-2
				¹⁴¹ Ce ^c	2.1E-4	1.7E-5	2.8E-6	2.1E-5
				wt loss	6.2E-2	5.2E-3	8.5E-4	6.4E-3
5	5.526	5.4	13	⁶⁰ Co	3.4E-4	2.0E-5	3.7E-6	2.0E-5
				⁶⁵ Zn	5.6E-5	3.3E-6	6.1E-7	3.4E-6
				¹²⁴ Sb	1.4E-3	8.5E-5	1.6E-5	8.8E-5
				¹³⁴ Cs ^b	5.0E-1	2.9E-2	5.5E-3	3.0E-2
				¹⁴¹ Ce ^c	2.5E-4	1.5E-5	2.7E-6	1.5E-5
				wt loss	5.3E-2	3.1E-3	5.7E-4	3.1E-3

^aIdentified from equation five in the text.

^bLeach rates become relatively meaningless for our purposes when large fractions (>1%) are leached out in a short time.

^cThere is a significant uncertainty (*i.e.*, a factor of 10 or more) in the ¹⁴¹Ce data because of the self-absorption of the weak (145-keV) gamma radiation in the lead ingot. Hence, these values are upper limits.

Table 20. Seven-day Leach Rates in 25°C Distilled Stagnant Water for PW-7a Beads in Various Configurations

Isotope Analyzed	Fraction Leached per d			
	23 g Ingot	7.5 g Ingot	5.5 g Ingot	Bare Beads ^a
⁶⁰ Co	8.4E-6	2.5E-5	2.0E-5	5 E-5
⁶⁵ Zn	9.2E-6	1.4E-5	3.3E-6	4 E-5
¹³⁴ Cs	2.1E-2	1.1E-2	2.9E-2	3 E-2

^aData taken from ANL-78-11.

(*i.e.*, g/cm²·d) show that the effect is much less than would be expected if the matrix were a solid, impervious ingot. Additional studies must be made on these as well as larger composites before definite conclusions can be drawn.

The results obtained thus far, as reported in Table 18 and ANL-78-11, indicate that waste forms can be produced with acceptably low leach rates (*i.e.*, 10⁻⁵ to 10⁻⁶ g/cm²·d). However, the final waste ingot must be sufficiently impervious so that the surface area exposed to the leaching medium consists approximately of the external surface area of the ingot. If the waste matrix has significant porosity, the radioactive waste products will be leached out relatively rapidly despite low leach rates.

The leachant used exclusively in these measurements was distilled water. Alternative leachants were tried in previous studies (ANL-78-11), but no dramatic effect attributable to the pH of the leachant was observed. The specific characteristics of the leachant in the final waste repository will undoubtedly affect the leach rate of the waste form to some extent. For instance, a high-carbonate leaching medium would probably reduce the leach rate for a lead matrix. Until such time as the groundwater characteristics of the final repository are defined, distilled water can be considered to be as representative a leachant as a mineralized aqueous solution.

The application of activation analysis techniques coupled with radiochemical separations and/or radiation counting techniques (ANL-78-11) seems to be a very useful method of establishing realistic leach rates of simulated waste forms. A paper describing in detail the procedures used in these leach rate studies is being prepared for publication.

VI. ESTABLISHMENT OF TENTATIVE CRITERIA FOR HULL TREATMENT (L. E. Trevorrow and B. J. Kullen)

A. Introduction

The hull-treatment criteria program is one of developing general overall guidance leading to future regulation of the handling, transport, and disposal of waste Zircaloy cladding hulls from the reprocessing of spent LWR fuel assemblies. The goal of these criteria is to ensure that the operations present minimal risk to operating personnel and to the public. To this end, effort has been concentrated on (1) collecting available information on, or relevant to, hulls generation, handling, treatment, packaging, storage, and transport, (2) collecting documented regulations and criteria that might have relevance to waste hulls handling, and (3) developing preliminary criteria based on the preceding information. These areas were described in detail in a previous progress report (ANL-77-36). Ultimately, the objective of this program is to establish final hull-treatment criteria, acceptable to industry, professional institutions (*e.g.*, The American National Standards Institute), and government agencies, that would result in safe design, safe operational practices, and effective administrative practices.

B. Progress in the Period

A rough draft, entitled *Development of Criteria for the Handling of Waste Cladding Hulls and Associated Metal Waste*, was outlined and written during the report period. The purpose of the draft, pending internal review, revision, and editing, is to serve as the document transmitting preliminary hull-treatment criteria to other organizations for review. It is expected that the reviews will result in feedback comments, prompting revisions of and additions to the draft from which a final document will be created approaching as broad a compromise of interests and objectives as possible.

The draft addresses five topics:

- (1) Assessment of Potential Hazards in the Handling of Zircaloy Hull Waste;
- (2) Description of the Cladding Hull Waste Stream;
- (3) Waste Cladding Hull Handling Operations;
- (4) Proposed Criteria for Waste Cladding Hull Management;
- (5) Impact of Proposed Criteria on Plant Flow Sheets.

In addition to the textual material outlined above, a large amount of supporting reference material was assembled in appendix form. Existing criteria were extracted from the Code of Federal Regulations on fuel reprocessing plant (FRP) design, packaging of zirconium forms and of radioactive materials, and the transport of zirconium and radioactive materials. Current documented guidance was excerpted, *i.e.*, guidance pertaining to plant design, operational safety, and administrative procedures. Sources of the guides were industry/institution standards and NRC Regulatory Guides. Other appendices (1) examined the implications of compliance with existing plant designs to

documented criteria, regulations, standards, and guides, (2) described possible hull-treatment technologies that might be used to meet the proposed handling criteria, (3) considered the relation of economics to the proposed criteria, (4) presented justification for proposed criteria, and (5) described a tree-structure base for the organization of hull-handling criteria.

Ongoing effort will be applied to producing an internally acceptable, clean draft manuscript of the proposed-criteria document, suitable for distribution to outside parties. Concurrently, a mailing list of suitable interested parties will be developed through correspondence and interviews. The finished draft will then be distributed for review and comment. Future activity will include the incorporation of outside commentary into the criteria draft and the eventual publication of the final report.

In the report period, compiling of a list of possible outside reviewers was begun. Sources of this information have been the technical literature and working committee lists appearing in various nuclear standards. The standards consulted were on the subjects of fire protection, transportation, fuel cycle, design criteria, physical protection of nuclear materials, and decommissioning criteria. To date, some 150 individuals and 80 organizations (industrial and institutional) have been identified. The list will be shortened to a number more compatible with the program schedule.

In addition to the work described above, three adjunctive studies were conducted during the period. These studies, which could have effects on the development of criteria, are presented below. First, as a result of internal review of the criteria draft, possible hulls hazards have been reevaluated; as described in Section C of this chapter, hazards have become visible which might affect the basis for criteria. In Section D of this chapter, a hull-criteria development methodology based on a tree-structure technique is described. Lastly, Section E of this chapter is an evaluation of zirconium fines behavior during the mechanical shearing of spent LWR fuels.

C. Reevaluation of the Criteria Base

A review of the hulls-management criteria generated to date has suggested that a small set of general criteria might be of value in further defining or putting into perspective the scope of the eventual set of design guides.

It being assumed that the prime objective of generated criteria is to eliminate risks to operating personnel and the public (risks from hazards imposed by cladding hulls), a direct issue is to define the worst possible hazard that should be considered likely during hulls management. Once the hazard is defined, it should be mandatory that plant design ensure that the consequences of an accident involving that hazard are limited. With this objective, the following overall criteria appear to be quite adequate.

- A detailed analysis shall be provided, as an adjunct to the plant design, describing the effects of total combustion* of the maximum allowable accumulation of hulls and/or fines.

* Assumed to be the maximum credible accident for hulls/fines.

- The plant design shall ensure adequate containment within radiation limits consistent with ALARA [CFR-10]* for combustion of the maximum allowable accumulation of hulls and/or fines.

- The plant design shall ensure that combustion of the maximum allowable accumulation of hulls and/or fines will not cause any protection/monitoring instrument or system to operate in a way that might result in increasing the combustion energy/material releases beyond the limits set by the combustion analysis.

- The plant design shall ensure that the energy or the material from the combustion of the maximum allowable accumulation of hulls and/or fines will not cause propagation of the accident to other accumulations of hulls and/or fines.

- The above criteria shall also apply to hulls and/or fines waste under conditions of packaging for storage or off-site shipment or to packaged hulls/fines waste in the site-storage mode. Exemption from these in-plant criteria may be allowed under either of the following extensions of plant design.

1. Packaging of hulls and/or fines shall be provided which reduces the effects of a combustion accident to acceptably low levels [CFR-10, CFR-40].

2. The hulls and/or fines waste shall be subjected to treatment which produces a waste form that is acceptably inert, as demonstrable by analysis and testing documented in the safety analysis report.

As an example of a possible impact of primary criteria on existing plant designs, Table 21 is presented to compare the apparent hulls-accumulation limits as found in the safety analyses for four plants. Three of the four designs call for maximum accumulations of hulls in storage containers ranging from 0.1 to ~1.6 Mg of waste. One design [EXXON] included a model characterizing the effect of combustion of ~1.2 Mg of cladding hulls in an open storage container located within a process cell. The postulated conclusion was that the cell would contain the combustion effects with only minimal atmospheric release, thereby protecting personnel and the public. Of interest was the prediction that cell ventilation filters would be loaded to only ~10% of their rated capacities as a result of the hull fire.

Also in Table 21 is another plant design [MFRP] which allows a potential maximum accumulation of ~1000 Mg of hulls waste (from 10 years of operation) in a single, large storage vault. Taking into consideration the EXXON combustion model discussed above, criteria stipulating that the plant must contain the combustion of the total amount of a single accumulation of hulls would force reevaluation of the design of a plant in which it is planned to collect as much as 1000 Mg of hull waste in a single location. It must be noted that although the MFRP design also includes a large sand-bed filter as a final ventilation-air barrier, no analyses were presented to quantify the effectiveness of the filter in containing combustion products from the burning of 1000 Mg of contaminated cladding-hull waste.

* Part 190 of the latest EPA code of regulations [CFR-40] may supersede current NRC limits [CFR-10].

Table 21. Cladding Hull Accumulations Based on Plant Designs

Plant	Container	Batch Limit, Mg	Total Curies after 10-y Cooling		
			TRU ^a	F.P. ^b	A.P. ^c
NFS ^d	0.1 m ³ drum	~0.1	3 E1	4 E1	1 E3
MFRP ^e	~1000 m ³ vault	~1000	3 E5	4 E5	1 E7
BNFP ^f	~1.6 m ³ engineered container	~1.6	5 E2	6 E2	2 E4
EXXON ^g	~1.2 m ³ engineered container	~1.2	4 E2	4 E2	1 E4

^aTransuranic activity.

^bFission product activity.

^cActivation product activity.

^dNuclear Fuel Services, West Valley, New York [NFS].

^eMidwest Fuel Reprocessing Plant, Morris, Illinois [MFRP].

^fBarnwell Nuclear Fuel Plant, Barnwell, South Carolina [AGNS].

^gNuclear Fuel Recovery and Recycling Plant (proposed), Oak Ridge, Tennessee [EXXON].

The basic criteria listed above, which would satisfy the need for protection of personnel and the public, might serve as first-order design guidance. However, lesser hazards in hulls management might arise--*i.e.*, hazards imposed by conditions that might be avoided by prudent design of systems and operations. Some examples of such conditions and resulting hazards are listed below. It should be noted that some of the conditions cited here are possible reiterations of general industrial zirconium-handling recommendations outlined in previous reports [KULLEN, LEVITZ] (ANL-77-36). Here, they apply to specific areas or functions and are used to demonstrate the importance of hazard awareness for prudent design.

CONDITION: Collection of very fine zirconium (and entrained oxide fuel) dust on ventilation air-treatment filters.

HAZARD: Combustion of zirconium dust could damage the filter media, which could result in release downstream of previously trapped radioactive material.

CONDITION: Segregation and localization of zirconium fines in a sealed storage container constructed of stainless steel.

HAZARD: Localized, rapid oxidation or spontaneous ignition of zirconium fines pockets at the walls or bottom of a container could generate zirconium-SS eutectic-melting temperatures (~1100°C [NELSON]), resulting in deterioration and possible breach of the container. Subsequent entrance of water (in the case of pool storage) or air (in the case of dry storage) could have catastrophic results.

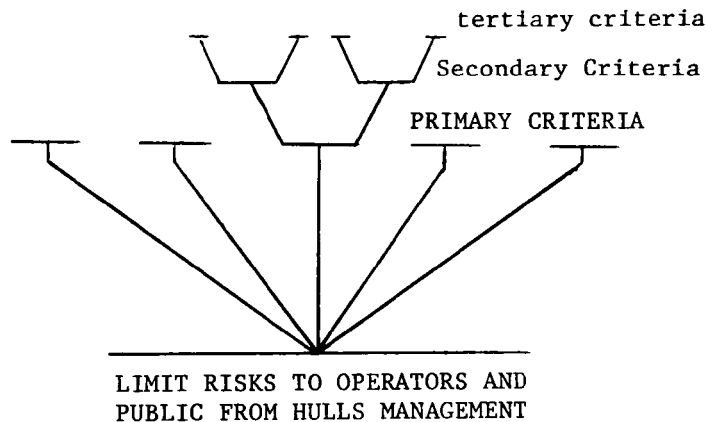
- CONDITION: Subjecting hull waste to a process(es) that could sensitize the surfaces of the zirconium waste.
HAZARD: The waste form would be more susceptible to pyrophoric behavior.
- CONDITION: Equipment designed so that fines material could become isolated and locally accumulated in routine operation.
HAZARD: Accumulated zirconium fines represent a most hazardous condition in terms of pyrophoric behavior.
- CONDITION: Mixing of hull waste with other materials in waste storage containers.
HAZARD: Some materials other than hulls (such as ion-exchange resins or loaded filter media) are themselves combustion hazards and as such could serve as a means of igniting the hull waste.
- CONDITION: The use of inert atmospheres to blanket operations whereby zirconium metal is mechanically upset.
HAZARD: Newly exposed surfaces on the resulting metal forms are unreacted and are pyrophorically sensitive when removed from an inert atmosphere.
- CONDITION: A design of process equipment for the treatment (deactivation or volume reduction) of hulls that does not limit the amount of hulls being treated.
HAZARD: Anomalies in process operation could cause runaway reactions that might overtax the containment capabilities of the plant.
- CONDITION: Arc or gas welding of covers onto hulls/fines waste containers without making provision for limiting sparks and metal and/or flux runoff.
HAZARD: This operation could ignite the contained hulls and/or fines waste.

Occurrence of accidents of the types described above would seem more likely to compromise plant operations than to threaten the safety of personnel or the public. Thus, it might well be to divide design criteria into two categories--first, guidance which will ensure the safety of operating personnel and the public, and secondly, guidance which will assure avoidance of a plant condition which might create a potential hazard. Stated simply, the two categories represent *direct* and *indirect* means of protecting operating personnel and the public.

Thus, it can be seen that future development of hulls management criteria, within the current program, not only must be responsive to the necessity of protecting operating personnel and the public from undue hazards, but also must contribute to prudent design.

D. A Tree-Structure Criteria Development Model

Another approach to waste management guidance is the development of a method or tool that can be used to propagate criteria in ascending levels of detail. In such a method, a set of criteria can be conceived of as a tree, stemming from a root premise representing the extreme generality--that hulls handling must be carried out without undue risk to operating personnel and the public. From this root, branchlike primary criteria can be developed as a first step towards additional detail and specification. Criteria might be structured either within the scope of hull hazards (*i.e.*, radioactive properties and potential pyrophoricity) or they might be structured to the general set of operations proposed for a typical fuel reprocessing plant (FRP). The criteria development scheme presented in Table 22 is rooted in safety in hulls management during FRP operations and waste-transport procedures. The table shows five primary-branch criteria for safety in hulls management: (1) design and construction of the FRP, (2) normal process operations, (3) maintenance operations, (4) abnormal operations, and (5) transport of hull waste away from a FRP. An example of the different branching levels of criteria is shown below.



From each of the primary criteria, additional stages of detail and specification, conceived of as additional branching, can be developed as secondary criteria. Obviously, further branching may be continued in stages of increasing detail. However, if the resulting criteria are not to be dictatorial, a limit must be placed upon finer branching before the degree of specification begins to infringe on the commercial operator's options in the design of plant, equipment, procedures, and conditions. Table 22 and the illustration show criteria taken to the third stage of detail.

Table 22. Development of Detail in Criteria

Primary Criteria	Secondary Criteria	Tertiary Criteria
Design and construction includes provisions to limit hulls hazards.	Plant layout of areas used for hulls operations and storage should provide physical convenience.	Dimensions, arrangement, and structure of areas used for hulls operations and storage should allow easy access and egress and offer adequate space and utilities.
	Hulls operating and storage areas should be durable.	Hulls operating and storage areas should withstand natural phenomena, fire, impact, explosions.
	Hulls storage capacity must limit maximum credible accident.	Hulls storage areas must have bins of limited volume.
	Hulls storage areas must be remote.	Hulls storage areas must be separated by distance and suitable shielding for fire, blast, and radiation from other processing areas and areas frequented by personnel.
	Hulls handling equipment must be fail-safe.	In case of failure of power or any component, containment and shielding must be preserved.
	Building and equipment involved in hulls handling must be durable.	Building and equipment involved in hulls handling must withstand all natural phenomena, fire, explosions.
Normal process operations at the FRP include provisions to limit hulls hazards.	Hulls handling equipment must meet defined quality standards.	Requirements for reliability, accuracy, and strength must be developed and used to test hulls handling equipment.
	Personnel must be informed on hulls hazards.	Personnel in plant operations, plant management, transport, and emergency units must receive initial instruction and periodic review of written set of information on potential hull hazards.
	Responsibility for hulls management must be defined.	Responsibility for safe management of hulls must be clearly defined for members of operating, management, transport, and emergency teams.
	Access to hulls operating and storage areas must be controlled.	Access to areas involved in processing or storage of hulls must be controlled and limited to necessary personnel.
		Hulls storage areas should not be routinely occupied by personnel.
		Hulls storage areas should not be used for storage of materials other than hulls.
	Information on hulls must be up to date.	A running inventory of the hulls at a fuel reprocessing plant must be available through accounting procedures.
		There must be constant surveillance of heat and radioactivity in areas containing hulls accumulations.
Radiation exposure from hulls must be limited.		Labeling of packages containing hulls waste must clearly identify contents.
		Doses to operating personnel and public from hulls operations must be assigned a limit that is an appropriate fraction of total ALARA dose from the entire fuel cycle.

(contd)

Table 22. (contd)

Primary Criteria	Secondary Criteria	Tertiary Criteria
Normal process operations at the FRP include provisions to limit hulls hazards. (contd)	Operating procedures for hulls handling must be defined.	<p>A manual of written procedures for hulls operations must be kept current.</p> <p>A mechanism for adopting changes or additions to hulls operating procedures must be defined in writing and must include a written safety analysis for each change or addition.</p> <p>PSARs must contain analysis of possible error in cases resulting in adverse consequences in hulls operating procedures.</p>
	Hulls processing and storage restricted to appropriate areas in plant.	Areas devoted to hulls processing and storage must offer appropriate ventilation, shielding, and contain all remote operation where necessary.
	Hulls containment must be reliable.	<p>Hulls must be contained in a nest of primary plus secondary vessels at all times.</p> <p>Packaging and vessels used in any storage of hulls, including that at reprocessing site, must conform to DOT specifications.</p> <p>All hulls containment must offer protection to operating personnel and public equivalent to 10CFR100.</p>
	Conditions of processes involving hulls must be chosen to limit hazards.	<p>Zr metal accumulation, both in processing and storage, must be mass-limited.</p> <p>Exposure of Zr metal to high temperatures, except as a process condition, must be avoided.</p> <p>Exposure of Zr metals to ignition sources, including static electricity sources, is to be avoided.</p> <p>Residence time of hulls waste at the FRP is to be limited.</p> <p>Hulls stored in metallic form should not be in contact with combustible materials.</p> <p>Exposure of hulls in metallic form to oxidizing environments, except as part of a controlled process, should be avoided.</p> <p>Compositions of mixtures of Zr metal and water should lie outside the range 3-25% water.</p> <p>Zr metal accumulations should not be subjected to violent mechanical forces.</p> <p>The production and accumulation of roughened Zr metal surfaces should be minimized.</p> <p>The production and accumulation of all Zr metal forms with high surface/volume or high surface/mass should be minimized.</p>
	Hulls waste forms must be consistent with limiting risk of hulls hazards.	Forms for storage must not be more dispersible, more leachable, more pyrophoric, or more reactive than the original hulls.

(contd)

Table 22. (contd)

Primary Criteria	Secondary Criteria	Tertiary Criteria
Normal process operations at the FRP include provisions to limit hulls hazards. (contd)	Hulls waste forms must be consistent with limiting risk of hulls hazards. (contd)	Hulls waste located outside plant containment must be in a form that does not result in release of aerosols, dust, vapor, or solution if exposed to the atmosphere.
Maintenance Operations at the FRP are consistent with limiting the hazards.	Maintenance of areas involving processing and storage of hulls must be defined and carried out.	<p>Hulls processing and storage areas must be inspected, according to a schedule outlined in writing, before plant operation starts.</p> <p>Equipment used in hulls processing, including containment, shielding, lifting, transport, monitoring, and control must be tested according to written schedule and procedures.</p> <p>Repair procedures for equipment used in processing and storage of hulls must be maintained in writing.</p> <p>Replacement of equipment involved in hulls processing and storage must be determined by its response to periodic tests and a decision system.</p> <p>Replacement of equipment used in processing and storage of hulls must be carried out according to written procedures.</p> <p>Decontamination of equipment used in processing and storage of hulls must be carried out according to written procedures when levels reach defined threshold.</p>
Abnormal operations at FRP must be consistent with limiting risks of hulls handling.	Accident counteraction plans must include both prevention and mitigation of hulls accidents.	<p>Equipment and instruments used in processing, storage, remote control, and surveillance of hulls operations must be capable of withstanding any credible accident and continuing operation after it.</p> <p>Radiation release in any hulls accident must be limited by building design, operating equipment, and emergency equipment to a fraction of total allowed for entire fuel cycle consistent with ALARA.</p> <p>Fire detection equipment must be appropriately located in areas where hulls are processed and stored.</p> <p>Equipment intended for suppression of hulls fires must be appropriate for use on metal fires.</p> <p>Fire suppression equipment must be appropriately located in areas where hulls are processed and stored.</p> <p>Explosions involving hulls must be localized by building design, mass limit, and storage and processing arrangements.</p> <p>All credible hulls accidents and their consequences should be described or modeled for a specific plant and should be available as a written catalogue.</p>

(contd)

Table 22. (contd)

Primary Criteria	Secondary Criteria	Tertiary Criteria
Abnormal operations at FRP must be consistent with limiting risks of hulls handling. (contd)	Accident counteraction plans must include both prevention and mitigation of hulls accidents. (contd)	Emergency procedures to be observed following each credible hulls accident must be available as a written catalogue.
Procedures for transport of hulls wastes must be consistent with limiting the risks.	Hulls transport must be carried out with appropriate containment and shielding.	Hulls transport packages must conform to DOT and NRC accident specifications for transport of radioactive materials and reactive metals. Hulls transport vehicles must be equipped with appropriate fire-suppression apparatus.

E. Zirconium Fines Behavior During Shearing Operations

A brief analysis was carried out of the hazards from pyrophoric materials likely to be present in the shearing of spent fuel assemblies. The equipment was assumed to consist of an argon-purged system, wherein a fuel bundle was mechanically fed into a two-step operation of bundle compaction followed by shearing of a short section of the entering end of the bundle. This operation was assumed to produce short segments that dropped through a chute into a basket. It was also assumed that some provision would be made for separating (e.g., by a cyclone) the dust generated in shearing from the argon purge stream. Although the analysis is based on a simple, basic concept of a shearing operation, the most important conclusions obtained are thought to be applicable to any design of a shearing operation.

To identify possible hazards imposed by the presence of zirconium in the conceptual fuel shear, a number of factors (see Table 23) conducive to pyrophoricity were presented, along with possible effects of the factors in the various components of the shear system. In general, the appearance of zirconium (Zircaloy) as a fine particulate was deemed the major pyrophoric hazard [KULLEN, LEVITZ]. Also suggested were three conditions of operation that should be avoided, conditions that would apply to any probable mechanical shear concept. They are

1. mechanical action that generates excessive zirconium dust and fine particles,
2. suspension of high concentrations of zirconium dust in a reactive atmosphere,
3. accumulation of zirconium and particles at a locale that might be exposed to a reactive atmosphere.

Because of the enclosed fuel-basket design of the conceptual shear, the problems related to fines generation and particle-size distribution were of interest. A review of past studies [FINNEY, WEST] indicated some results that, although quite obvious, need to be kept firmly in mind when developing design criteria. First, the amount of material dislodged (i.e., separated from discrete chopped-fuel segments) during shearing is inversely proportional

Table 23. Factors Conducive to Zircaloy Pyrophoricity
in a Conceptual Fuel-Shear Design

Factors Conducive to Pyrophoricity ^a	Sites of Potential Pyrophoric Hazards in Shear Process			
	Surfaces of Chute and Basket Holder	Argon Blanket	Basket	Dust Separator
Small Particle Size	D ^b	D	D	D
High Surface/Volume or High Surface/Mass	D	D	D	D
Roughened Zirconium Surfaces	---	---	D	---
Moisture (3-25%)	P ^c	P	P	P
Oxidizing Environment (air, O ₂ , acids)	---	---	---	---
Combustible Material (<i>e.g.</i> , organic lubricants)	P	---	---	---
Mechanical Agitation	D ^d	---	D	D
Accumulation of Metal	P	---	D	D
Zirconium Aerosols	---	P	---	P
High Temperatures	---	---	---	---
Ignition Sources (friction)	P	---	P	P
Problem Alloys	---	---	---	---

^aDerived from [KULLEN].

^bD denotes definite occurrence.

^cP denotes possible occurrence.

^dChute only.

to the length to which segments are chopped (see Fig. 14). The amount of Zircaloy dislodged was found to be much smaller than the amount of dislodged ceramic UO_2 fuel for any given segment length. For 2.5-cm cuts, for example, only about 2 wt % of the total Zircaloy cladding was dislodged, but about 50 wt % of the ceramic fuel separated from the segments. Reducing the cutting length to 1.3-cm segments resulted in essentially total dislodgment of UO_2 ; Zircaloy loss increased to only about 4 wt %. Figure 15 is a plot of particle sizes for both dislodged Zircaloy and dislodged UO_2 as a result of shearing 2.5-cm segments. From these data, Table 24 was derived to quantify the zirconium hazardous particle-size ranges in comparison with the UO_2 fines that will also appear in the total dislodged-material fraction of sheared fuel. The rather important implication of these data is that the Zircaloy is diluted a thousandfold with inert UO_2 powders and is *not* likely to be pyrophorically hazardous in the interim between shearing and introduction of the chopped fuel into nitric acid for dissolution. It became apparent that Zircaloy fines become a hazard only after the diluting UO_2 fines are dissolved, allowing concentrated zirconium powders to accumulate.

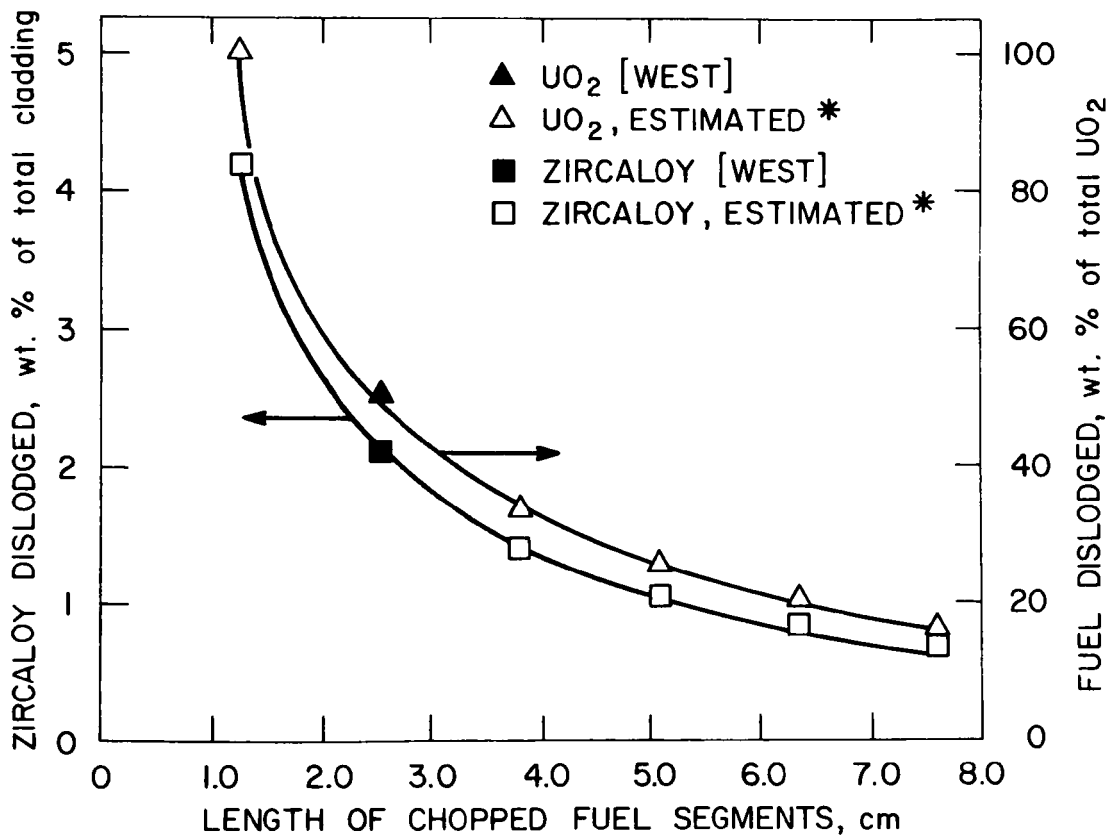


Fig. 14. Quantity of Dislodged Material as a Function of Chopped-Fuel Length

* Estimated from data on stainless steel-clad fuel [FINNEY].

The above information may indicate that emphasis on fines hazards for operations preceding the fuel-dissolution step is unnecessary. Further, it may be desirable to increase the emphasis on fines-handling criteria for operations during and after fuel dissolution.

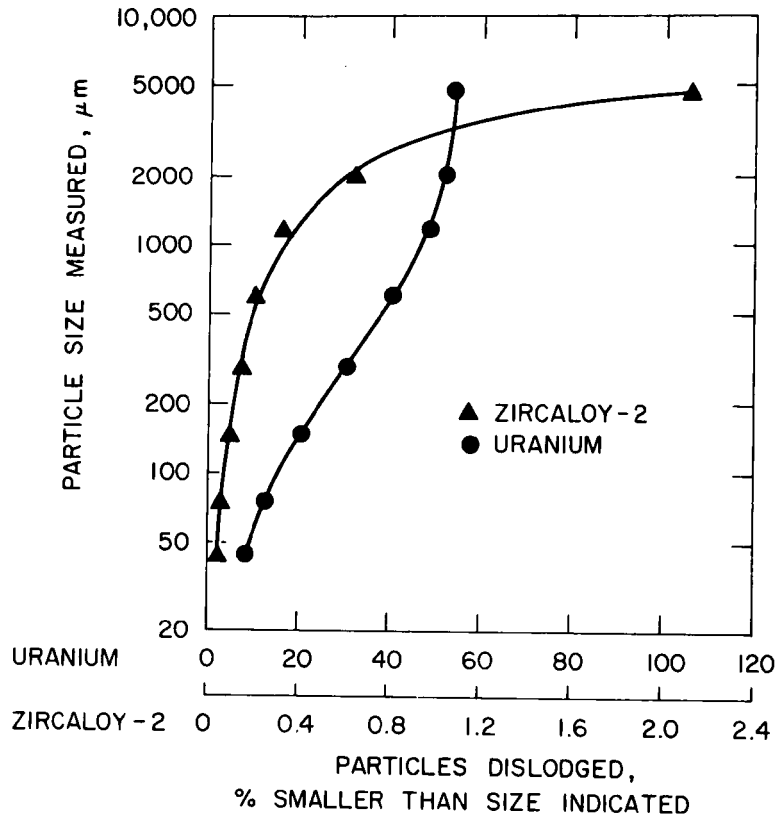


Fig. 15. Size Distribution of Zircaloy-2 and Uranium Particles Dislodged from Shearing Zircaloy-2-Clad UO_2 Prototype Fuel Rods Into 2.5-cm Lengths. (Reproduced from [WEST]). Conditions: (1) Fuel: a stacked array (8×8) of unsecured Zircaloy-2 fuel tubes, 1.12-cm OD \times 0.081-cm wall, filled with UO_2 pellets with a 0.0064-cm annular clearance. (2) Shear: horizontally actuated ORNL 250 Mg with a stepped blade operating at 3.10 cm per s

Table 24. Estimated Amounts and Ratios of Particles
from Shearing of LWR Fuel

Particle Size Range, μm^a	General Risk Category for Metallic Zr ^a	Wt of Zircaloy in Size Range, kg/Mg fuel ^b	Wt of UO_2 in Size Range, kg/Mg fuel ^b	Ratio, Zircaloy/ UO_2
60-1000	Fire Hazard	6×10^{-1}	4×10^2	1.5×10^{-3}
<60	Explosive	3×10^{-1}	1×10^2	3×10^{-3}

^a[KULLEN, LEVITZ].

^bEstimated from the percentages given in Fig. 15 and the assumption of 1.1 Mg of UO_2 and 290 kg of Zircaloy per Mg of uranium in fuel.

VII. TRANSPORT PROPERTIES OF NUCLEAR WASTES IN GEOLOGIC MEDIA

(M. G. Seitz, P. G. Rickert,* A. M. Friedman,*
S. M. Fried,* and M. J. Steindler)

A. Introduction

Fission products and some transuranic elements are contained in wastes generated in nuclear reactor fuel during power production. Because the waste is radioactive and represents a hazard to health, it must remain isolated from the biosphere. Some fission products and actinide elements are long-lived, necessitating that the waste be isolated for long periods of time until they become radiologically innocuous. A method being considered for permanently disposing of the waste is to emplace it in deep geologic formations (geologic repositories).

As part of the evaluation of the safety of a geologic repository, the duration of long-term isolation of the wastes must be assessed. Groundwater infiltrating the repository is considered the most credible mechanism for mobilizing nuclides from a disrupted repository in a well-chosen geologic site. Our experimental program was undertaken to give information on the migration of radionuclides in aqueous solution-rock systems.

The current concept of migration by infiltration assumes that groundwater passes through a breached repository and leaches trace amounts of radionuclides from the solidified waste. The water then carries the radionuclides into the adjacent geologic formations, and constituents of the solution react with the rock. If it is assumed that the radionuclides are freely leached from the repository, it is their reactions with rock materials that determine their migratory behavior. Experiments described in this report were performed to determine the reactions of radionuclides in solution-rock systems.

B. Rock and Solution Characterization

Analyses to characterize the rocks used in the program were performed on granulated samples of the rocks. The rock samples were each aliquots from ~150 g of material that was homogenized by crushing in a hard steel mortar. Various types of analyses have been performed on 32 of the rocks studied in the program.

Aqueous solutions were prepared for analyses by contacting powdered samples of the rocks with distilled water. The mixtures of rocks and water were each stirred for ~4 weeks at ambient temperatures, the powdered rock was allowed to settle, and the solution was decanted and passed through a 0.45- μ m-pore Millipore or a 0.4- μ m-pore Nuclepore filter. The solutions obtained by this procedure were clear and free of visible particulate.

The stirring procedure is used to prepare rock-equilibrated waters (REW) for the experimental program. Since the composition of a REW solution is established during extended periods while water is continuously mixed with granulated rock, little change in the chemistry of REW would be expected upon subsequent contact of the water with rock during experiments. The procedure

* Chemistry Division, Argonne National Laboratory.

of preequilibrating water with rock contrasts to the use of solutions of arbitrary composition; for the latter, there is, in general, no way of ensuring that no major change in solution composition will occur upon contact with the rock.

Analyses by X-ray diffraction of powdered samples of three of the rocks used in column-infiltration experiments described in this report are given in Table 25. A mineral fraction of the chalk was obtained by removing the acid-soluble components (mainly calcite), *i.e.*, by treating the powdered rock with acetic acid buffered to pH 5 with sodium acetate. The insoluble components of the chalk were determined to be quartz and hydrous minerals by X-ray diffraction.

Table 25. X-Ray Diffraction Analyses of Rocks
Used in Nuclide Migration Experiments

Sample Description	Mineral Phases Identified		
	Major	Minor	Trace
Chalk, Selma	Calcite (CaCO_3)	Quartz (αSiO_2)	Kaolinite, Montmorillonite
Acid-Insoluble Residue of Selma Chalk (20% of the Chalk's Weight)	Quartz	Kaolinite Montmorillonite	
Shale, Pierre	Quartz, Feldspar	Meta-halloysite type pattern	
Limestone, Salem Formation	Calcite		

The analyses by X-ray diffraction were sufficient to allow major and minor minerals occurring in the rocks to be determined. Since no mineral fractions were separated, no specific chemical information within mineral groups (such as the feldspars or the montmorillonites) was obtained.

Spectrochemical analyses of rock samples were determined from d-c arc and copper electrode emission spectra. The spectrochemical analyses indicate the major and minor cations present in the samples and give upper concentration limits for cations that are not detected. The analyses will be used as a guide to further analyses of the samples for specific cations.

The REW solutions are being analyzed for major cations by atomic-absorption spectroscopic procedures. Anionic species such as chloride, nitrate, etc. will be determined by colorimetric techniques. Total alkalinity will be determined by titration.

The total dissolved-solids contents of REW solutions were estimated by evaporating the water and drying the residue at 180°C. These weights per liter of solution are given in Table 26 for the three rocks used in the experiments described in this report. The acidity (pH) and the oxidation potential of deaerated REW solutions are also given in Table 26.

Table 26. Total Dissolved Solids, Hydrogen Ion Concentrations, and Oxidation Potentials of Pre-Equilibrated Deaerated Solutions

Rock Used to Equilibrate Solutions	Total Dissolved Solids, mg/L (dried at 180°C) ^a	Hydrogen Ion Concentration, pH	Oxidation Potential, ^b V
Chalk, Selma	111	8.0	0.269
Shale, Pierre	173	7.8	0.269
Limestone, Salem Formation	42	7.6	0.277

^a Solutions were filtered through 0.4- μ m-pore filters.

^b Oxidation potentials of the deaerated solutions were measured using a standard calomel electrode. A Zobel reference solution was measured to have an oxidation potential of 0.425 V.

Residual solid concentrations in the water samples represent estimates of the extents of reaction of the rocks with waters. The values listed in Table 26 are comparable to or exceed the total dissolved solids (in mg/L) of some natural waters [ROSTER]. However, the residual solids contents measured in REW are considerably below (lower by ~ 2 orders of magnitude) that measured in some near-surface groundwaters [COLOMBO]. These near-surface groundwaters are believed to contain organic constituents that account for most of the residual solids and that would not be expected in deep groundwater.

C. Column Infiltration Experiments

In interpreting the results of column infiltration experiments, simplifying assumptions have been made concerning the water-rock systems. One of these assumptions is that the rock can be represented as a continuous, homogeneous medium. Various tests of homogeneity were applied to examine columns used in calcine infiltration experiments with cesium (ANL-78-11) with the conclusion that the complex behavior of cesium was due to chemical properties of the cesium rather than to the hydrodynamic properties of the columns. As an additional aid to examining the characteristics of rock columns, experiments were run in which tritiated water was used to trace the migrating water front in columns. Four rock-aggregate columns, two of shale and two of chalk, were prepared in a manner analogous to that used to prepare previous columns (ANL-78-11). Columns were formed by packing successive layers at total of 20 g of rock aggregate in a Buchner funnel. Shale columns prepared in this manner had a measured volume of 16.7 cm³ and a measured porosity of 27%; chalk columns had a volume of 20 cm³ and a porosity of 40%. The columns were saturated

with REW, then by 0.5 mL of REW containing tritiated water (2.35×10^4 dpm/0.5 mL), and then by REW containing no tritium. The eluates were collected in fractions, and the tritium contents of the eluates were analyzed by liquid scintillation counting. Counting solutions were made by adding 1 mL aqueous solution to 19 mL of organic scintillation liquid (Insta-Gel, Packard Instr.). The volumes of the eluates and the activities of tritium in the eluates are given in Table 27. The eluate fractions were collected by manually replacing a tube containing the eluate with an empty tube. This resulted in unequal fraction sizes (Table 27).

The percentages of the total activity in the eluates are given in Table 27 (fifth column) and were calculated based on the measured activities of the initial tritiated water. The percentages of activity were summed for succeeding samples to give the cumulative percent of the activity recovered from the columns, which are also given in Table 27 (sixth column). It is seen from the table that most of the activity was recovered in the first 20 to 40 mL of eluate volume. All of the activity was recovered from the shale columns, as evidenced by the cumulative percent being close to 100. The cumulative percentages calculated for the chalk columns were low in one case (90% in Expt. 63-3) and high in another (128% in Expt. 63-4). For Expt. 63-4, the volume of one eluate fraction was not recorded but was estimated from the length of time the sample was collected, it being assumed that the flow rate was constant. This eluate was calculated to contain 64% of the activity in the system, and an error in the estimated volume of the sample may be responsible for the cumulative percentage exceeding 100. Thus, the high value for this experiment may reflect an error in procedure.

No plausible reason is known for the low cumulative percentage of tritium in Expt. 63-3 with the chalk column. Losses of activity (for example, by evaporation) were minimized, as evidenced by the quantitative recovery of activity from the shale columns.

The activity of the eluates versus the volume of the eluates is plotted in Fig. 16 for column 63-1. In addition to the data, a curve derived from a mixing model is plotted in the figure. The mixing model was developed to account for the dilution of the activity in the liquid that was above the rock columns. The volume of liquid above the rock column was maintained at about 10 mL. The activity of the solution entering the column was calculated by assuming that REW solution containing no activity continuously flowed into the liquid above the rock columns and mixed with that liquid and thereby diluted its concentration of tritium. The volume of REW solution flowing into the liquid above the column was taken to be equal to the volume of tritiated solution entering the column. The agreement between the mixing model and the experimental data indicates that all of the characteristics of the eluate-activity curve reflect the mixing in the volume of solution above the columns.

From Table 27, it can be seen that the dispersive effects in the migrating waters are not large and that most of the activity is contained in a volume of solution comparable to the volume of the shale columns (16.6 cm^3). Tritium penetrated the columns with little water flow; all of the tritium was eluted in a solution having a few times the volume of the column. This contrasts with cesium that, as seen by the experiments (ANL-78-11), would only penetrate a column of shale after ~ 20 column volumes of eluate passed through the column.

Table 27. Activities of Tritium in Eluates from Four Column-Infiltration Experiments

Experiment	Eluate No.	Eluate Volume, mL	Eluate Activity, cpm	Eluate Activity, % of Total	Total Eluate Activity, cumulative percent
63-1, Shale Column	1	0.1	34.3	0.0	0.0
	2	12.8	1.59×10^4	68	68
	3	4.8	3.35×10^3	15	83
	4	11.5	3.23×10^3	14	97
	5	3.3	3.58×10^2	2	99
	6	6.0	3.37×10^2	1	100
63-2, Shale Column	1	0.2	8.9	0.01	0.0
	2	12.8	1.98×10^4	84	84
	3	6.0	2.02×10^3	9	93
	4	12.5	1.17×10^3	5	98
	5	5.0	1.57×10^2	1	99
	6	6.0	7.74×10^1	0.3	99
63-3, Chalk Column	1	0.2	1.0	0.004	0.0
	2	0.5	--	--	0.0
	3	8.5	8.11×10^3	34	34
	4	1.5	2.08×10^3	9	43
	5	4.0	5.39×10^3	23	66
	6	12.5	5.04×10^3	21	87
	7	8.0	3.67×10^2	2	89
	8	23.0	3.06×10^2	1	90
	9	10.7	20.3	0.08	90
	10	27.0	24.3	0.07	90
	11	20.0	4.0	0.01	90
	12	6.0	--	--	90
63-4, Chalk Column	1	0.4	3.0	0.01	0.01
	2	0.9	11.9	0.05	0.06
	3	9.0	9.53×10^3	40	40
	4	1.5	2.04×10^3	9	49
	5	12.8 ^a	$(1.52 \times 10^4)^b$	$(64)^b$	113
	6	40.0	3.22×10^3	14	127
	7	17.0	81.6	0.3	127
	8	38.0	1.10×10^2	0.4	128
	9	17.5	--	--	128
	10	27.0	--	--	128
	11	20.0	--	--	128
	12	6	--	--	128

^aEluate volume was not measured but was estimated from the flow rate and the length of time the sample was collected.

^bCalculated. See text.

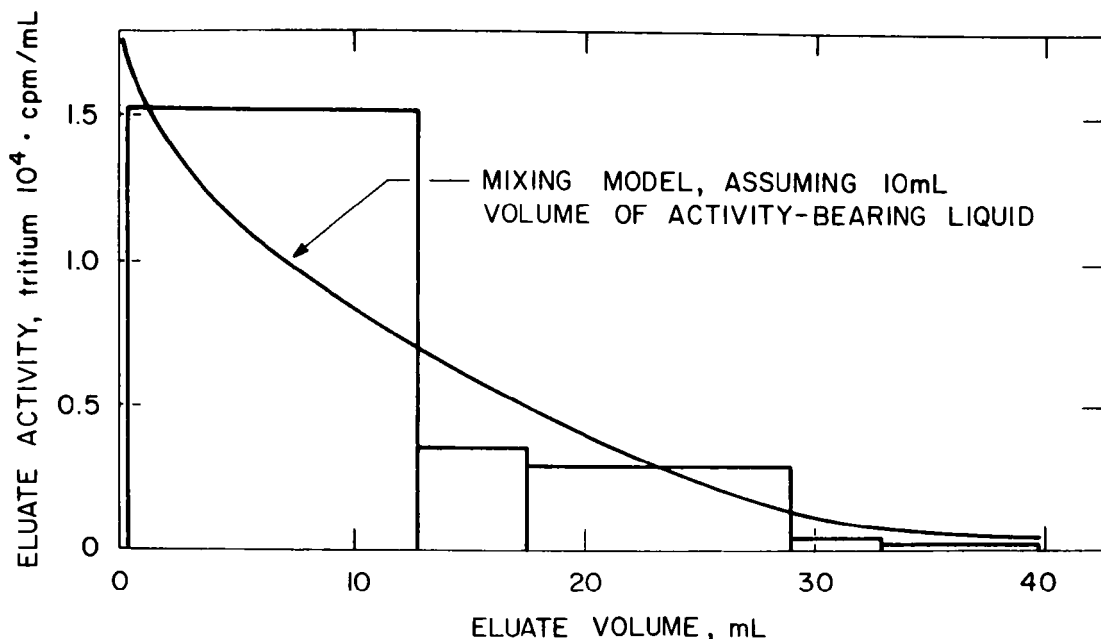


Fig. 16. Elution Curve for Tritium in a Shale (Pierre) Column of 17-cm³ Volume. Expt. 63-1

Moreover, the cesium persisted in eluates of a hundred column volumes or more without ever being fully elutriated from the columns. Thus, dispersive effects in the water front are clearly too small to account for the behavior of cesium, and the large dispersion was due to chemical reactions with the rock.

D. Static-Absorption Experiments

Experiments were also performed to investigate the apparent synergistic behavior seen in previous static-absorption experiments. In the previous work (ANL-78-11), the addition of solutions containing plutonium to solutions containing americium often had a significant effect on the partitioning of americium between rock and solutions. The source of the apparent synergistic behavior was postulated to be auxiliary chemicals in the plutonium solution rather than the plutonium itself.

The plutonium solutions used in the experiments reported here were purified by passing them through cation exchange columns twice, rather than once, to increase their purity. The plutonium solutions were otherwise treated in a manner similar to that previously used, *i.e.*, the solution was dried, the plutonium was redissolved in distilled water, etc.

In four tests in which dissolved plutonium was added to an americium solution that had reacted with limestone tablets, no synergistic effect was observed. This result strongly suggests that the synergistic effect seen previously was not caused by plutonium. The results suggest that the synergistic effect is caused by an auxiliary chemical(s) which was removed by the purification procedure.

There is another possible reason for the absence of synergistic behavior--the americium used in the most recent experiments was somehow different from that used previously, *i.e.*, was not sensitive to the addition of plutonium. For example, a difference in the chemical form of the americium or the presence of plutonium or auxiliary chemicals in the initial americium solution might have masked synergistic behavior.

E. Conclusions

The use of tritiated water appears to be a useful method for examining the behavior of water fronts advancing through the columns. Dispersive effects are so small in the columns that the effects observed in the experiments can be attributed entirely to the mixing of tritium activity with solutions above the columns. However, because most of the activity comes through the column in a small volume of eluate, it is necessary to collect fractions smaller than can be collected by manually changing collecting tubes to determine details of the elution curve.

Apparatus consisting of solvent pumps, stainless steel tubing, sample injection valves, and fraction collectors will be examined for use in rock infiltration experiments. The apparatus has the potential to (1) maintain controllable and constant flow rates, (2) inject nuclide samples without disturbing the flow of solution through the columns, (3) minimize solution dead space within the system, and (4) fractionate the eluate into small aliquots of sequentially eluted solution. This apparatus should allow development of the full potential of the tritiated-water technique.

Synergistic behavior was found to be absent in experiments in which plutonium-bearing aqueous solutions were added to aqueous solutions containing americium that had reacted with rock. This result suggests that plutonium does not have a synergistic effect on the behavior of americium. The results suggest further that added plutonium purification steps removed those chemicals from the plutonium spike that interfered with the absorption of americium. Alternatively, the americium solution may have changed, making it insensitive to the addition of the plutonium solution.

VIII. TRACE-ELEMENT TRANSPORT IN LITHIC MATERIAL
BY FLUID FLOW AT HIGH TEMPERATURE
(M. G. Seitz and R. A. Couture)

A. Introduction

The objective of this work is to examine trace-element transport produced by aqueous fluid flow in geologic materials at high temperatures.

Many geologic phenomena are thought to originate by mass transport from fluids at high temperatures. During metamorphism of sediments, for example, large masses of aqueous solutions may be driven out of rock by pressure gradients. Also, during emplacement of a pluton (a large body of rock which has crystallized at depth in the earth's crust), large masses of fluids may be driven off by contact heating. The residual rock may be uniform in composition, in which case equilibrium behavior derived from hydrostatic experiments may best describe the evolution of the rock. However, in many geologic bodies, the reactions produce two or more mineralogically distinct zones of rock (metasomatic zoning). Metasomatic zoning has been studied extensively, both in theory and from field evidence [TURNER, THOMPSON, HOFMANN-1972, HOFMANN-1973, KORZHINSKII]. Mass transport by fluid flow is the only mechanism capable of establishing both the zoning and large concentration gradients over the distances involved.

Trace elements may move along the observed gradients. In some cases, trace element migration may be of considerable economic or practical interest. Selective extraction of soluble trace elements during metamorphism may give rise to ore bodies or pegmatites. Soluble or volatile elements extracted by hydrothermal fluids in geothermal areas may cause pollution or fouling of equipment and wells used in geothermal power plants.

Mass transport by fluid flow at high temperature may adversely affect isolation of radionuclides in solidified nuclear waste. Deeply buried waste is subject to heating from the earth's thermal gradient in addition to radiogenic self-heating. The average temperature at a depth of 5 km on the continents is near 180°C. In current waste disposal concepts, temperatures of about 300°C are allowed at the rock-waste interface. In addition, a geologic waste repository could conceivably be subject to heating from intrusive bodies (magma). The experimental procedures and concepts to be developed in this program are expected to be directly applicable to the evaluation of nuclide migration from a waste repository at high temperatures.

In the program, measurements of transport properties of trace elements in minerals and rocks will be made at temperatures up to 600°C. The objectives of this report are to provide an introduction to this project, to report on new experimental apparatus designed for the work, and to outline possible uses of the apparatus.

B. Experimental Method and Theoretical Consideration

Concepts of simple chemical equilibrium are not adequate to describe the transport of major elements or trace elements. Absorption of trace elements by rocks or minerals may involve the formation of new solids, recrystallization of surface layers, or diffusion inside a crystal. Because of slow kinetics,

such reactions may depend greatly on flow rate and may be impossible to model with thermodynamic data derived from static experiments. Moreover, the calculation of flow rate, a simple but important factor, depends on parameters such as pore size, pore tortuosity, and viscosity, all of which can be affected by chemical reactions. Model calculations of chemical transport by fluid flow predict rock zonation generally similar to that found in nature. The models, however, lack accurate diffusion and reaction rates of chemical species, preventing comparisons of model predictions to specific natural rock formations. This problem is complicated because in the major element species the behavior of rate parameters is often nonlinear in relation to chemical concentration.

An alternative method of understanding the origin of these formations is by laboratory experimentation on mineral and rock-solution reactions during fluid flow (infiltration). In this method, liquid is forced through packed columns of rock or mineral, and the effluent is analyzed. Substances will be introduced into the stream in trace quantities and will be eluted to determine their relative migration rates. In cases in which a substance is not eluted, the columns can be sectioned, and the solids analyzed.

The experiments in this program will investigate the motion of trace elements because, aside from previously mentioned kinetic factors and other complications, they are expected to exhibit simpler behavior than major elements. In natural rock formations, trace elements are exchanged onto the surface layer or into the lattice of a mineral, where they are expected to obey the relatively simple laws of dilute solutions. Furthermore, large changes in the trace element concentrations in the fluid phase may be recognized at the onset of infiltration metasomatism before metasomatism leads to the destruction of the rock matrix. On the other hand, only in exceptional cases could proportionately large changes in major element concentrations occur without recrystallization or destruction of the crystal lattices in the rock matrix. These features considerably simplify model calculations and experimentation on trace element migration.

Concentration profiles similar to those arising by elution of chromatographic columns are predicted. Whether trace-element migration does in fact exhibit this behavior at high temperatures will be observed in this experimental program.

C. Other Applications of Infiltration Experiments

Infiltration experiments are uniquely applicable to a wide range of chemical and geological problems, in addition to trace element migration. Such experiments are especially well suited to determining rates and reversibility of reactions between solid and liquid, including reactions at the solid surface which are otherwise difficult to study. In hydrothermal systems, infiltration experiments have an advantage over static experiments: the fluid composition can be readily changed during the course of the experiment. By sampling the initial liquid and the effluent, the rate of reaction can be determined as a function of solution composition, solid solution impurities in the surface layer, history of the solid, and flow rate. In this way, the solubilities and rates of dissolution or formation of minerals can be studied.

For example, by measuring small changes in pH of sea water passing through columns of carbonate minerals, Weyl [WEYL] determined that when crystals of calcite (CaCO_3) or dolomite [$\text{CaMg}(\text{CO}_3)_2$] grow in sea water, the rate of growth decreases with increased flow rate, evidently because of increased solubility of the surface layer. He determined that the increased solubility is due to magnesium in the surface layer (or excess magnesium in the case of dolomite), the amount of which increases with rapid flow and decreases with aging (recrystallization) of the solid in the absence of flow. This means that it is erroneous to speak of a single solubility of calcite, since the solubility depends on the history of the solid. Weyl determined that the magnesium-rich surface layer is sufficiently soluble to severely limit the rate of formation of inorganic calcite or dolomite in the oceans [WEYL]. In fact, the formation of dolomite is unknown in normal sea water at ambient temperatures, in agreement with Weyl's findings.

Thus, in general, the degree of incorporation of trace elements into a surface, and hence the rate of migration by fluid flow, may be dependent on flow rate, as it is in the cases of calcite and dolomite. Conversely, formation of a solid may be greatly hindered by surface impurities.

There are many implications of Weyl's findings and potential applications of similar techniques. For example, Weyl was able to relate the solubility characteristics of natural calcite samples to the environment of formation. Using filtration experiments, one might also study kinetics of dolomite formation at high temperatures or might study a number of hydrothermal reactions involving refractory minerals. Finally, infiltration experiments are applicable to studies of leaching of solid wastes by groundwater at high temperatures. Leaching of solid wastes by groundwater may well depend in complicated ways on solution composition and flow rate, just as the formation of calcite in sea water does.

D. Experimental Apparatus

Apparatus for work in the initial stage of the program is depicted in Fig. 17. In this apparatus, columns and sample injection valve are connected by high-pressure stainless steel tubing and are enclosed in a convective oven that can be heated to temperatures up to 300°C . One or two mineral or rock columns upstream from the sample injection valve are used to react the aqueous solvent with the lithic material prior to the solvent entering the reaction column. This design serves to minimize in the reaction column, those chemical reactions which do not involve the trace element, thereby isolating trace-element reactions from the major-element reactions. The trace element solution is introduced into the final column by the sample injection valve. In some experiments, the first two columns may not be used. In such a case, the sample injection valve can be located outside the oven.

The pressure in the system is controlled by a back-pressure regulator valve ($0-4.8 \times 10^4$ kPa, $0-70 \times 10^3$ psi) located outside the oven. Fluid flow control is provided by a high-pressure solvent-metering pump capable of delivering solvent at flow rates from 0.01 to 10.0 mL/min and at pressures to 7×10^4 kPa (1.0×10^4 psi).

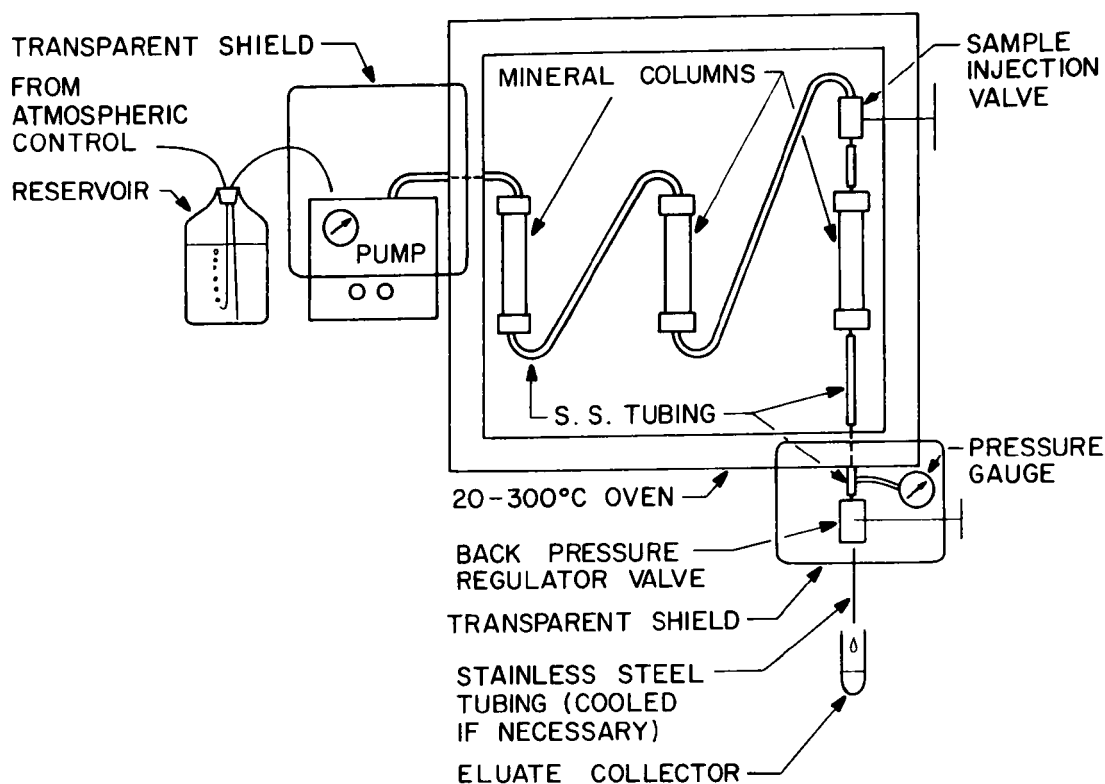


Fig. 17. Apparatus for Study of the Transport of Fluids Through Rock at High Temperatures and Pressures

A fraction collector at the low-pressure side of the pressure regulator valve is used to collect the eluate for subsequent analysis.

It is planned to install equipment to control initial pressures of CO_2 and O_2 . It is also planned to install pH-measuring equipment since the pH of the eluate is a sensitive indicator of major element reactions in the column.

The equipment on hand is capable of operation up to 290°C and 5×10^4 kPa (7300 psi). A different back-pressure regulator valve, different column seals, and different sample injection procedure which may be needed at high temperatures and pressures appear to be available from commercial suppliers.

The equipment has been partly tested and appears to work well. In order to verify the suitability of the pumps and columns for work with clays, a column of kaolinite was prepared by compacting a thin slurry of the clay under pressure. The kaolinite has a mean equivalent spherical diameter of $0.8 \mu\text{m}$. In a column 1 cm in diameter and 3.5-cm high, the pressure drop was 9.6×10^3 kPa (1.4×10^3 psi) at room temperature at the nominal flow rate of 0.05 mL/min water. Thus, the high pressures generated by the pumps are required to infiltrate clays, and the equipment appears to be well suited for the work in the program.

It was deemed that the inside surfaces of the high-pressure components should be lined with inert material to minimize reactions with the aqueous solution. Lining the capillary tubing is difficult, but attempts are being made to get it gold-plated or coated with inert plastic (Teflon). A supply of nickel tubing has been ordered which may be more inert than stainless steel and which can be substituted for stainless steel if coating is not possible. A heavy oxide coating on the nickel or stainless steel may also provide protection from chemical reaction.

E. Planned Experimental Program

The initial experiments will be conducted in relatively simple systems, using clay minerals. Clay minerals are abundant in most sedimentary rocks and occur as alteration products in igneous and metamorphic rocks. Because many clay minerals have high exchange capacities, they may determine the trace element migration characteristics of rocks in which they are present. Initial experiments are planned on the sorption of cesium and strontium on kaolinite (hydrous aluminum silicate) and talc (hydrous magnesium silicate). These have low exchange capacities (3-15 meq/100 g). Experiments are planned with smectites and glauconite, which have higher exchange capacities (70-100 meq/100 g and 11-20 meq/100 g, respectively).

Trace-element migration studies are also planned for common rock-forming minerals such as quartz or feldspar. Among the feldspars, replacement of plagioclase by albite (Na plagioclase) is well known in spilites (Na-rich basalts). The replacement is likely to be preceded by modifications in trace element chemistry, which could be revealed by infiltration experiments. If strontium does show chromatographic-type behavior, knowledge of the migration properties would be an important tool in recognizing and analyzing geologic formations undergoing processes of infiltration metasomatism.

In most initial experiments, it is planned to study the migration of cesium and strontium. If continuity of this program is maintained, it is planned to begin work with actinides by 1980.

REFERENCES

AGNS

Allied-Gulf Nuclear Services, *Final Safety Analysis Report; Barnwell Nuclear Fuel Plant Separations Facility*, DOCKET 50-332 (October 1973).

Allan

C. R. Allan and R. V. Jolliffe, *Explosive Dissemination of Compacted Powders*, AD-849998 (EA-TR-4263), Edgewood Arsenal, Maryland (February 1969).

ANL-77-36

M. J. Steindler, Milton Ader, G. J. Bernstein, K. F. Flynn, T. J. Gerding, L. J. Jardine, B. J. Kullen, W. J. Mecham, B. B. Saunders, W. B. Seefeldt, M. G. Seitz, A. A. Siczek, and L. E. Trevorow, *Chemical Engineering Division Fuel Cycle Programs, October-December 1976*, ANL-77-36.

ANL-78-11

M. J. Steindler, Milton Ader, R. E. Barletta, G. J. Bernstein, K. F. Flynn, T. J. Gerding, L. J. Jardine, B. J. Kullen, R. A. Leonard, W. J. Mecham, R. H. Pelto, B. B. Saunders, W. B. Seefeldt, M. G. Seitz, A. A. Siczek, L. E. Trevorow, A. A. Ziegler, D. S. Webster, and Leslie Burris, *Chemical Engineering Division Fuel Cycle Programs, January-September 1977*, ANL-78-11.

Avogadro

A. Avogadro and J. W. Wurm, *Pyrochemical Separation of Plutonium From Irradiated Fuels*, ANL-TRANS-702 (December 1968).

Bell

D. C. Bell, *Post Calcination Treatment of Commercial Wastes in Waste Management Development Technical Progress Report July-September 1976*, Allied Chemical Corp. (Idaho), ICP-1106, p. 11 (November 1976).

Bonner

W. F. Bonner, H. T. Blair, and L. S. Romero, *Spray Solidification of Nuclear Waste*, Battelle Pacific Northwest Laboratories, BNWL-2059 (August 1976).

Breschet

C. Breschet and P. Miquel, *Proc. Int. Solv. Extr. Conf., ISEC 71, Vol. 1, Society of Chemical Industry, London*, pp. 565-576 (1971).

Brodda

B. G. Brodda and D. Heinen, *Nucl. Tech.* 34, 428 (1977).

Brown-1957

P. G. M. Brown, J. M. Fletcher, and A. G. Wain, *Report A.E.R.E. C/R 2260* (1957).

Brown-1958

P. G. M. Brown, J. M. Fletcher, C. J. Hardy, J. Kennedy, D. Scargill, A. G. Wain, and J. L. Woodhead, *Second United Nations Intern. Conf. Peaceful Uses of Atomic Energy, Geneva, Vol. 17, p. 118* (1958).

Brown-1960

P. G. M. Brown, J. Inorg. Chem. 13, 73 (1960).

Burger

L. L. Burger and E. D. McClanahan, Nucl. Tech. 50, 153 (1958).

Busby

M. R. Busby, J. E. Kahn, and J. P. Belk, *Effects of Explosion-Generated Shock Waves in Ducts*, Proceedings of the Fourteenth Air Cleaning Conference held at Sun Valley, Idaho, August 2-4, 1976, pp. 210-220.

CFR-10

Code of Federal Regulations 10 Energy, Parts 0 to 199 (Revised as of January 1, 1977), U.S. Government Printing Office, Washington, D.C. (1977).

CFR-40

Code of Federal Regulations 40 Protection of Environment Parts 100 to 399 (Revised as of July 1, 1977), U.S. Government Printing Office, Washington, D.C. (1977).

Chiotti

P. Chiotti and K. J. Gill, Trans. Met. Soc. AIME 221, 573 (1961).

Chitty

A. Chitty and D. R. Slade, AERE/X/PR-2506 (May 1959).

Colombo

P. Colombo, A. J. Weiss, and A. J. Francis, *Evaluation of Isotope Migration--Land Burial*, BNL-NUREG-50695, Quarterly Progress Report, January-March 1977 (September 1977).

Craig

J. A. Craig, R. E. Balzhiser, and D. V. Ragone, Trans. Met. Soc. AIME 242, 1809 (1968).

Dresner

L. Dresner and C. V. Chester, *Attenuation of Shock Waves in Long Pipes by Orifice Plates, Rough Walls, and Cylindrical Obstacles*, ORNL-4288 (July 1968).

EXXON

Exxon Nuclear Company, Inc., *Nuclear Fuel Recovery and Recycling Center; Preliminary Safety Analysis Report*, DOCKET 50-564 (1976).

Fee-1975A

D. C. Fee and C. E. Johnson, *Phase Equilibria and Melting Point Data for Advanced Fuel Systems*, ANL-AFP-10 (June 1975).

Fee-1975B

D. C. Fee and C. E. Johnson, *Chemical Compatibility Between Cladding Alloys and Advanced Fuels*, ANL-AFP-9 (May 1975).

Finney

B. C. Finney, B. A. Hannaford, G. A. West, and C. D. Watson, *Shear-Leach Process: Semicontinuous and Batch Leaching of Sheared, Unirradiated Stainless-Steel-Clad and Zircaloy-2-Clad UO₂ and UO₂-ThO₂*, ORNL-3984 (July 1969).

Fletcher-1958

J. M. Fletcher, *J. Inorg. Nucl. Chem.* 8, 277 (1958).

Fletcher-1959

J. M. Fletcher, P. G. M. Brown, E. R. Gardner, G. J. Hardy, A. G. Wain, and J. L. Woohhead, *J. Inorg. Nucl. Chem.* 12, 154 (1959).

Gershinskii

A. E. Gershinskii, A. A. Khoromenko, and E. I. Cherepov, *Kinetics of Interaction Between Films of Al and SiO₂*, *Izv. Akad Nauk SSSR* 12, 627-30 (1976).

Goldenson

J. Goldenson and J. Wilcox, *Carrier Dusts for Toxic Aerosols, II Preliminary Dispersal Tests*, AD-499904, Technical Command, Army Technical Center, Maryland (January 30, 1951).

Gorbunov

V. F. Gorbunov, G. P. Novoselov, and S. A. Ulanov, *The Precipitation of Plutonium Dioxide From Fluoride Melts*, translated from *Atomnaya Energiya* 37, 435 (November 1974).

Gregory

W. S. Gregory *et al.*, *Tornado Depressurization and Air Cleaning Systems*, Proceedings of the Fourteenth Air Cleaning Conference held at Sun Valley, Idaho, Aug. 2-4, 1976, pp. 171-193.

Hahn

H. T. Hahn and E. M. VanderWall, *J. Inorg. Nucl. Chem.* 26, 191 (1964).

Hansen

W. N. Hansen, NAA-SR-7660 (1963).

Healy

T. V. Healy, *Proc. Management of Radioactive Wastes from the Nuclear Fuel Cycle*, I.A.E.A., Vienna, Vol. 1, p. 201 (1976).

Hishida

M. Hishida and M. Hori, *Experiment on Pressure Wave Propagation (1) The Result of Experiment on Branches and Bends*, JAPFNR-187 (November 1974).

Hofmann-1972

A. Hofmann, *Chromatographic Theory of Infiltration Metasomatism and Its Application to Feldspars*, *Amer. J. Sci.* 272, 69-90 (1972).

Hofmann-1973

A. Hofmann, *Theory of Metasomatic Zoning, a reply to Dr. D. S. Korzhinskii*, *Amer. J. Sci.* 273, 960-964 (1973).

Hofmann-1974

P. Hofmann, *Studies on the Reactivity of Steels With Simulated Fission Products in the Presence of UO_2 and UC and Possible Ways of Improving the Compatibility Behavior of Oxide Fuel Pins*, EURFNR-1177 (1974) [German Version KFK-1831].

Holley

C. E. Holley, Jr., *J. Nucl. Mater.* 51, 36 (1974).

Jardine

L. J. Jardine, Argonne National Laboratory, private communication to M. J. Steindler (May 1975).

Johnson

I. Johnson, *Compounds of Interest in Nuclear Reactor Technology*, Met. Soc. AIME, Special Report No. 13, 171 (1964).

Kateley

J. A. Kateley, M. J. Tschetter, and P. Chiotti, *J. Less-Common Metals* 26, 145 (1972).

Kisbaugh

A. A. Kisbaugh, USAEC Report DP-818 (1963).

Knighton

J. B. Knighton, I. Johnson, and R. K. Steunenberg, *Uranium and Plutonium Purification by the Salt Transport Method*, Symposium on Reprocessing of Nuclear Fuels, CONF-690801, Nuclear Metallurgy, Vol. 15, P. Chiotti, Ed. (1969).

Koch

V. G. Koch, *Zur Wiederaufarbeitung von Kernbrennstoffen durch Flüssig-Flüssig - Extraction mit quartären Ammoniumnitraten*, Kerntechnik 7, 394 (1965); also in *Reprocessing by Quaternary Ammonium Nitrates: Laboratory Studies in Solvent Extraction Chemistry of Metals*, Proc. Int. Conf. Harwell, September 1965, H. A. C. McKay, I. L. Jenkins, and A. Naylor, Eds., McMillan, London, p. 247 (1967).

Korzhinskii

D. S. Korzhinskii, *Theory of Metasomatic Zoning, a reply to Dr. Albrecht Hofmann*, *Am. J. Sci.* 273, 958-959 (1973).

Kot

C. A. Kot, *Airblast Attenuation*, Technical Manuscript S-1R (AD-505592L) (February 1971).

Kriebel

A. R. Kriebel, *Airblast in Tunnels and Chambers, Final Report*, DASA-1200-11 Supplement 1 (October 1972).

Kullen

B. J. Kullen, N. M. Levitz, and M. J. Steindler, *Management of Waste Cladding Hulls. Part II. An Assessment of Zirconium Pyrophoricity and Recommendations for Handling Waste Hulls*, ANL-77-63 (November 1977).

Levitz

N. M. Levitz, B. J. Kullen, and M. J. Steindler, *Management of Waste Cladding Hulls. Part I. Pyrophoricity and Compaction*, ANL-8139 (February 1975).

Luna

R. E. Luna, H. W. Church, R. M. Elrick, D. R. Parker, and L. S. Nelson, *Combustion and Smoke Formation Following Exposure of Actinide Metals to Explosions*, U.S. Energy Research and Development Administration Report SAND-76-6246, Sandia Laboratories (1976).

Lyon

W. L. Lyon and E. E. Voiland, *The Preparation of Uranium Dioxide From a Molten Salt Solution of Uranyl Chloride*, HW-62431 (October 1959).

Maya

L. Maya and C. D. Bopp, Reports ORNL/TM-5993 (1977) and ORNL/TM-6092 (1977).

MFRP

General Electric Company, Nuclear Energy Div., *Safety Analysis Report-Midwest Fuel Recovery Plant*, DOCKET 50-268 (December 1970).

Moffat

A. J. Moffat and R. D. Thompson, Report IDO-14543 (1961).

Nelson

R. G. Nelson, *Densification Process*, pp. 45-48, *Nuclear Waste Management and Transportation Quarterly Progress Report April through June 1975*, A. M. Platt (compil.), BNWL-1936 (September 1975).

NFS

Nuclear Fuel Services, Inc., *Safety Analysis Report - NFS' Reprocessing Plant - West Valley, New York*, DOCKET 50-201 (1973).

Orth

D. A. Orth, J. M. McKibben, and W. C. Scotten, *Int. Solv. Ext. Conf.*, p. 514 (1971).

Peppard

D. F. Peppard, G. W. Mason, A. F. Bollmeier, and S. Lewey, *Extraction of Selected Metallic Cations by a Highly Hindered $(\text{GO})_2 \text{PO}(\text{OH})$ Extractant in Two Different Diluents from an Aqueous Chloride Phase*, *J. Inorg. Nucl. Chem.* 33, 845 (1971).

Petkus

E. J. Petkus and M. A. Bowden, *Chemical Engineering Division Semiannual Report, July-December 1964*, ANL-6925, p. 97 (May 1965) and E. J. Petkus, T. R. Johnson and R. K. Steunenberg, *The Preparation of Uranium Monocarbide by Reaction in a Liquid Metal Medium*, ANL-7301 (March 1967).

Porter

J. B. Porter, *Analysis of Hydrogen Explosion Hazards*, DP-1295 (July 1972).

Porzel

F. B. Porzel, *Design Evaluation of the Boiling Water Reactor (ANL) in Regard to Internal Explosions*, ANL-5651 (January 1957).

Pushlenkov

M. F. Pushlenkov, N. N. Shchepetilnikov, G. I. Kuznetsov, F. D. Kasimov, A. L. Yasnovitskaya, and G. N. Yakovlev, *Int. Solv. Ext. Conf.*, p. 493 (1974).

Rand

M. H. Rand, *Atomic Energy Review*, Special Issue No. 5, IAEA, Vienna (1975).

Rice

P. A. Rice, R. E. Balzhiser, and D. V. Ragone, *The Thermodynamics of Nuclear Materials*, IEAE, Vienna, p. 331 (1962).

Robinson

W. C. Robinson and P. Chiotti, *J. Less-Common Metals* 10, 190 (1966).

Röster

H. S. Röster and H. Lange, *Geochemical Tables*, Elsevier Publishing Company, New York (1972).

Samsel

E. G. Samsel and J. R. Berreth, *Nucl. Technol.* 33, 68 (1977).

Schlea

C. S. Schlea, H. E. Henry, M. R. Caverly, and W. J. Jenkins, *USAEC Report DP-809* (1963).

Siddal

T. D. Siddall, *Trialkyl Phosphates and Dialkyl Alkylphosphonates in Uranium and Thorium Extraction*, *Ind. Eng. Chem.* 51, 41 (1959).

Smailos

E. Smailos, *Reaction Behavior of Fission Products in Carbide and Nitride Fuel Based on Simulation Investigations*, EURFNR-1179 (1974) [German Version KFK-1953].

Sokhina

L. P. Sokhina, F. A. Bogdanov, A. S. Solovkin, E. G. Teterin, and N. N. Shesterikov, *Russian J. Inorg. Chem.* 21(9), 1358 (1976).

Solovkin-1969

A. S. Solovkin, P. G. Krutikov, and A. N. Panteleeva, *Russian J. Inorg. Chem.* 14(12), 1780 (1969).

Solovkin-1971

A. S. Solovkin, P. G. Krutikov, and G. N. Yakovilev, *Russian J. Inorg. Chem.* 16(5), 763 (1971).

Standage

A. E. Standage and M. S. Gani, *Reaction Between Vitreous Silica and Molten Aluminum*, *J. Amer. Ceram. Soc.* 50, 101-5 (1967).

Steunenberg

R. K. Steunenberg, R. D. Pierce, and I. Johnson, *Status of the Salt Transport Process for Fast Breeder Reactor Fuels*, Symposium on Reprocessing of Nuclear Fuels Conf. 690801, Nuclear Metallurgy, Vol. 15 (1969).

Teterin-1971A

E. G. Teterin, N. N. Schesterikov, P. G. Krutikov, and A. S. Solovkin, Russian J. Inorg. Chem. 16(1), 77 (1971).

Teterin-1971B

E. G. Tererin, N. N. Shesterikov, P. G. Krutikov, and A. S. Solovkin, Russian J. Inorg. Chem. 16(3), 416 (1971).

Thompson

J. B. Thompson, Jr., *Local Equilibrium in Metasomatic Processes*, in Researches in Geochemistry, P. H. Abelson (ed.), John Wiley and Sons, New York, pp. 427-457.

Toth

L. M. Toth and L. O. Gilpatrick, J. Inorg. Nucl. Chem. 35, 1509 (1973).

Tsujino

T. Tsujino *et al.*, Ind. Eng. Chem. Proc. Des. Dev. 15, 396 (1976).

Turner

F. J. Turner and J. Verhoogen, *Igneous and Metamorphic Petrology*, 2nd ed., McGraw-Hill, New York, pp. 565-569 (1960).

Viecelli

J. Viecelli, *Air Blast Protection in Tunnels*, URCL-14848-T (March 1968).

Vogler

S. Vogler and J. Pavlik, *Chemical Engineering Division Semiannual Report, July-December 1964*, ANL-6925, p. 101 (May 1965).

Walsh

W. J. Walsh, J. J. Stockbar, T. F. Cannon, and L. Anderson, in *Chemical Engineering Division Annual Report-1969*, ANL-7675, p. 22 (April 1970).

Wenz

D. A. Wenz and I. Johnson, *Reaction of PuO_2 With Molten $MgCl_2$* , Inorg. Nucl. Chem. Lett. 4, 735 (1968).

West

G. A. West and C. D. Watson, *Safety Studies of the Shear-Leach Processing of Zircaloy-2-Clad Spent Nuclear Fuels*, ORNL-4061 (October 1967).

Weyl

P. K. Weyl, *The Solution Behavior of Carbonate Minerals in Sea Water*, Studies in Tropical Oceanography 5, 178-228 (1967).

Winsch-1962

I. O. Winsch and T. F. Cannon, *Chemical Engineering Division Summary Report for Oct, Nov, Dec 1961*, ANL-6477, p. 55 (March 1962).

Winsch-1974

I. O. Winsch, T. R. Johnson, R. D. Pierce, and W. E. Miller, *Melt Decladding of Fast Reactor Fuel*, ANL-8142 (November 1974).

Yagodin

G. A. Yagodin, D. A. Sinegribova, and A. M. Chekmarev, *Int. Solv. Extr. Conf.*, p. 2209 (1974).

Distribution of ANL-78-37Internal:

M. Ader	A. Melton
G. Bernstein	M. V. Nevitt
L. Burris	R. Pelto
F. A. Cafasso	B. Saunders
E. J. Croke	W. B. Seefeldt
P. R. Fields	M. Seitz
K. Flynn	A. Siczek
S. Fried	J. Simmons
A. M. Friedman	M. J. Steindler (15)
B. R. T. Frost	L. E. Trevorrow
T. J. Gerding	D. S. Webster
L. Jardine	A. Ziegler
G. Kesser	A. B. Krisciunas
B. Kullen	ANL Contract File
S. Lawroski	ANL Libraries (5)
R. Leonard	TIS Files (6)
W. J. Mecham	

External:

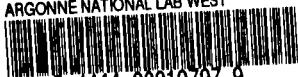
DOE-TIC, for distribution per UC-10 and UC-70 (292)
 Manager, Chicago Operations Office
 Chief, Office of Patent Counsel, CH
 President, Argonne Universities Association
 Chemical Engineering Division Review Committee:
 C. B. Alcock, U. Toronto
 R. C. Axtmann, Princeton U.
 R. E. Balzhiser, Electric Power Research Inst.
 J. T. Banchemo, U. Notre Dame
 T. Cole, Ford Motor Co.
 P. W. Gilles, U. Kansas
 R. I. Newman, Allied Chemical Corp.
 G. M. Rosenblatt, Pennsylvania State U.
 R. C. Adkins, NUSAC, Falls Church, VA
 H. M. Agnew, Los Alamos Scientific Lab.
 T. W. Ambrose, Battelle Pacific Northwest Lab.
 C. K. Anderson, Combustion Engineering
 F. H. Anderson, Allied Chemical Corp., Idaho Falls
 J. F. Bader, Westinghouse Electric Corp., Pittsburgh
 Battelle-Columbus Labs.
 R. C. Baxter, Allied-General Nuclear Services
 J. E. Bennett, Clemson U.
 M. Binstock, Kerr-McGee Nuclear Corp.
 B. C. Blanke, USDOE-DA, Miamisburg, OH
 D. Bowersox, Los Alamos Scientific Lab.
 K. Bowlman, General Electric Co., San Jose
 R. G. Bradley, Office of Nuclear Waste Management, USDOE
 M. G. Britton, Corning Glass Works
 C. L. Brown, Battelle Pacific Northwest Lab.
 R. Brown, Allied Chemical Corp., Idaho Falls

H. L. Browne, Bechtel, Inc.
 J. K. Bryan, Clemson U.
 L. L. Burger, Battelle Pacific Northwest Lab.
 D. Camp, Lawrence Livermore Lab.
 D. O. Campbell, Oak Ridge National Lab.
 J. Carp, Edison Electric, New York City
 W. T. Cave, Mound Lab.
 B. H. Cherry, GPU Services Corp.
 E. D. Clayton, Battelle Pacific Northwest Lab.
 F. E. Coffman, USDOE-MFE
 J. J. Cohen, Lawrence Livermore Lab.
 W. J. Coleman, Battelle Pacific Northwest Lab.
 C. R. Cooley, Office of Nuclear Waste Management, USDOE
 G. R. Corey, Commonwealth Edison, Chicago
 R. Cunningham, USNRC, Nuclear Materials Safety & Safeguards
 R. E. Dahl, Hanford Engineering Development Lab.
 J. C. Dempsey, Office of Nuclear Waste Management, USDOE
 R. L. Dickeman, Exxon Nuclear Co., Inc., Bellevue
 M. Dickerson, Lawrence Livermore Lab.
 B. R. Dickey, Allied Chemical Corp., Idaho Falls
 J. Dietz, Los Alamos Scientific Lab.
 R. L. Dillon, Battelle Pacific Northwest Lab.
 R. F. Duda, Westinghouse Electric Corp., Pittsburgh
 G. H. Dyer, Bechtel Corp.
 Eastern Environmental Radiation Lab., HEW
 D. Eldred, General Electric Co., Sunnyvale
 E. D. Erickson, Rocky Flats Plant
 D. Ferguson, Oak Ridge National Lab.
 J. L. Fletcher, Hanford Engineering Development Lab.
 Foster Wheeler Corporation, Library (HQAP)
 R. Fullwood, Science Applications, Inc., Palo Alto
 General Electric Co., San Jose (DOE)
 A. Giambusso, USDOE-AIA
 R. W. Gilchrist, Clemson U.
 S. Goldsmith, Battelle Pacific Northwest Lab.
 R. L. Grant, Boeing Engineering and Construction Div., Seattle
 J. L. Heffter, NOAA, Silver Spring
 R. S. Hemper, Battelle Pacific Northwest Lab.
 T. B. Hindman, Jr., USDOE-SR, Aiken
 A. H. Hines, Jr., Florida Power Corp.
 C. A. Hirenda, Proposal Management, Inc., Philadelphia
 R. Hoskins, Tennessee Valley Authority
 H. A. Hurstadt, Virginia Polytechnic Inst.
 R. H. Ihde, Babcock & Wilcox Co., Lynchburg
 W. Johnson, Yankee Atomic Electric Co.
 B. F. Judson, General Electric Co., San Jose
 W. A. Kalk, Holmes & Narver, Inc., Anaheim
 S. V. Kaye, Oak Ridge National Lab.
 G. R. Keepin, Los Alamos Scientific Lab.
 C. J. Kershner, Mound Lab.
 F. J. Kiernan, Aerojet Energy Conversion Co., Washington
 K. Killingstad, Battelle-Human Affairs Research Centers, Seattle
 H. J. C. Kouts, USNRC
 C. W. Kuhlman, Office of Nuclear Waste Management, USDOE

L. T. Lakey, Exxon Nuclear Co., Richland
 G. Lehmkul, Rocky Flats Plant
 D. Lester, Battelle Pacific Northwest Lab.
 S. Levine, USNRC, Div. of Reactor Safety Research
 F. W. Lewis, Middle South Utilities, Inc., New Orleans
 W. H. Lewis, Nuclear Fuel Services, Rockville
 R. C. Liikala, Battelle Pacific Northwest Lab.
 J. L. Liverman, Office of Nuclear Waste Management, USDOE
 H. E. Lyon, USDOE-SS
 L. Machta, NOAA, Silver Spring
 J. C. Mailen, Oak Ridge National Lab.
 W. J. Maraman, Los Alamos Scientific Lab.
 T. L. McDaniel, Babcock & Wilcox Co., Lynchburg
 W. H. McVey, USDOE-NPD
 R. B. Minogue, USNRC, Office of Standards Development
 E. Morgan, Babcock & Wilcox Co., Lynchburg
 B. C. Musgrave, Allied Chemical Corp., Idaho Falls
 M. I. Naparstek, Burns & Roe, Inc., Paramus, NJ
 NASA, John F. Kennedy Space Center
 L. W. Nelms, Todd Company, Galveston
 Y. Ng, Lawrence Livermore Lab.
 R. D. Oldenkamp, Atomics International
 D. Orloff, U. South Carolina
 R. C. Orphan, Lawrence Livermore Lab.
 D. A. Orth, Savannah River Plant
 B. Paige, Allied Chemical Corp., Idaho Falls
 J. H. Pashley, Oak Ridge Gaseous Diffusion Plant
 G. B. Pleat, Office of Nuclear Waste Management, USDOE
 H. Postma, Oak Ridge National Lab.
 C. A. Preskitt, IRT Corp., San Diego
 J. J. Reilly, Brookhaven National Lab.
 C. Rhoades, U. South Carolina
 G. K. Rhode, Niagara Mohawk Power Corp., Syracuse
 L. M. Richards, Atlantic Richfield Co., Los Angeles
 G. L. Ritter, Exxon Nuclear Corp., Richland
 R. W. Roberts, USDOE-ANE
 D. M. Rohrer, Los Alamos Scientific Lab.
 H. E. Roser, USDOE, Albuquerque Operations Office
 K. J. Schneider, Battelle Pacific Northwest Lab.
 R. L. Seale, U. Arizona
 T. A. Sellers, Sandia Labs.
 J. Shefcik, General Atomic Co.
 W. G. N. Slinn, Oregon State U.
 B. Smenoff, Hudson Inst. Croton, NY
 L. E. Smith, Carolina Power & Light Co., Raleigh
 A. Squire, Hanford Engineering Development Lab.
 T. Stanford, U. South Carolina
 C. Stephens, Virginia Electric Power Co., Richmond
 M. J. Stephenson, Oak Ridge National Lab.
 J. A. Stiegler, Sandia Labs.
 S. Stoller, The S. M. Stoller Corp.
 E. Straker, Science Applications, Inc., La Jolla
 K. Street, Lawrence Livermore Lab.

G. Stukenbroeker, NL Industries, Wilmington, Del.
 J. L. Swanson, Battelle Pacific Northwest Lab.
 R. Uhrig, Florida Power & Light Co., Miami
 USDOE Div. of Nuclear Fuel Cycle and Prod., Raw Matr.
 USDOE Div. of Basic Energy Sciences
 USDOE Div. of RRT, Engineering
 USDOE Div. of RRT, Technology
 USDOE Idaho Operations Office
 USDOE New Brunswick Laboratory
 USDOE San Francisco Operations Office
 USDOE Southern California Energy Office
 V. Van Brunt, U. South Carolina
 H. H. Van Tuyl, Battelle Pacific Northwest Lab.
 V. C. A. Vaughn, Oak Ridge National Lab.
 K. Vickers, Phrasor Technology, Pasadena
 E. E. Voiland, General Electric Co., Morris, IL
 B. L. Vondra, Oak Ridge National Lab.
 R. D. Walton, Jr., Office of Nuclear Waste Management, USDOE
 C. D. Watson, Oak Ridge National Lab.
 L. L. Wendell, Battelle Pacific Northwest Lab.
 G. W. Wensch, USDOE-AIA
 W. J. Wilcox, Oak Ridge Gaseous Diffusion Plant
 A. K. Williams, Allied-General Nuclear Services, Barnwell
 R. O. Williams, Rocky Flats Plant
 D. D. Wodrich, Atlantic Richfield Hanford Co.
 R. Wolfe, Office of Nuclear Waste Management, USDOE
 D. Zeigler, Rocky Flats Plant
 Arizona, U. of, Dept. of Nucl. Engineering
 C. F. Bonilla, Columbia U.
 W. Brandt, U. of Wisconsin-Milwaukee
 R. G. Cochran, Texas A&M U.
 D. A. Daavettila, Michigan Technological U.
 A. H. Emmons, U. Missouri
 E. R. Epperson, Michigan Technological U.
 Fermi National Accelerator Lab., Library
 P. J. Fulford, Purdue U.
 H. E. Hungerford, Purdue U.
 H. S. Isbin, U. Minnesota
 Y. W. Kang, National Accelerator Lab.
 W. R. Kimel, U. Missouri
 Maine Univ., Prof. in charge of Chem. Engr. Lib.
 Marquette U., Dept. of Chemistry
 Michigan Technological U., Library
 D. W. Moeller, Kresge Ctr. for Environmental Health, Boston
 G. Murphy, Iowa State U.
 H. Rosson, U. Kansas
 L. Schwendiman, Pacific Northwest Lab.
 E. R. Stansberry, Purdue U.
 B. S. Swanson, Illinois Inst. of Technology
 H. G. Swope, Madison, Wis.
 B. W. Wilkinson, Michigan State U.
 W. E. Wilson, Washington State U.
 W. F. Witzig, Pennsylvania State U.

ARGONNE NATIONAL LAB WEST



3 4444 00010797 9